Active heat capacity : models and parameters for the thermal performance of buildings

Jóhannesson, Gudni

1981

DIVISION OF BUILDING TECHNOLOGY
LUND INSTITUTE OF TECHNOLOGY

ACTIVE HEAT CAPACITY

MODELS AND PARAMETERS FOR THE THERMAL PERFORMANCE OF BUILDINGS

GUÐNI JÓHANNESSON

REPORT TVBH - 1003
LUND, SWEDEN 1981

L'épaisseur des murs était pour lui un véritable régal.

Marcel Aymé: Le passe-muraille.

ACKNOWLEDGEMENTS

The present work was sponsored by the Swedish Council for Building Research which is gratefully acknowledged.

It has been initiated and carried out under the supervision of Prof. Lars Erik Nevander, head of the Division of Building Technology at Lund Institute of Technology. His encouragement and constructive criticism over the years has been of great value.

Several other people have supported me during this work, such as: Dr. Gerd Hauser at the University of Essen, who kindly permitted me to use his computer results, Dr. Ann-Charlotte Andersson, a colleague at the Division, who implemented my results on two-dimensional frequency response into her computer program and Dr. Johan Claesson at the Division of Mathematical Physics, a true discussion partner on mathematical and physical problems.

Typing was done by Lena Thorell, Birgitta Salmi and Inger Karlsson. Lilian Johansson drew the figures. Their patience and helpfulness has been invaluable.

To my wife Bryndis Sverrisdóttir, and to Gunnhildur and Sverrir, who have had to put up with my absence during this long winter, I express my sincerest thanks.

Lund, April 1981

Gudni Jóhannesson

CONTENTS

SUMMARY		5
LIST OF SYMBOLS		7
1	INTRODUCTION	11
1.1	Background	11
1.2	Scope	12
1.3	Fields of application	13
2	THE BUILDING ENCLOSURE - A PARAMETER SURVEY	15
2.1	The room system	15
2.2	Solar radiation	16
2.3	Ventilation	16
2.4	Internal sources of heat	17
2.5	Discretization of the room system	17
3	STEADY STATE RELATIONS	21
3.1	Heat transmission through opaque surfaces	22
3.1.1	One-dimensional heat flow	22
3.1.2	Two-dimensional heat flow - thermal bridges	22
3.2	Heat transfer at internal surfaces	24
3.2.1	Convective heat transfer	24
3.2.2	Long wave radiation	27
3.2.3	Combined convection and radiation, practical heat transfer coefficients	32
3.3	Heat transfer by ventilation	39
3.4	Solar radiation and its contributions to the heat balance	40
3.4.1	Solar radiation towards a surface	40
3.4.2	Heat balance for outer surfaces	40
3.4.3	Window heat balance	42
4	NON-STEADY HEAT CONDUCTION IN BUILDING COMPONENTS	47
4.1	The frequency domain solution	47
4.1.2	Solution for a multilayer construction	51
4.1.3	Solution of frequency response for two-dimensional heat flow problems	53

4.2	Solution by Laplace transform and related procedures	59
4.3	Finite-difference methods - RC-models	61
5	SIMPLIFIED MODELS FOR SURFACE HEAT EXCHANGE - CONSTRUCTION CHARACTERISTICS	65
5.1	Model specifications	65
5.1.1	Quantities of interest for calculating the room climate	65
5.1.2	Limits to generality and applicability	66
5.1.3	Presentation and evaluation of model characteristics - the Bode diagram	70
5.2	Introduction and evaluation of different models and parameters	73
5.2.1	Frequency response - the admittance procedure	75
5.2.2	The ω - RC transform	84
5.3	The proposed parameter	99
5.3.1	Active heat capacity	100
5.3.2	A basis for an approximative method for calculation of the active heat capacity	101
5.3.3	An approximative calculation method to estimate the active heat capacity	112
5.4	Models for constructions with two dimensional heat flow	114
6	CALCULATION OF ROOM HEAT BALANCE	117
6.1	Models for room heat balance	118
6.1.1	Alternative ways to simplify the room heat balance	120
6.1.2	Principles for combination of surface admittances	127
6.1.3	Influence of heat capacity of the room air	133
6.1.4	The two-node model for room heat balance	136
6.2	Calculation methods for one-surface models	138
6.2.1	The steady state solution	138
6.2.2	The frequency response	139
6.2.3	Solution with finite differences	143

7	APPLICATIONS TO NON-STEADY HEAT TRANSFER PROCESSES IN BUILDINGS	149
7.1	Calculation object	150
7.2	Overheating problems	151
7.3	Intermittent heating	155
7.4	Energy consumption and thermal inertia	158
LIST OF REFERENCES		161

SUMMARY

This thesis concerns the characterization and evaluation of non-steady heat transfer in building components and building enclosures. The major aim of the underlying research has been to assemble and develop simplified calculation procedures for this purpose.

The room system is transformed into a set of nodal points. Each nodal point is characterized by its temperature. The temperatures and generated heat flows at the nodal points are related by a matrix of heat transfer operators. To establish a simple model for heat balance calculations three main items are treated: simplification of the heat transfer operators, the description of the solar gain through windows and reduction of the number of nodes.

The heat transfer operators that can be treated as steady state are delt with in Chapter 3. The convective surface heat transfer and the long-wave radiation exchange between surfaces are non-linear processes. The latter also has to be solved simultaneously for all surfaces.

From a study of a room with two isothermal surfaces it is concluded that a generally applicable modified surface heat transfer coefficient including the radiation exchange is not to be found. An alternative simplification discussed is to regard the radiation exchange between the surfaces as infinite. An important consequence of this assumption is that all the opaque surfaces of the room can be represented by a single node.

The heat transfer through windows under the influence of solar radiation is complicated since the radiation absorbed in different window panes causes a rise in temperature and thereby disturbs the heat flow pattern. If the window is treated as a series of linear resistances from air to air the total power gain through the window can be treated as three independent components: The short wave radiation transmitted through the window, the short wave radiation absorbed in the window panes and the ordinary thermal admittance. The two first are tabulated for different types of windows and sun protection as fractions of the total solar gain through a

double-glazed window.

For non-steady heat conduction in opaque constructions solutions are given in the frequency domain and by finite differences while solutions by the Laplace transform and the response factor method are found to be unsuitable for the purpose of this work. A numerical solution for the frequency response of constructions with two dimensional heat flow is also given.

Based on the frequency response at an angular velocity corresponding to the 24 h period optimum parameters for different types of RC-models are derived. The simplest network is a single capacitance giving the same ratio between the amplitudes of heat flow and temperature as the real surface. This quantity is called the active heat capacity of the wall. To estimate this quantity a simplified calculation procedure is given.

The active heat capacity is meant to characterize the building component but even to be applied for an approximate calculation of the room heat balance. For the combination of surfaces with different active heat capacities addition rules are established that take into account the limited mutual radiation exchange between the surfaces. In that way the room is transformed into a model with two nodes, one representing the surface temperature and one representing the room air. An explicit solution is given in the frequency domain. A solution in the time domain allows the thermal loads to be represented as time series and the mode of operation can be freely defined and varied during the calculated period.

Finally some calculated examples are given where the simplified procedure is applied on: overheating problems, intermittent heating and energy consumption in relation to thermal inertia. In a few cases the results are compared to the results of a computer program.

LIST OF SYMBOLS

	quantity	unit
A	area	m^2
A	element of transfer matrix	-
a	thermal diffusivity	m^2/s
a	short-wave radiation absorptance	-
B	element of transfer matrix	-
b	temperature variation coefficient	K/s
†C	heat capacity	J/K
C_A	active heat capacity	J/Km^2
C	foundation modulus	Pa/m
C	element of heat transfer matrix	-
c	specific heat capacity	J/kgK
D	bending stiffness	m^3Pa
D	element of heat transfer matrix	-
E	element of heat transfer matrix	-
F	element of heat transfer matrix	-
F_S	surface factor	
F	configuration factor	
F	short-wave radiation transmittance	-
f	decrement factor	-
G	element of heat transfer matrix	-
Gr	Grashof number	

$$Gr = \frac{g\beta}{\nu^2}\Delta\vartheta l^3$$

G	transfer function	
H	element of transfer matrix	-
I	incident solar radiation	W/m^2
K_1-K_9	calculation constants	
k	coefficient of thermal transmittance (steady state)	W/m^2K
k	wave number of temperature wave	m^{-1}
L{}	the Laplace transform of	
l	length	m
M	moment	Nm
m	areal thermal resistance	m^2K/W
Nu	Nusselt number	-

	quantity	unit
$Nu = \frac{\alpha_c l}{\lambda}$		
n	ventilation rate	h^{-1}
Pr	Prandtl number	-
$Pr = \frac{\nu}{a}$		
Q	heat flow	W
q	density of heat flow rate	W/m^2
^{+}R	thermal resistance	K/W
R	radiosity	W/m^2
r	length	m
r	amplitude	
s	conductance	W/K
s	variable of Laplace transform	
T	thermodynamic temperature	K
T_D	dynamic transmittance	W/m^2K
t	time	s
u	real part of a complex number	
V	volume	m^3
v	imaginary part of a complex number	
W	displacement	m
x	length coordinate	m
y	length coordinate	m
Y	admittance	W/m^2K
Y'	modified admittance	W/m^2K
Z	thermal impedance	m^2K/W
α	overall coefficient of surface heat transfer	W/m^2K
α_C	convective coefficient of surface heat transfer	W/m^2K
α_S	radiative coefficient of surface heat transfer	W/m^2K
β	angle	rad
β	expansion coefficient	K^{-1}
Δ	difference	
Δ	Laplace operator	
ε	emissivity	
θ	phase difference	rad, degrees

	quantity	unit
ϑ	Celcius temperature	C
λ	thermal conductivity	W/mK
ν	kinematic viscosity	m^2/s
ξ	ratio	
ρ	reflectance	
ρ	density	kg/m^3
σ	Stefan Boltzmann constant	W/m^2K^4
ϕ	phase difference	rad, degrees
ϕ	generated heat	W/m^3
ω	angular velocity	rad/s

†

When plane constructions are studied the thermal resistance R and the heat capacity C are both related to 1 m^2 area.

1 INTRODUCTION

This thesis concerns the characterization and evaluation of non-steady heat transfer in building components and building enclosures as applied to the field of climatization. The major aim of the underlying research project has been to assemble and develop simplified calculation procedures for this purpose.

1.1 BACKGROUND

In recent time a number of computer programs have been developed around the world in order to evaluate non-steady state heat transfer processes in building. The rapid increase in the availability of computer power has led the progress towards more and more detailed calculation models. With an increasing number of input parameters and a more sophisticated description of the physical phenomena one tries to gain good accordance with some real process as observed by measurements. The expected outcome of the efforts being made in this field is that the temperatures or the heat-flows of a certain building enclosure can be predicted for given meteorological and operating conditions. With an increasing degree of accuracy the extensive computer programs are of course very valuable for the evaluation of different system solutions.

It is, however, a paradox that with increasing complexity of the physical model the computer program will have the character of a black box. The user will accept the resulting design values for the heating or the cooling plant without reflecting over the separate physical processes that lead on to this result. The calculations are also as a rule carried out by the heating and ventilating consultant while the thermal performance of the building is to a great extent affected by other categories, such as architects, constructors and acoustic experts at earlier stages of the building process. It is therefore of crucial importance to give those categories qualitative and quantitative knowledge concerning how their different choices of materials, construction alternatives and geometries influences the energy, power and investment needed for the maintenance

of a comfortable indoor climate. At the early stage of the building design process the use of extensive computer programs is both unthinkable and unnecessary. What is needed is rather a whole spectrum of evaluation procedures such as simple guide-lines for the orientation of windows, tables or simple calculation procedures for characterization of the building components, calculation rules to estimate extreme temperatures in relation to mass, window treatment and ventilation pattern and finally detailed computer programs to calculate the power loads for the resulting solution.

1.2 SCOPE

The paramount goal of this work has been to provide tools so that the non-steady state characteristics of the building components can be taken into account at the earlier stages of the building design process.

The first step in this direction has been to derive parameters that describe the characteristics of the building component. The specifications are, that the parameters, in a way understandable to most people, provide information about their contribution to the non-steady process at the same time as they can, together with other influencing factors such as window size, ventilation pattern and meteorological data, serve as a basis for an approximate calculation of the heat balance.

The second step has been to provide approximate formulae for the non-steady heat balance. The specifications read as follows.

- The complexity of the calculation procedures is limited so that the heat balance for a single room over one day can be calculated with the aid of a desk calculator within reasonable time limits, say 3 h.

- The simplifications made in order to derive the simplified formulae should not lead to restrictions in the choice of heat transfer data for materials surfaces etc.

- The time dependent parameters that can be considered in the calculations are outside temperature, solar radiation, window screening, venti-

lation, internal power load and room air and surface temperatures.

In general this thesis does not question the assumptions and simplifications that are common for most great computer systems. An important exception is that non-steady two dimensional heat flow is considered for certain building components.

The simplifications made in the deduction of the simplified formulae are chosen in a way to give optimum accuracy for the 24 hour frequency components of a non-steady state process.

The boundary conditions for the calculation, i.e. meteorological data, internal power load etc. are only treated to a degree necessary to provide examples for comparative calculations.

1.3 FIELDS OF APPLICATION

As it has been outlined above the main purpose with those calculation procedures is not to replace the computer programs but rather to affect the design process so that the solution finally treated by the computer will be close to the optimum one. The simplified procedures can also be implemented in the computer programs either to make a qualified guess on initial conditions and thereby speed up the convergence to a periodic heat balance or for long term energy balance calculations where a detailed consideration of the building mass would take unreasonably long time for the computer.

The simplified procedure should also benefit educational and training purposes. The students should be able to make quantitative calculations on their own and study the influences of different parameters.

Furthermore in the developing countries where buildings are being designed for difficult climatic conditions and without an access to computer power the simplified calculation procedures described in this report should be valuable.

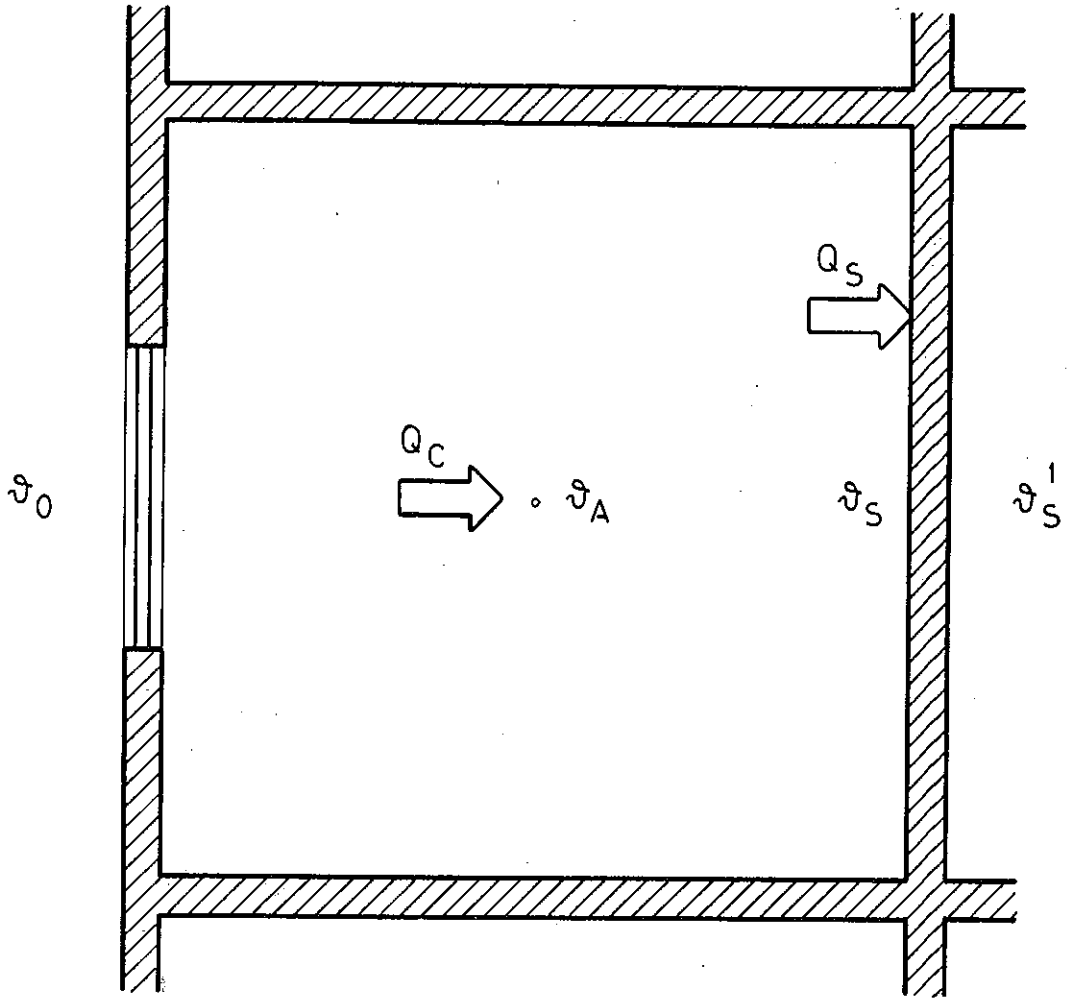

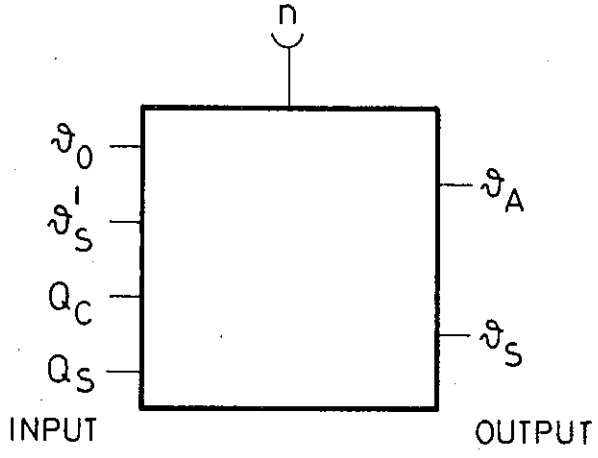

FIG. 2.1. The room system with different variables of the heat balance.

2 THE BUILDING ENCLOSURE - A PARAMETER SURVEY

In this chapter is presented a set of parameters necessary for the description of the heat transfer processes, followed by a discussion on how the different influencing phenomena can be expressed in terms of the parameters.

2.1 THE ROOM SYSTEM

In figure 2.1 a room system is shown. The heat balance for the room can be expressed in terms of a set of external temperatures and a set of internal heat gains. These are therefore referred to as input variables while the temperatures resulting from the calculations, i.e. the air and wall temperatures, are the output variables. It is characteristic of this relationship that the input variables are dependent on the output variables, except for the outside temperature ϑ_0. The air temperatures of the adjacent rooms ϑ'_A can be set equal to ϑ_A for rooms with the same geometry and orientation. The convective heat loss through ventilation is dependent on the inside air temperature. The internal heat gains both for the room air Q_C and for the surfaces Q_S can be regulated on basis of the resulting temperatures.

The choice of input variables is rather arbitrary especially for the internal heat gains Q_C and Q_S which we shall see later on are no basic data but have to be calculated from several other variables. It is also questionable if Q_S and Q_C also should represent the heat exchange generated by the temperature differences in the system. To avoid confusion the following definition is made.

> The internal heat gain to the air and the surfaces denoted by Q_C and Q_S respectively is the generated heat which can be expressed in terms of no more than one temperature variable.

The definition above implies for instance that the internal heat gain does not include ventilation and transmission loss but heat generated by the heating system, persons, machinery and transmitted solar radiation. In some cases this definition will be violated especially for such quantities that for the sake of simplification are assumed to be independent of the resulting temperatures.

2.2 SOLAR RADIATION

Solar radiation will affect the indoor climate in three different ways.

Firstly, the solar radiation, transmitted through the window is absorbed by the surfaces of the room. Since the room air does not absorb any radiation the total amount of transmitted radiation is added to Q_S, i.e. considered as heat generated at the surfaces.

Secondly, the solar radiation absorbed in the window panes will cause a rise in temperature. In those cases where the window heat balance is not treated separately the part of the absorbed energy entering the room is added to Q_c.

Thirdly, the rise in temperature on the outer surfaces caused by solar radiation will generate heat flow through the construction. This is taken into consideration by calculating a new equivalent outside temperature from a heat balance at the surface.

2.3 VENTILATION

The ventilation loss from the room is considered as a heat exchange between the room air and an external air supply with a known temperature, for instance the outside air or the air in an adjacent room. The resulting heat flow to the room air will in most cases be put proportional to the momentaneous temperature-difference at which the exchange of air masses takes place. But this heat flow can also be considered in the case where the air flow takes place through a canal with some given dynamic properties.

In some cases the ventilation rate for a room varies with time. The ventilation rate thus has to be treated as an independent variable affecting the heat transfer characteristics of the system.

2.4 INTERNAL SOURCES OF HEAT

Under operating conditions heat is either supplied to or removed from the room system as a result of many different processes - generally of two types: heat supplied or removed for the sake of climatization, and heat generated by the different activities in the room. The latter type is sometimes referred to as gratis heat.

The internal heat sources can be considered either as supplying heat to the room air or generating it at the surfaces of the room. Preheaters for the ventilation air and cooling batteries have a stronger coupling to the room air, while heat foils exemplify heat sources at the surface. For other sources such as radiators, machines and persons, heat is generated both to the air and to the surfaces in proportion that are variable and difficult to calculate.

In the following, internal heat sources will be assumed to generate heat to the room air only, if not specified otherwise. This implies that the total amount of heat is added to Q_c.

2.5 DISCRETIZATION OF THE ROOM SYSTEM

In the description above the distribution of the different quantities within the room has not been specified. A continous variation of such quantities as air temperature, surface temperatures, and power generated within the room cannot be allowed in the calculation model since this would lead to an unreasonably complex solution.

The room is therefore transferred into a set of nodal points representing the different surfaces, the room air and the external temperatures. This means that for each set of surfaces and for the room air the distribution of temperature and induced power is assumed to be uniform.

The heat transfer between the different nodal points of the system is described by a matrix of heat transfer operations showing the time-dependent heat transfer by conduction, radiation and convection.

The complexity of the calculation problem and the accuracy of the physical model are mainly affected by the number of nodal points chosen to represent the room system but also by the models chosen for the heat transfer between different nodal points.

Consequently for calculations that are to be done manually or with a simple desk calculator, it can be stated that a system of two different unknown temperatures, i.e. a system with two nodes, is a practical upper limit.

In other words, since one nodal point is reserved for the room air, all the inside surfaces have to be set to the same temperature. The resulting system of nodal points is shown in figure 2.2. The exterior temperature of the surfaces ϑ'_s can, in some cases, equal the air temperature of the very room being calculated, sometimes it equals the outside air temperature, or is a weighted average of different external temperatures. The heat transfer operators of the network will be discussed later.

In certain circumstances the indoor air temperature can be considered as linearily dependent on the surface temperatures. After a suitable transform two different surface temperatures could be solved manually. A possible network is shown in figure 2.3.

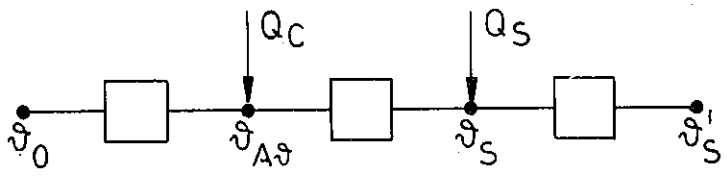

FIG. 2.2. System with two nodal points describing the heat flow within a room.

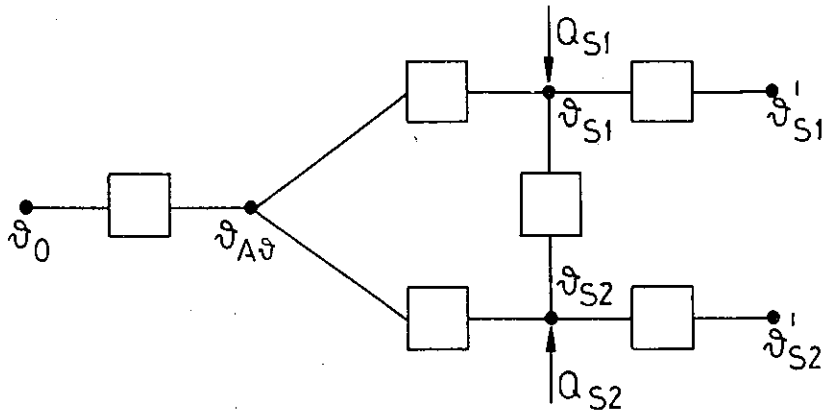

FIG. 2.3. System with three nodal points describing the heat flow within a room.

3 STEADY STATE RELATIONS

Time variable processes dealt with in heat balance calculations can be roughly considered as consisting of two components. A steady state component calculated from the average of the input variables over a longer period of time, and a non-steady component calculated from the variations of the input variables.

This is of course true only as far as the room system can be considered linear. The consequence, however, is that the accuracy of e.g. the maximum temperature during the day will be no better than the accuracy of the average room temperature.

This chapter contains a review of the relations and expressions necessary for the calculation of a heat balance for a room system, which can be treated independently of time.

Time dependent parts of the heat balance will be treated in Chapter 4.

The physical processes involved are as a rule too complicated to be treated exactly in practical calculations, especially when one is trying to establish simplified models. Therefore different simplifications are discussed.

One severe problem in calculations of thermal performance of buildings is that the material properties given in most building codes only apply to special purposes. They are therefore multiplied by a safety factor which corresponds to certain extreme conditions. The thermal conductivity is as a rule increased by 10 - 30% to be on the safe side with regards to calculations of maximal heating power in wintertime, and surface condensation risk.

In other cases a too high thermal conductivity of materials will give the reverse picture. In summertime transmission loss through the walls will increase, which under certain circumstances will give a lower average room temperature. Furthermore, higher thermal conductivity for the materials of an inner wall will, as shown below, increase the accessibility of the wall mass and result in a temperature amplitude which is smaller than in reality. With lower amplitude both the maximum temperature and maximum power need will be underestimated.

3.1 HEAT TRANSMISSION THROUGH OPAQUE SURFACES

3.1.1 One-dimensional heat flow

One dimensional heat flow rate per area can either be expressed in terms of the temperature difference between two surfaces and the resistance m, m^2K/W, between those

$$q = \frac{\Delta\vartheta}{m} \qquad (3.1)$$

or in terms of the temperature difference between two ambient temperatures and the coefficient of thermal transmittance k, W/m^2K.

$$q = k \cdot \Delta\vartheta \qquad (3.2)$$

3.1.2 Two-dimensional heat flow - thermal bridges.

Two-or three-dimensional heat flow in building constructions can as a rule only be calculated accurately with such numerical procedures as finite difference methods or finite elements. For practical non-steady-state calculations the implementation of two- or three-dimensional time-dependent finite difference models for wall joints, window splays etc. would seem unthinkable. Therefore thermal bridges are often left out in calculations of this type since they do not fit into the simple one-dimensional model for a plane wall construction.

Anderson (1978) shows that ignoring the thermal bridges will, for certain types of buildings, cause the transmission heat loss to be underestimated by up to 30 or 40%. Under summer conditions in cases where only a small part of the total heat load is gained by transmission through the opaque surfaces, this will play a smaller role. However, in energy balance calculations during the heating season the increased accuracy won by taking into account the mutual dependence of the time dependent variables will be jeopardized by ignoring the heat loss through the thermal bridges.

It is convenient to divide thermal bridges into two groups: Thermal bridges within the building components and thermal bridges at joints between the building components. Another more explicit definition with

approximately the same meaning would be thermal bridges covered by the exposed inner surfaces of the exterior constructions and thermal bridges that are not. The latter definition is more natural considering that in non-steady state calculations only the exposed surface can be treated. Figure 3.1 gives examples of those two types of thermal bridges.

In practical calculations concerning the non-steady state even the steady state solution for the various thermal bridges involved is too tedious to be carried out numerically. Chasing a simple, accurate and generally applicable formula for thermal bridges has proved to be the alchemy of building physics. However, several authors have presented their studies of special cases either in the form of tables or simple formulae based on some physical reasoning with empirical parameters adjusted in order to fit a sample of numerically solved alternatives. Such work covering a wide range of construction alternatives is presented in the French Rules Th (1977). Other references are Nevander (1961), Johannesson (1976), Verhoven and Liem (1976) and Andersson (1978). Thermal bridges in sheet metal constructions are treated by Johannesson and Åberg (1981).

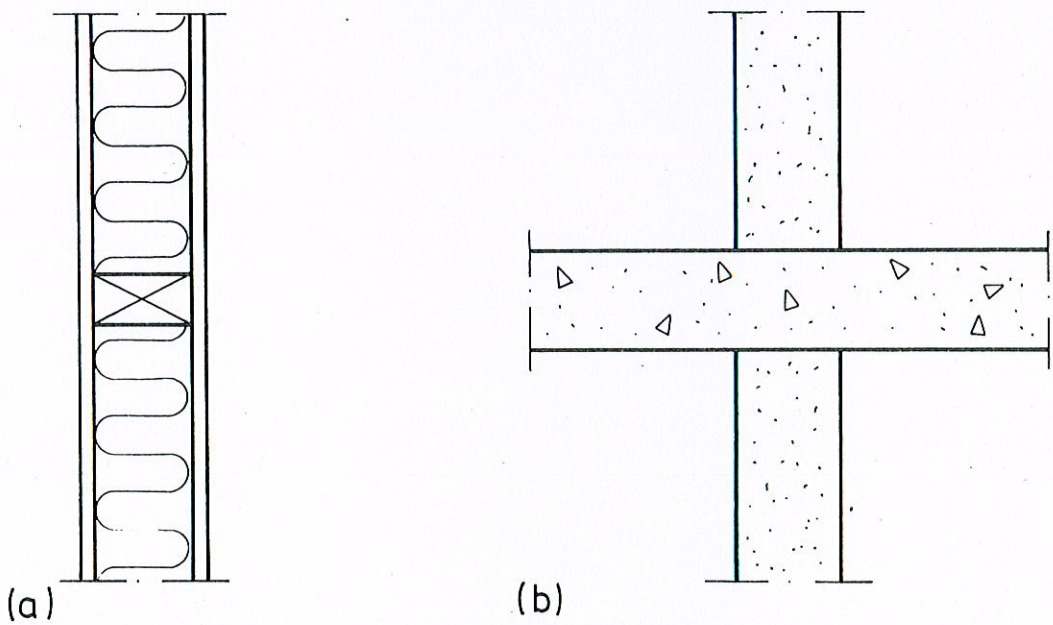

FIG. 3.1. Thermal bridges. In a covered by the exposed inner surface. In b not covered by the exposed inner surface.

3.2 HEAT TRANSFER AT INTERNAL SURFACES

The heat transfer between internal surfaces and the surroundings consists mainly of two processes i.e. convective heat transfer between the surface and the room air, and heat transfer by long wave radiation between the surface and surrounding surfaces. Even vapour transfer between the surface and the room air can, under certain circumstances, contribute significantly to the total heat transfer but this is not considered below.

3.2.1 Convective heat transfer

The surface coefficient of convective heat transfer for plane surfaces varies with several parameters such as the orientation of the surface in relation to the direction of the heat flow and gravitation, temperature difference, air movements and geometry.

Even for simple, idealized cases strict mathematical solutions are not available. However, dimensional analysis yields a generalized relationship between those quantities that are involved in the process of natural convection. The relation between the Nusselt number Nu, the Grashof number Gr and the Prandtl number Pr can be described by

$$Nu = C\ (Gr \cdot Pr)^n \qquad (3.3)$$

within a wide range. The parameter C is mainly dependent on orientation geometry and state of flow while the exponent n is in fact a function of the variable $Gr \cdot Pr$ even though it can be given a constant value within certain ranges. The exponent n takes the value 1/4 for laminary air flow along the surface and 1/3 for turbulent air flow. The transition from laminary to turbulent air flow is assumed to take place at Grashof number around 10^8. Since Grashof number depends on a characteristic length, the transition will take place at some distance in the direction of the convection flow.

From the definition of the Nusselt number it is seen that the convective surface heat transfer coefficient can be expressed as

$$\alpha_c = \frac{\lambda \cdot Nu}{l} \tag{3.4}$$

$$\alpha_c = \frac{\lambda \cdot C(Gr \cdot Pr)^n}{l} \tag{3.5}$$

If all components of Gr · Pr are assumed to be constant except for the length and the temperature difference, and considering the fact that the convective flow becomes turbulent within 1 meter, the average heat transfer coefficients for different orientations can be expressed in terms of the temperature difference only.

Below, results from three different sources are put together. Wieczynski (1977) quotes the results of Davis and Griffith concerning the heat transfer due to natural convection on big plates of concrete, and the results by Min et al (1956) on convective heat transfer at the surfaces of indoor partitions. The third set of expressions was given by Kollmar and Liese (1957). Min et al give the same expression for heat transfer from the ceiling to the air as from the air to the floor. In the same way they state that a warm floor is equivalent to a cold ceiling.

TABLE 3.1. Some different results on convective surface heat transfer.

	Min et al	Davis and Griffith	Kollmar and Liese
Warm floors (cold ceilings)	$\alpha_c=1.79\cdot\Delta\vartheta^{0.32}$	$\alpha_c=2.63\cdot\Delta\vartheta^{0.25}$	$\alpha_c=2.6\cdot\Delta\vartheta^{0.25}$
Warm ceilings (cold floors)	$\alpha_c=0.14\cdot\Delta\vartheta^{0.25}$	$\alpha_c=1.31\cdot\Delta\vartheta^{0.25}$	$\alpha_c=0.6\cdot\Delta\vartheta^{0.25}$
Walls	$\alpha_c=2.16\cdot\Delta\vartheta^{0.31}$	$\alpha_c=1.97\cdot\Delta\vartheta^{0.25}$	$\alpha_c=2.0\cdot\Delta\vartheta^{0.25}$

The original results of Min et al are a little dependent on a characteristic length but the results shown above are those for a quadratic room with wall height 2.6 m and floor area 16 m^2.

The agreement between the three different results is best for walls, while the difference is slightly greater for warm floors and of a different order of magnitude for warm ceilings or cold floors. This could be expected since the situation must be sensitive to convection currents generated at other surfaces of the room.

In simpler linear systems there is a need for applicable average values either for the separate surfaces or for the room as a whole. In table 3.2 daily mean values of the convective heat transfer coefficients according to the Swedish computer program BRIS are shown for different surfaces and different operating conditions.

TABLE 3.2. The calculated heat transfer coefficients due to convection on the inner surface. In the table are given daily mean values of the heat transfer coefficients due to convection on different inner surfaces according to the standard version of the program BRIS. From Wieczynski (1977).

Surface	Daily mean values of heat transfer coefficient due to convection α_C (W/m^2K)			
	SUMMER		WINTER	
	No cooling	Cooling	Convective heating	Radiator heating
Ceiling	0.58	0.58	-2.16	0.48
External wall	1.02	2.45	-2.46	-2.22
Side walls	2.02	2.39	-1.41	0.21
Floor	2.56	2.89	-0.04	0.99
Back wall	2.02	2.37	-1.24	0.31
Window	3.02	1.91	-4.33	-4.29

sign (-) shows that heat flux is from indoor air to surface

An interesting way of measuring the average convective heat transfer coefficient has been presented by Jensen (1978). By studying the response of the room air to variable convective power load at relatively high frequences (periods of the magnitude of 1 min) he shows that the temperature variations can be expressed in terms of the convective surface heat transfer coefficient, the room air capacity and the geometry of the room. By identification of such a process he finds that a suitable average α_c for the room to be about 2.0 W/m^2K.

3.2.2 Long wave radiation

The heat induced by long wave radiation at a non transparent surface j in an enclosure consisting of n diffuse surfaces, each characterized by a uniform temperature and emittance can, according to Love (1968), be expressed as

$$Q_j = \sum_{k=1}^{n} A_k R_k F_{kj} - A_j R_j \qquad (3.6)$$

The rate of heat flow leaving a diffuse surface is called the radiosity of the surface and is given the symbol R. F_{kj} is the configuration factor or the view factor and may be defined as the fraction of diffuse energy leaving area A_i that is directly incident on area A_j.

The radiosity can be expressed as the sum of the emitted and reflected radiation per area at the surface.

$$R_j = \varepsilon_j \sigma T_j^4 + \frac{\rho_j}{A_j} \sum_{k=1}^{n} R_k F_{kj} A_k \qquad (3.7)$$

ρ is the reflectance and ε is the emittance of the surface. σ is the Stefan Boltzmann constant $5.67 \cdot 10^{-8}$ W/m^2K^4.

As the view factors in the different directions are given as

$$F_{kj} \cdot A_k = F_{jk} A_j \tag{3.8}$$

the radiosity can be written as

$$R_j = \varepsilon_j \cdot \sigma T_j^4 + \rho_j \sum_{k=1}^{n} R_k F_{jk} \tag{3.9}$$

It can be noted at this point in accordance with the brief definition above that for a plane or a convex surface k

$$F_{kk} = 0 \tag{3.10}$$

The solution of equation 3.9 has to be carried out for the n surfaces simultaneously and it therefore represents a system of n linear algebraic equations for which the explicit solution can be written as

$$\begin{bmatrix} R_1 \\ \vdots \\ R_n \end{bmatrix} = \sigma \begin{bmatrix} (1 - \rho_1 F_{11}) & -\rho_1 F_{12} & \cdots & -\rho_n F_{1n} \\ -\rho_2 F_{21} & (1 - \rho_2 F_{22}) & & \vdots \\ \vdots & & \ddots & \vdots \\ -\rho_n F_{n1} & \cdots & \cdots & (1 - \rho_n F_{nn}) \end{bmatrix}^{-1} \begin{bmatrix} \varepsilon_1 T_1^4 \\ \vdots \\ \varepsilon_n T_n^4 \end{bmatrix} \tag{3.11}$$

Mathematically the configuration factors are expressed by the formula

$$F_{kj} = \frac{1}{\pi A_k} \int_{A_1} \int_{A_2} \frac{\cos\beta_k \cos\beta_j}{r^2} dA_1 dA_2 \tag{3.12}$$

If two points on the surfaces k and j respectively are connected by a line β_j and β_k are defined as the angle between the connecting line and the normal to the surfaces at the surfaces j and k respectively, as shown in figure 3.2 while r is the length of the line segment between those two points.

The solution of (3.12) by direct integration is rather tedious and will in many cases have to be carried out by a numerical procedure. For many

special cases the solutions are to be found in various publications in forms of formulae, tables or diagrams. Eckert and Drake (1959), McAdams (1954), Kreith (1965), Love (1968) and Bruggen (1978).

There are certain relations between the configuration factors which can be utilized to reduce the calculation work needed for a given geometry. The relation stated in equation (3.8), which can be established from the symmetry of the integral in (3.12), means that between two surfaces the configuration factor only has to be calculated in one direction.

From the definition of the configuration factor it is evident that the sum of all fractions is equal to unity so that for a closed space with surfaces numbered from 1 to n

$$\sum_{j=1}^{n} F_{kj} = 1 \qquad (3.13)$$

Furthermore if the surface j is divided in two partial surfaces j' and j'', the configuration factor from the surface k to the surface j is given by

$$F_{kj} = F_{kj'} + F_{kj''} \qquad (3.14)$$

And in a similar way

$$F_{kj'} = F_{kj} - F_{kj''} \qquad (3.15)$$

The practical advantage of equation (3.15) is illustrated in figure 3.3. The explicit solution for F_{kj} and $F_{kj''}$ is documented in the textbooks mentioned above giving $F_{kj'}$ as the difference between those two.

Two important simple cases are a) two parallell plane surfaces at a relatively small distance and b) a plane or convex surface completely surrounded by another surface see figure 3.4. For both cases the configuration factor F_{12} equals unity.

$$F_{12} = 1$$

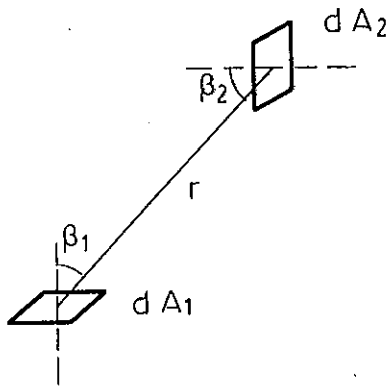

FIG. 3.2. Long wave radiation between two surface elements.

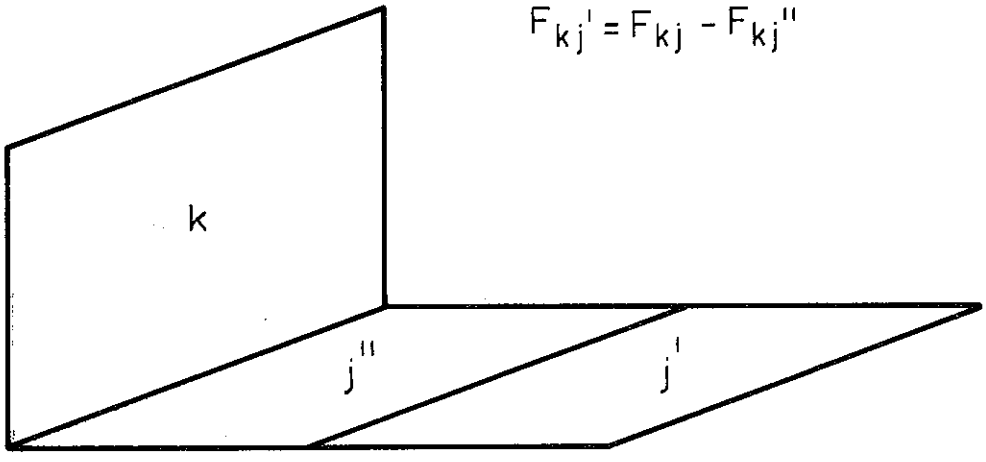

FIG. 3.3. Illustration of the addition rule for configuration factors.

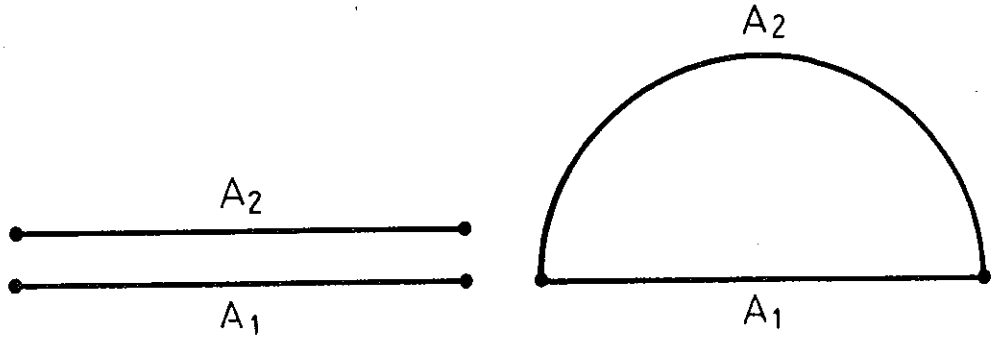

FIG. 3.4. Two simple geometrical configurations for which the radiation can be explicitly solved.

Once the configuration factors are known the radiosities at different surfaces can be calculated from equation (3.11). Where three or more surfaces are involved the inversion of the matrix should be carried out numerically. The explicit solution for two surfaces reads as follows.

$$R_1 = \frac{\sigma\left[(1-\rho_2F_{22})\varepsilon_1T_1^{\,4}+\rho_1F_{12}\varepsilon_2T_2^{\,4}\right]}{(1-\rho_1F_{11})(1-\rho_2F_{22})-\rho_1\rho_2F_{12}\cdot F_{21}} \tag{3.16}$$

$$R_2 = \frac{\sigma\left[\rho_2F_{21}\varepsilon_1T_1^{\,4}+(1-\rho_1F_{11})\varepsilon_2T_2^{\,4}\right]}{(1-\rho_1F_{11})(1-\rho_2F_{22})-\rho_1\rho_2F_{12}F_{21}} \tag{3.17}$$

For long wave radiation the emittance ε and reflectance ρ of a surface are with good approximation related as

$$\rho = 1 - \varepsilon \tag{3.18}$$

From the equations (3.8), (3.16) and (3.18) it can be deduced that the heat generated by long wave radiation at the surface 1 for the configurations in figure 3.4 is given by the formula

$$Q_1 = A_1\ \varepsilon_{12}\cdot\sigma\cdot(T_2^{\,4} - T_1^{\,4}) \tag{3.19}$$

in which

$$\frac{1}{\varepsilon_{12}} = \frac{1}{\varepsilon_1} + \frac{1}{\varepsilon_2} - 1 \tag{3.20}$$

for the parallell surfaces and

$$\frac{1}{\varepsilon_{12}} = \frac{1}{\varepsilon_1} + \frac{A_1}{A_2}\left(\frac{1}{\varepsilon_2} - 1\right) \tag{3.21}$$

for the surrounded surface. If $A_2 >> A_1$

$$\varepsilon_{12} \simeq \varepsilon_1 \tag{3.22}$$

It is useful to define a surface heat transfer coefficient due to long wave radiation at a surface in analogy with the convective heat transfer coefficient. From the case with two different isothermal surfaces, the heat transfer coefficient due to long wave radiation at the surface 1 α_s can be defined in such a way that

$$\alpha_s = \frac{Q_1}{A_1(T_2 - T_1)} \tag{3.23}$$

From equation (3.19)

$$\alpha_s = \varepsilon_{12}\ \sigma\ \frac{(T_2^{\ 4} - T_1^{\ 4})}{(T_2 - T_1)} \tag{3.24}$$

As the temperature difference normally is small compared with the total value α_s can be expressed as

$$\alpha_s \cong 4 \cdot \varepsilon_{12} \cdot \sigma \cdot T_m^{\ 3} \tag{3.25}$$

$$T_m = \frac{T_1 + T_2}{2} \tag{3.26}$$

3.2.3 Combined convection and radiation, practical heat transfer coefficients

As can be seen from 3.2.1 and 3.2.2 a detailed treatment of the surface heat transfer within a room can only be made with excessive computer power. The complexity and non-linearity of the system is best illustrated by the fact that, for a normal room where one of the surfaces has three different isothermal areas, 18 configuration factors have to be calculated by complicated formulae. The calculation of the radiosities demands an inversion of an 8 x 8 matrix and the calculations of the heat balance for the nine defined temperatures of the system have to be carried out by iteration since the heat transfer parameters are non-linearly dependent on the resulting temperatures.

The simplifications of the surface heat transfer process can be divided in two categories, i.e. linearization and reducing the number of transfer paths.

As for the linearization, three functions have to be considered

- o For natural convection
  $\Delta T^{0.25}$
  $\Delta T^{0.33}$
- o For long wave radiation
  T^3

Figure 3.5 shows the deviation from the formulae in table 3.1 if the temperature difference is fixed at 2 K. At very low temperature difference the deviation becomes large but, on the other hand, the heat flow is small so this is of less importance.

The error in the calculated heat flow introduced by fixing the α_c is therefore small considering present knowledge of the niveau of the convective heat transfer coefficient for a surface. The resulting α_c is also relatively insensitive to the chosen temperature difference for all normal cases where one might expect the average temperature difference to be between 1 and 3 K.

Figure 3.6 shows the deviation from equation (3.25) as a function of the mean temperature, T_m, if the radiation exchange is calculated with a fixed mean temperature at 20°C or 293 K. The error introduced is approximately 1% per degree.

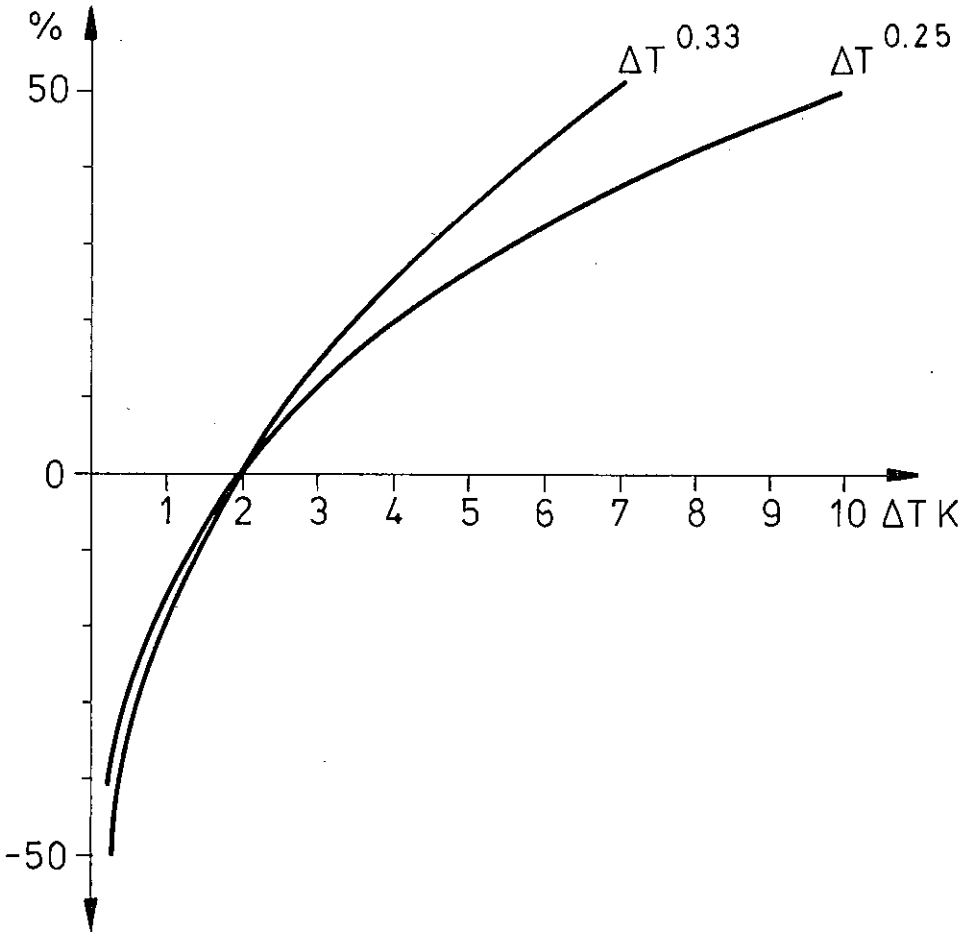

FIG. 3.5. The deviation from the formulae in table 4.2.2 if the temperature difference is fixed at 2 K.

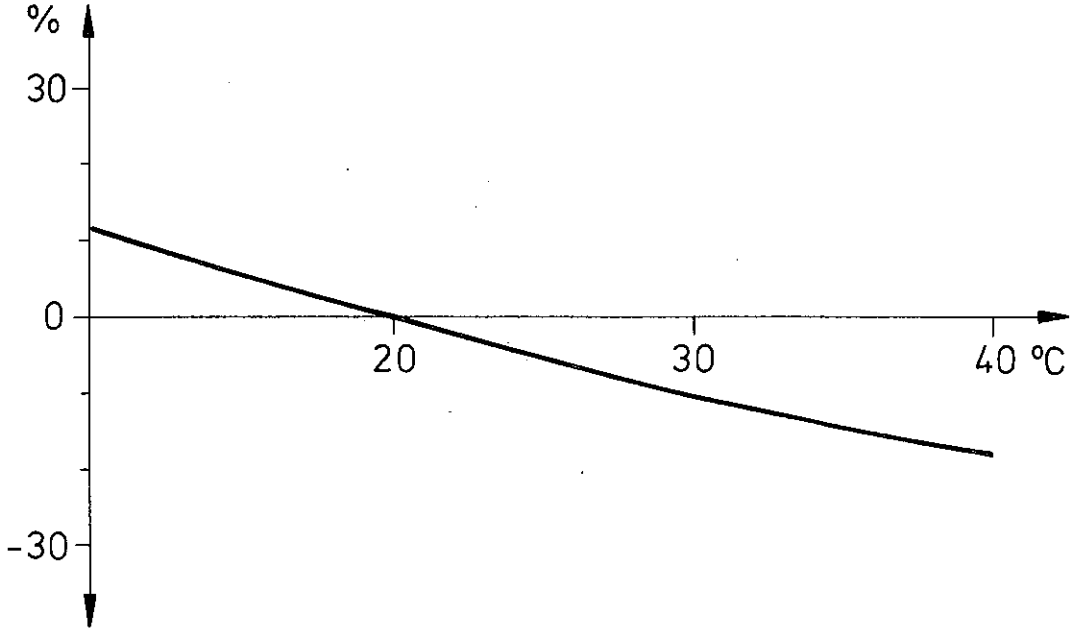

FIG. 3.6. The deviation from equation (3.25) as a function of the mean temperature if the radiation exchanged is calculated using a fixed mean temperature, 20 ^{o}C or 293 K.

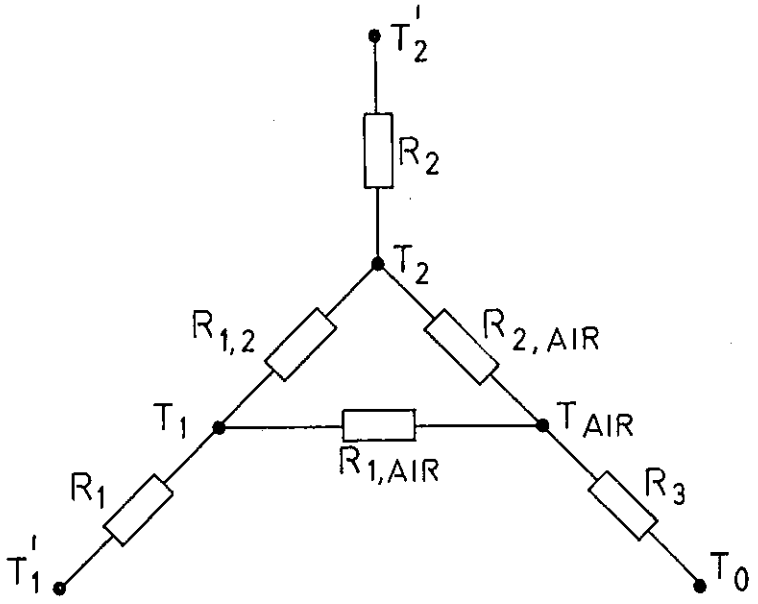

FIG. 3.7. A nodal representation of a room system with linear heat transfer coefficients, two different isothermal surfaces and under steady conditions. c.f. figure 2.3. $T = \vartheta + 273$.

The reduction of the number of heat flow paths can be carried out either by assuming two or more surfaces as isothermal or by combining the heat transfer coefficients for both convection and long wave radiation, to an equivalent heat transfer coefficient between the surface and the room air. To illustrate this, consider a room with a plane surface of area A_1 and at temperature T_1 while the rest of the surfaces have an area A_2 and temperature T_2. The resulting heat transfer due to long wave radiation between the surfaces can be calculated from the equations (3.21), (3.24) and (3.23).

A nodal representation of this room system is given in figure 3.7. Assuming that the heat transfer coefficients within the room are linear, the resistances can be expressed as follows:

$$R_{12} = \frac{1}{A_1 \alpha_s} \qquad (3.27)$$

$$R_{2,AIR} = \frac{1}{A_2 \cdot \alpha_{c2}} \tag{3.28}$$

$$R_{1,AIR} = \frac{1}{A_1 \ \alpha_{c1}} \tag{3.29}$$

A common simplification of the internal heat transfer process is to exclude the long wave radiative heat transfer between the surfaces. Instead the convective heat transfer coefficients at the surfaces are increased to such a degree that the resulting total heat transfer between the surfaces via the room air equals the sum of the convective and radiative heat transfer when those two heat transfer processes are treated separately.

If the emittances for both surfaces are set equal to 0.9 and the mean temperature is 293 K then α_s can be calculated from equation (3.25) and (3.21).

$$\alpha_s = \frac{4\sigma T_m^3}{\frac{1}{\varepsilon_1} + \frac{A_1}{A_2}\left(\frac{1}{\varepsilon_2} - 1\right)} \tag{3.30}$$

The value of α_s depending on the ratio between A_1 and A_2 is shown in figure 3.8.

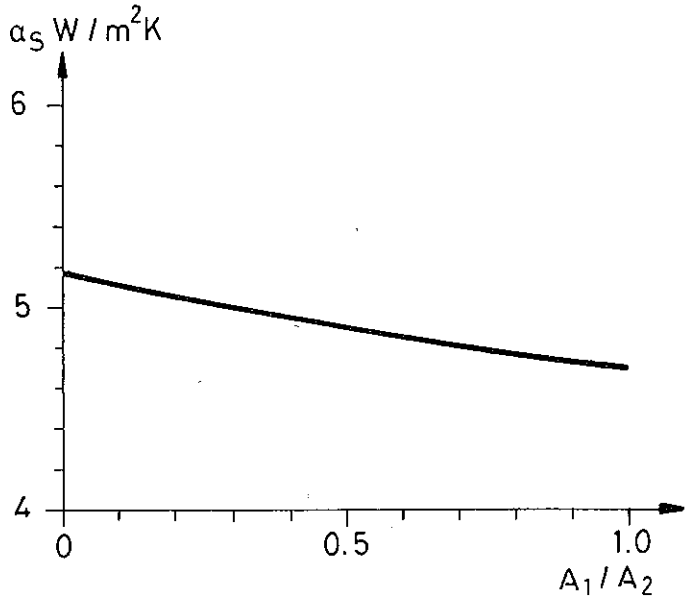

FIG. 3.8. α_s plotted against the ratio A_1/A_2 within a room.

The total thermal resistance between the surfaces is given by the expression

$$R = \frac{R_{1,2}(R_{2,AIR} + R_{1,AIR})}{R_{1,2} + R_{2,AIR} + R_{1,AIR}} \tag{3.31}$$

The correction of the convective α-values is now assumed to take place by multiplying them with a constant ξ. This gives the equation

$$R = \frac{1}{\xi}(R_{1,AIR} + R_{2,AIR}) \tag{3.32}$$

Equality of the above expressions and putting in equations (3.27 - 3.29) gives the solution for one type of surfaces denoted ξ'.

$$\xi' = 1 + \frac{\alpha_s}{\alpha_{c1}} + \frac{A_1}{A_2}\frac{\alpha_s}{\alpha_{c2}} \tag{3.33}$$

If α_{c2} equals α_{c1}, an expression for the fictitious convective surface heat transfer coefficient at the surface 1 is given by

$$\alpha'_{c1} = \xi' \cdot \alpha_{c1} = \alpha_{c1} + \alpha_s(1 + \frac{A_1}{A_2}) \tag{3.34}$$

Typical values as 2.5 W/m^2K for α_{c1} and 1/6 for the ratio A_1/A_2 give

$\alpha'_{c1} = 8.43\ W/m^2K$

Another interesting case is when the surface 2 is a partition between two rooms with identical conditions resulting in the steady state in zero net heat flux at the surface. That is, T_2' equals T_2 in figure 3.7. In the same way as before, α_{c1} can be corrected to account also for the heat flow via the surface 2.

The correction factor ξ'' then becomes

$$\xi'' = 1 + \frac{1}{\frac{\alpha_{c1}}{\alpha_s} + \frac{A_1}{A_2}\,\frac{\alpha_{c1}}{\alpha_{c2}}} \tag{3.35}$$

This gives the corrected surface heat transfer coefficient as

$$\alpha''_{c1} = \alpha_{c1} + \frac{1}{\frac{1}{\alpha_s} + \frac{A_1}{A_2}\cdot\frac{1}{\alpha_{c2}}} \tag{3.36}$$

Using the same typical values as above:

$$\alpha''_{c1} = 2.50 + 3.79 = 6.29\ W/m^2K$$

A particularly interesting consequence of equation (3.34) is that the effect of the differences in convective surface heat transfer coefficients for the two surfaces are evened out by the radiation exchange between the surfaces. This implies that the differences in α_c for warm ceilings given by the references in table 3.1 are of less importance, since a variation in α_c for a single surface from 0.2 to 1.5 W/m^2K in the example above would give an equivalent surface heat transfer coefficient α_c between 4.0 and 5.3 W/m^2K.

The above analysis shows that, even in the steady state, a generally applicable modified convective surface heat transfer coefficient including the radiation exchange is not to be found. The optimally chosen coefficient will depend on the mode of operation of the room system and what physical properties are being studied. It should be noted that if both surfaces are concave e.g. if surface 1 consists of a wall plus the ceiling one has to go back to the equations (3.16) and (3.17) for a correct treatment. The transforms also cause a displacement of the air temperature which means that power fed into the room air represented by the node T_1 in figure 3.7, will be erroniously placed after the transform since the node T_1 is then a fictitious temperature. This is especially significant in the non-steady state as will be illustrated later on in this text.

In cases where the temperature difference between the different surfaces is of less significance than the temperature difference between the surfaces and the room air a useful simplification is to assume that all surfaces have the same temperature. In figure 3.7 this would be realized by putting R_{12} equal to zero. This leads back to the two-point model presented in figure 2.2.

3.3 HEAT TRANSFER BY VENTILATION

In the treatment of surface heat transfer in 3.2 it has been assumed that the air temperature is uniformly distributed within the room. Consequently it must be assumed for the ventilation process that the different air flows entering the room are perfectly mixed with the room air. Therefore the air flow leaving the room has the temperature given to the room air.

This may be formulated in the following expression describing the net ventilation loss from the room

$$Q_v = \frac{\rho c V}{3600} (\vartheta_{AIR} \Sigma n_j - \Sigma n_j \cdot \vartheta_j) \qquad (3.37)$$

n_j is the inflow rate expressed as a ventilation rate, h^{-1}, for air with the temperature ϑ_j, ^oC.

The validity of the above assumption is violated in rooms with a significant thermal gradient. In industrial buildings with high ceilings the air temperature under the ceiling can exceed the temperature in the occupied zone by the order of 6 K. If the outlet is placed right under the roof the temperature of the exhaust air is underestimated by the order of 3 K by using the average air temperature ϑ_{AIR} in equation (3.37).

3.4 SOLAR RADIATION AND ITS CONTRIBUTIONS TO THE HEAT BALANCE

3.4.1 Solar radiation towards a surface

The solar radiation towards a given surface can be achieved from different sources. The most direct way is to calculate the radiation with formulae which have been developed and tested over the years. Such formulae are given by Kreith (1965), Sandberg (1973) and Kimura (1977). Knowing the latitude of locality, orientation of surface, and making assumptions on cloudiness and the quality of the atmosphere, the variation of solar radiation during a chosen period can be calculated.

Calculations can also be based on measured values for the nearest weather station. There are , however, few weather stations that record direct and diffuse solar radiation data and therefore the solar radiation towards different surfaces has to be estimated with the aid of theoretical and empirical formulae. Kimura gives two different procedures for calculating the components of solar radiation based on weather data. One is for breaking down the global radiation into direct and diffuse components and the second one is for calculating the solar radiation with the observed cloudiness as a parameter.

For many locations the solar radiation from a clear sky is given by tables or diagrams that can be directly used in calculations for extreme summer conditions.

3.4.2 Heat balance for outer surfaces

The heat balance of outer opaque surfaces contains different heat flows to and from the surface. This can be expressed by the formula containing the most important factors

$$q_S + q_G + q_E = q_C + q_R + q_0 \qquad (3.38)$$

in which

q_S = solar radiation absorbed by the surface W/m^2

q_G = long wave atmospheric radiation absorbed by the surface, W/m^2

q_E = long wave radiation from the ground absorbed by the surface, W/m^2
q_C = convective heat transfer from the surface to the ambient air, W/m^2
q_R = long wave radiation emitted by the surface, W/m^2
q_0 = heat flow from the surface into the construction, W/m^2

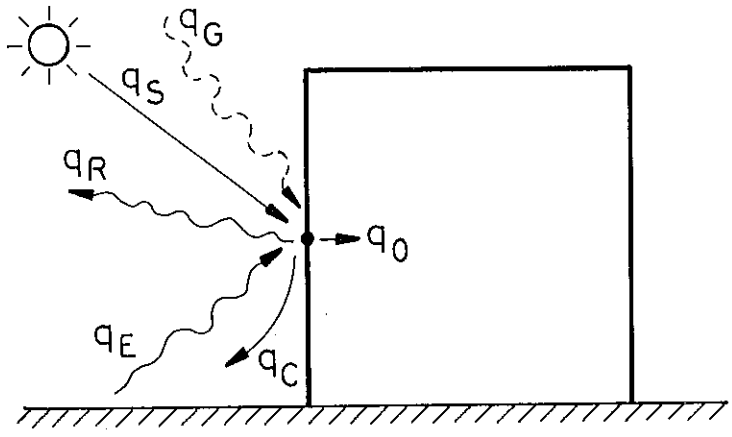

FIG. 3.9. Heat balance at an outer surface of a building.

A detailed treatment of the different components is given by Kimura (1977). A simplified approach is to define an equivalent outside air temperature in such a way that the sum of the different external heat flow components is equal to the heat flow between the equivalent temperature and the surface temperature when the surface heat transfer coefficient, α_{SC}, is defined as the sum of the radiative and the convective heat transfer coefficient at the surface α_S and α_C.

Such an equation was given by Höglund (1973).

$$\vartheta_E^* = \vartheta_0 + \frac{q_S}{\alpha_{SC}} + \frac{\alpha_S}{\alpha_{SC}} (\vartheta_G - \vartheta_0) \tag{3.39}$$

in which

ϑ_E^* = equivalent outside temperature, ^oC
ϑ_0 = outside air temperature, ^oC
ϑ_G = the mean radiating temperature as seen from the surface, ^oC.

3.4.3 Window heat balance

The heat transmission through windows is complicated by the fact that the transmission of solar radiation and the potential heat flow through the window cannot be regarded as parallel, independent processes. The solar radiation absorbed in the different panes causes a rise in temperature and thereby disturbs the heat flow pattern.

If the window can be treated as a series of thermal resistances m_j with nodal points between them each representing the temperature of a single pane as in figure 3.10 the heat balance for the window with n different layers can be expressed by the matrix equation.

$$\begin{bmatrix} \vartheta_1 \\ \vdots \\ \vartheta_n \end{bmatrix} = \begin{bmatrix} (\frac{1}{m_1} + \frac{1}{m_2}) & -\frac{1}{m_2} & \cdots & 0 \\ -\frac{1}{m_2} & (\frac{1}{m_2} + \frac{1}{m_3}) & \ddots & \vdots \\ \vdots & \ddots & \ddots & -\frac{1}{m_n} \\ 0 & \cdots & -\frac{1}{m_n} & (\frac{1}{m_n} + \frac{1}{m_{n+1}}) \end{bmatrix}^{-1} \begin{bmatrix} a_1 \cdot I + \frac{1}{m_1}\vartheta_i \\ a_2 \cdot I \\ \vdots \\ a_{n-1} I \\ a_n I + \frac{1}{m_{n+1}}\vartheta_0 \end{bmatrix} \tag{3.40}$$

In which a_j is the fraction of the incoming solar radiation I W/m^2 absorbed by pane j. This implies that all a_j's are dependent.

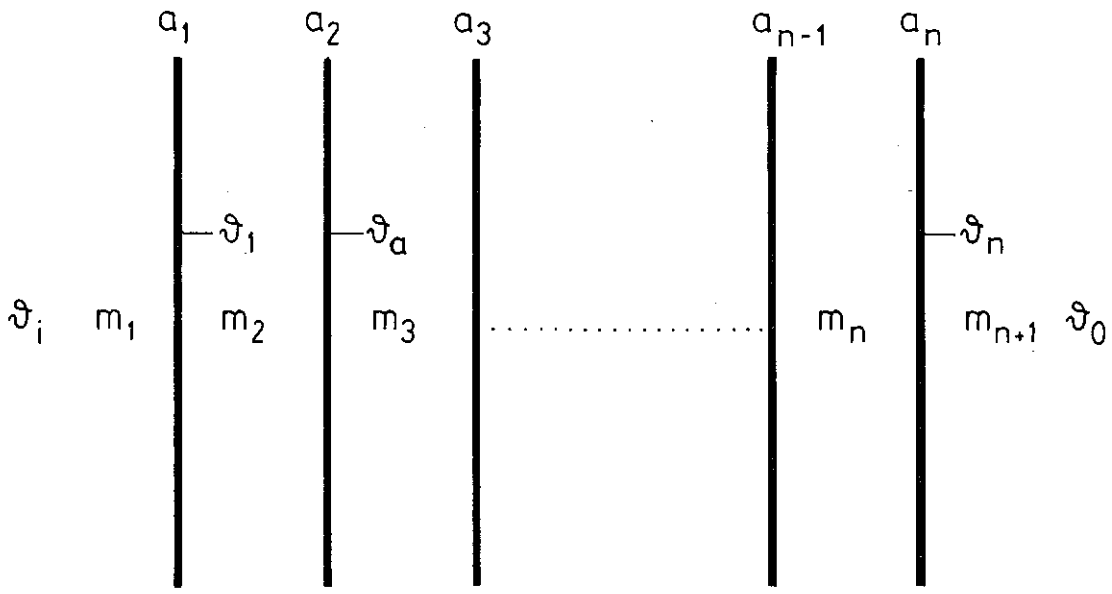

FIG. 3.10. Window with n panes each absorbing a fraction of the incoming solar radiation given by a.

A solution of the system for two panes gives the heat flow from the inner pane to the room as

$$q = \frac{1}{m_1}(\vartheta_1 - \vartheta_i) = \frac{1}{m_1 + m_2 + m_3}\left[m_3(a_1 I + a_2 I) + m_2 a_1 I + (\vartheta_0 - \vartheta_i)\right] \tag{3.41}$$

Or in more conventional terms

$$q = I \cdot k\left[m_3(a_1 + a_2) + m_2 a_2\right] + k(\vartheta_0 + \vartheta_i) \tag{3.42}$$

The practical consequence of the above expression is that the fraction of the incoming radiation that is absorbed in the window panes and fed into the room by convection and long wave radiation is approximately constant, independent of the internal and external temperatures. This

also applies for windows with more than two panes.

The total transmittance F is defined as the fraction of the incident solar radiation that reaches the interior of the room. The fraction F_2 entering the room by convection and long wave radiation is given by the first term in equation (3.42) and the short wave radiation part is expressed as

$$q = F_1 \cdot I \tag{3.43}$$

in which F_1 is the transmittance of the window.

The total transmitted solar radiation is therefore given by the formula

$$q = I\left\{F_1 + k\left[m_0(a_1 + a_2) + m_{12}\, a_2\right]\right\} = I(F_1 + F_2) \tag{3.44}$$

A mathematical procedure to calculate the absorptance of each window pane and the transmittances for a multiglazed window is given in Isfält (1974). The transmittance for several types of windows with different kinds of solar shading are to be found in the literature e.g. ASHRAE Handbook of Fundamentals. Some examples are given in table 3.3.

A complication is that the transmitted radiation is dependent upon the angle of incidence of the solar radiation. Figure 3.11 shows the total transmittance through three different types of windows as a function of the angle of incidence. At angles up to 50^0 the total transmittance is approximately constant while it decreases almost linearly to zero when the angle exceeds 50 - 60^0. Consequently the total transmittance is different for the three components of the incident radiation i.e. direct, diffuse and ground reflected radiation.

Given that the curve-forms for different window types are similar, the transmittances in table 3.3 are a percentage of the transmittance through a normal double-glazed window. Thus, knowing the transmittances through a double-glazed window, the transmittances for any window given in the tables are easily calculated. Tables and diagrams for the daily variations of transmitted radiation through a certain type of window are to be found in various publications. For Sweden see Brown and Isfält (1969).

TABLE 3.3. Shortwave solar gain F_1 and convective solar gain F_2 for varios types of glazing and shading. The values are taken from Bring and Isfält (1979). They are given as a fraction of the total radiation through a double glazed window. Observe that F_1 and F_2 have different interpretation in the original text.

Glazing and type of shading	F_1 %	F_2 %
single glazed	109	3
double glazed	93	7
ext. pane heat absorbing	40	20
ext. pane heat reflecting	8	6
ext. venetian blinds	11	28
mid. venetian blinds	14	51
mid. white weave	17-54	14-8*
mid. grey weave	10-43	30-21*
mid. dark weave	4-33	42-30*
triple glazed	80	11
ext. venetian blinds	6	5
ext. gap venetian blinds	9	21
int. gap venetian blinds	11	37
int. venetian blinds	13	53

* The amount of heat absorbed increases with increased density of the weave.

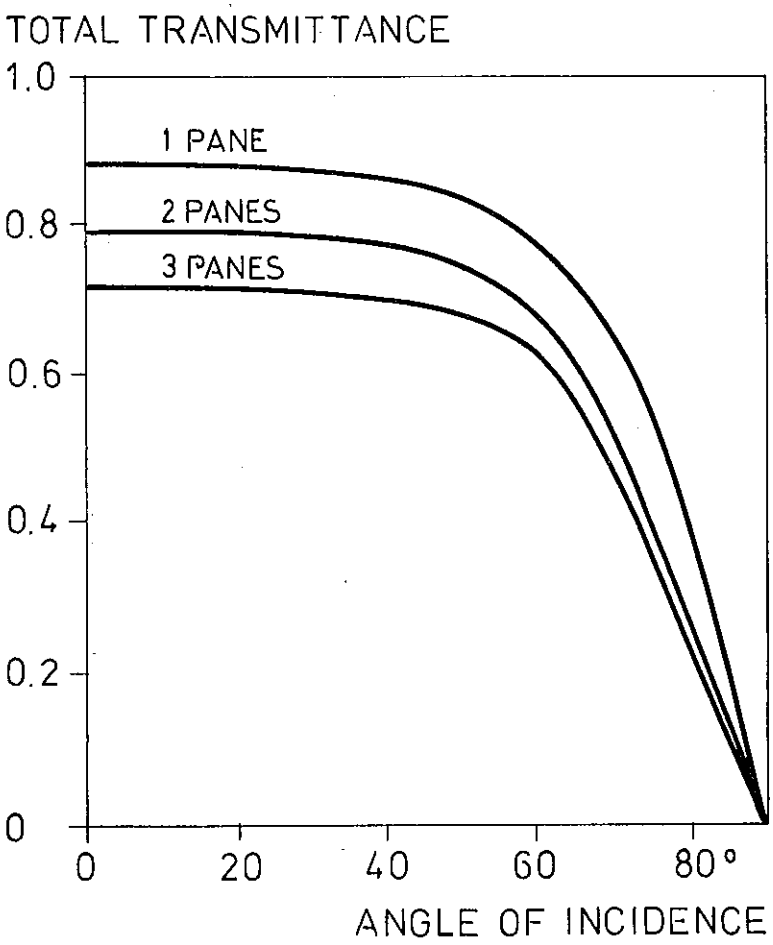

FIG. 3.11. Total transmission as a function of the angle of incidence.

4 NON STEADY HEAT CONDUCTION IN BUILDING COMPONENTS

The exchange of heat at the surfaces of a room is a time dependent process. The heat transfer in the wall is governed by the equation

$$\Delta\vartheta + \frac{\phi}{\lambda} = \frac{1}{a} \cdot \frac{\partial\vartheta}{\partial t} \tag{4.1}$$

in which the thermal diffusivity, m^2/s is given as

$$a = \frac{\lambda}{\rho c} \tag{4.2}$$

The source term, ϕ W/m^3, is set equal to zero in the following applications except at the surfaces of the wall where it represents the net heat gain by absorbed short-wave radiation, convection and long wave radiation.

$$\phi \cdot dV = (q_S + q_C + q_R) \cdot dA \tag{4.3}$$

In this chapter solutions to equation (4.1) for multilayer constructions are used to derive parameters which characterize the building component from the non-steady state point of view and which are suitable for further evaluation and characterization of the non-steady heat transfer processes within the room system.

4.1 THE FREQUENCY DOMAIN SOLUTION

The solutions derived in this section are only valid for harmonic boundary values. This means that all known temperatures and heat flows at the boundaries are written in the form

$$\vartheta = \bar{\vartheta} + \sum_{j=1}^{N} \hat{\vartheta}_j \, e^{i(\omega_j t + \phi_j)} \tag{4.4}$$

$$q = \bar{q} + \sum_{j=1}^{N} \hat{q}_j \, e^{i(\omega_j t + \phi_j)} \tag{4.5}$$

$\bar{\vartheta}$ and $\bar{q}_j$ are mean values, $\hat{\vartheta}_j$ and $\hat{q}_j$ are the amplitudes of the differ-

ent frequency components and ϕ_j is the phase difference in relation to the fundamental oscillation, $e^{j\omega t}$.

Since we are dealing with a linear system, i.e. the thermal diffusivity is assumed to be independent of time and temperature, each frequency component of the input values can be treated separately giving resulting heat flows and temperatures within the system as oscillations with the same frequency but different amplitudes and phase differences. The final result for each quantity is then achieved by summation of the partial results over the frequencies involved.

The following analysis is therefore restricted to one frequency component given by

$$\tilde{\vartheta} = \hat{\vartheta} e^{i(\omega t + \phi)} \tag{4.6}$$

In the following calculation each harmonic quantity is expressed as a product of a complex quantity representing amplification, phase difference and the fundamental oscillation

$$\tilde{\vartheta} = \hat{\vartheta}\, e^{i\phi} \cdot e^{i\omega t} \tag{4.7}$$

In a cartesian coordinate system this corresponds to a vector of length $\hat{\vartheta}$ rotating counter-clockwise with angular velocity ω around the origo and the angle ϕ ahead of the chosen fundamental oscillation as given in figure 4.1. Accordingly, the harmonic oscillation can also be expressed as a product of a complex number and the fundamental oscillation.

$$\tilde{\vartheta} = (u + iv)\, e^{i\omega t} \tag{4.8}$$

in which

$$u = \hat{\vartheta} \cos \phi \tag{4.9}$$

$$v = \hat{\vartheta} \sin \phi \tag{4.10}$$

In the same way, if u and v are known from calculations, the amplitude and phase difference for the oscillation can be calculated from

$$\hat{\vartheta} = u^2 + v^2 \tag{4.11}$$

$$\phi = \arctan\left(\frac{v}{u}\right) \tag{4.12}$$

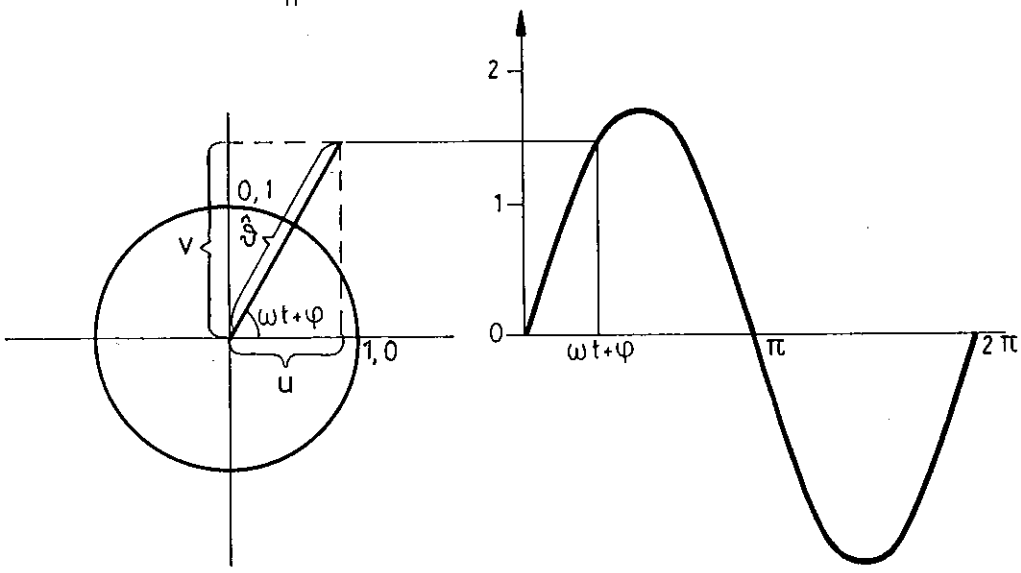

FIG. 4.1. Harmonic oscillation expressed in the complex plane.

An important feature of a harmonic quantity is that the time derivative is calculated by simply multiplying the quantity with the factor $i\omega$

$$\frac{\partial \tilde{\vartheta}}{\partial t} = i\omega\,(u + iv)\,e^{i\omega t} \tag{4.13}$$

This means that the differential equation (4.1) with no heat sources becomes

$$a\,\Delta\tilde{\vartheta} = i\,\omega\tilde{\vartheta} \tag{4.14}$$

Equation (4.14) can be solved analytically for one-dimensional heat flow in a multilayer wall. A numerical procedure for the solution of two and three dimensions is presented in next section.

Since the factor $e^{i\omega t}$ is common to all harmonic quantities and the equation or system of equations that are dealt with are linear, a useful convention is to exclude this factor from the calculations and simply write the harmonic quantities in the form

$$\tilde{\vartheta} = (u + iv) \tag{4.15}$$

For a finite layer with thickness l, thermal conductivity λ, specific heat c and density ρ Carslaw and Jaeger (1959) give the relation between temperatures and heat flow at the boundaries for a certain angular velocity ω by the matrix equation.

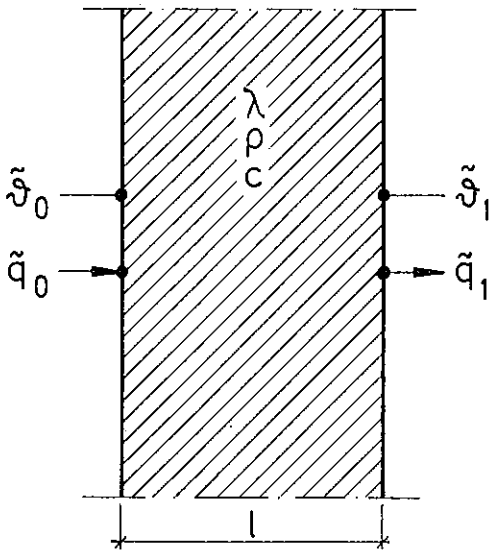

FIG. 4.2. Finite layer with harmonic boundary values.

$$\begin{bmatrix} \tilde{\vartheta}_1 \\ \tilde{q}_1 \end{bmatrix} = \begin{bmatrix} A & B \\ C & D \end{bmatrix} \begin{bmatrix} \tilde{\vartheta}_0 \\ \tilde{q}_0 \end{bmatrix} \tag{4.16}$$

A, B, C and D are complex numbers.

$$A = \cosh \; kl \; (1 + i) \tag{4.17}$$

$$B = - \frac{\sinh \; kl \; (1 + i)}{\lambda \, k \; (1 + i)} \tag{4.18}$$

$$C = - \lambda k (1 + i) \sinh \; kl \; (1 + i) \tag{4.19}$$

$$D = \cosh \; kl \; (1 + i) \tag{4.20}$$

$$k = \sqrt{\omega / 2a} \tag{4.21}$$

$$a = \frac{\lambda}{\rho c} \tag{4.22}$$

Equation (4.16) can be solved for two unknown quantities, for example if the temperature oscillations on both sides are known the heat flows on both sides can be calculated.

4.1.2 Solution for a multi-layer construction

If a construction consists of more than one layer the matrix for each layer can be calculated separately and then the matrix for the construction can be calculated by successive multiplication of the matrices for the different layers

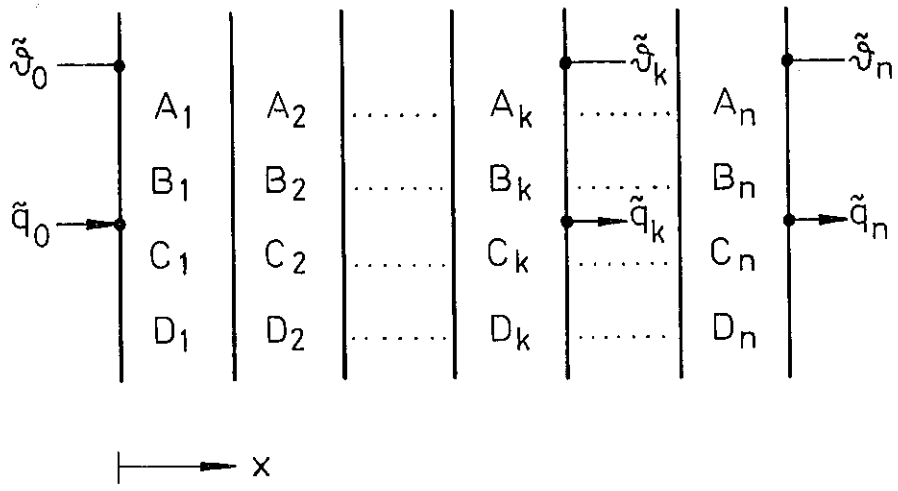

FIG. 4.3. Multi-layer construction with homogeneous sublayers.

$$\begin{bmatrix} \tilde{\vartheta}_n \\ \tilde{q}_n \end{bmatrix} = \begin{bmatrix} A_n & B_n \\ C_n & D_n \end{bmatrix} \begin{bmatrix} A_{n-1} & B_{n-1} \\ C_{n-1} & D_{n-1} \end{bmatrix} \cdots\cdots \begin{bmatrix} A_1 & B_1 \\ C_1 & D_1 \end{bmatrix} \begin{bmatrix} \tilde{\vartheta}_0 \\ \tilde{q}_0 \end{bmatrix} \tag{4.23}$$

or

$$\begin{bmatrix} \tilde{\vartheta}_n \\ \tilde{q}_n \end{bmatrix} = \begin{bmatrix} A & B \\ C & D \end{bmatrix} \begin{bmatrix} \tilde{\vartheta}_0 \\ \tilde{q}_0 \end{bmatrix} \tag{4.24}$$

if the matrix

$$\begin{bmatrix} A & B \\ C & D \end{bmatrix} = \begin{bmatrix} A_n & B_n \\ C_n & D_n \end{bmatrix} \begin{bmatrix} A_{n-1} & B_{n-1} \\ C_{n-1} & D_{n-1} \end{bmatrix} \cdots \begin{bmatrix} A_1 & B_1 \\ C_1 & D_1 \end{bmatrix} \tag{4.25}$$

For a layer k which can be considered as purely resistive with no thermal capacity such as air gaps, contact resistances and surface resistances the matrix can be written simply as

$$\begin{bmatrix} A_k & B_k \\ C_k & D_k \end{bmatrix} = \begin{bmatrix} 1 & -m_k \\ 0 & 1 \end{bmatrix} \tag{4.26}$$

In the same manner if the layer can be considered purely as capacitive the matrix is written

$$\begin{bmatrix} A_k & B_k \\ C_k & D_k \end{bmatrix} = \begin{bmatrix} 1 & 0 \\ -i\omega l \rho c & 1 \end{bmatrix} \tag{4.27}$$

Looking back at the matrix equation for multilayer wall, equation (4.24) the question arises which quantites are going to be calculated. Outside temperatures are usually known, the inside temperatures are either known or variables in an energy balance while the heat flows at the surfaces result from calculations. The matrix equation (4.24) is therefore rewritten to give a new matrix equation which gives the heat flows in terms of the temperatures on both sides.

$$\begin{bmatrix} \tilde{q}_n \\ \tilde{q}_0 \end{bmatrix} = \begin{bmatrix} E & F \\ G & H \end{bmatrix} \begin{bmatrix} \tilde{\vartheta}_n \\ \tilde{\vartheta}_0 \end{bmatrix} \tag{4.28}$$

$$E = D/B \tag{4.29}$$

$$F = C - DA/B \tag{4.30}$$

$$G = 1/B \tag{4.31}$$

$$H = - A/B \tag{4.32}$$

4.1.3 Solution of frequency response for two-dimensional heat flow problems

In most applications the heat flow through the building components can be considered as one-dimensional with regard to the non-steady part of the heat exchange between the room and the building component. In some cases, however, an extended knowledge of the multi-dimensional nature of the heat-flow processes is essential to provide a skilful choice of a simplified model.

Examples of such cases are heat flow into the ground under a building and the heat exchange between a room and a wall or a ceiling that is intermittently covered with layers of light insulating acoustical absorbents.

Many computer programs are available which solve two- or three-dimensional non-steady heat flow problems in the time domain. They solve the change of state for finite time steps for given initial and boundary values. Even if the curve form of the boundary values can be chosen freely within the limits given by the necessary discretization of input data, this is of minor advantage since the boundary values are a result of the heat balance for the room and therefore not known a priori. Such studies are therefore often carried out with sinusoidal temperature variations at the boundaries. A more straight forward procedure can be achieved by establishing a numerical solution of equation (4.14) in the frequency domain. An approach proposed by Claesson (1980).

Consider equation (4.14) in two dimensions

$$a\left(\frac{\partial^2 \vartheta}{\partial x^2} + \frac{\partial^2 \vartheta}{\partial y^2}\right) = i\cdot\omega\vartheta \qquad (4.33)$$

Making use of the convention introduced earlier, expressing ϑ with a complex number u + iv, the equation can be expressed as

$$\frac{\partial^2 u}{\partial x^2} + i\,\frac{\partial^2 v}{\partial x^2} + \frac{\partial^2 u}{\partial y^2} + i\,\frac{\partial^2 v}{\partial y^2} = i\,\frac{\omega}{a}\,u - \frac{\omega}{a}\,v \qquad (4.34)$$

This equation can be separated into two different equations, one for the real and one for the imaginary part.

$$\frac{\partial^2 u}{\partial x^2} + \frac{\partial^2 u}{\partial y^2} = - \frac{\omega}{a} v \tag{4.35}$$

$$\frac{\partial^2 v}{\partial x^2} + \frac{\partial^2 v}{\partial y^2} = \frac{\omega}{a} u \tag{4.36}$$

The equations (4.35) and (4.36) are identical to the equation for two-dimensional steady state heat flow with heat sources. The equations are coupled as the source term of the equation for the real part depends on the imaginary part and vice versa.

Applying the Laplace operator once more on both sides of equation (4.35)

$$\Delta\Delta u = - \frac{\omega}{a} \Delta v \tag{4.37}$$

and since equation (4.36) gives Δv expressed as a function of u, it can be substituted to form a differential equation with u as the only variable.

$$\Delta\Delta u + \frac{\omega^2}{a^2} u = 0 \tag{4.38}$$

and in the same way for the imaginary part

$$\Delta\Delta v + \frac{\omega^2}{a^2} v = 0 \tag{4.39}$$

These equations are analogous to a well known equation from building mechanics, giving the displacement of a plate W with bending stiffnes D resting on an elastic foundation with modulus of foundation C.

$$\Delta\Delta W + \frac{C}{D} W = 0 \tag{4.40}$$

The solution to this equation is given in many finite element packages for structural analysis. The finite elements programs are often equipped with preprocessors for input of data and generation of nodes and elements so that the only preparation needed for their use is to identify the material data and find suitable formulations for the boundary conditions.

At the boundaries between two different material fields the temperature problem implies that the heat flow is continuous at the border since no heat is removed or generated there. If we have two different surfaces s_1 and s_2 as in figure 4.4 the heat balance at the boundary gives

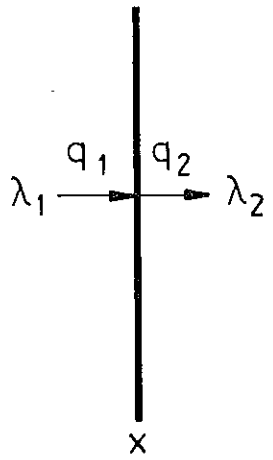

FIG. 4.4. Boundary between two surfaces with different thermal conductivities.

$$q_1 = q_2 \tag{4.41}$$

$$- \lambda_1 \left(\frac{\partial u}{\partial x}\right)_1 = - \lambda_2 \left(\frac{\partial u}{\partial x}\right)_2 \tag{4.42}$$

$$- \lambda_1 \left(\frac{\partial v}{\partial x}\right)_1 = - \lambda_2 \left(\frac{\partial v}{\partial x}\right)_2 \tag{4.43}$$

For the normal formulation of the plate problem, however, a discontinuity in the first derivative cannot exist for elastic deformations and the below equation is therefore always valid at the boundaries.

$$\left(\frac{\partial W}{\partial x}\right)_1 = \left(\frac{\partial W}{\partial x}\right)_2 \tag{4.44}$$

The consequence of this discrepancy is that the finite elements programs for plates cannot be applied for heat flow problems with more than one material field without modifying the mathematical formulation of the elements. Problems also arise in giving the boundary conditions as heat transfer between the surface and an ambient temperature, since the thermal resistance at the surface would normally be represented by a material layer with suitable properties.

A solution for two dimensional frequency response based on finite element techniques is mentioned by Augenbroe (1978) and has been successfully used by Vierveyzer (1978) for the calculation of time dependent energy loss through crawl space basements.

There is another way to formulate the heat flow problem in terms of finite differences: assume the construction to be divided into rectangular cells as in figure 4.5. Each cell is characterized by its dimensions dx and dy, material data λ, ρ and c and the temperature of the geometrical centrum $\tilde{\vartheta}$. If the dimensions of the cells are sufficiently small so that the temperature can be assumed to vary linearly between the cells, the heat transfer between two adjacent cells a and b can be expressed as

$$Q_{ab} = \frac{2\,dy}{\frac{dx_a}{\lambda_a} + \frac{dx_b}{\lambda_b}} (\tilde{\vartheta}_a - \tilde{\vartheta}_b) \tag{4.45}$$

if the heat flow between the cells is going in the x-direction. Similar expression is valid for the y-direction. From equation (4.45) a conductance s_{ab} can be defined giving the heat transfer rate per degree between the cells a and b.

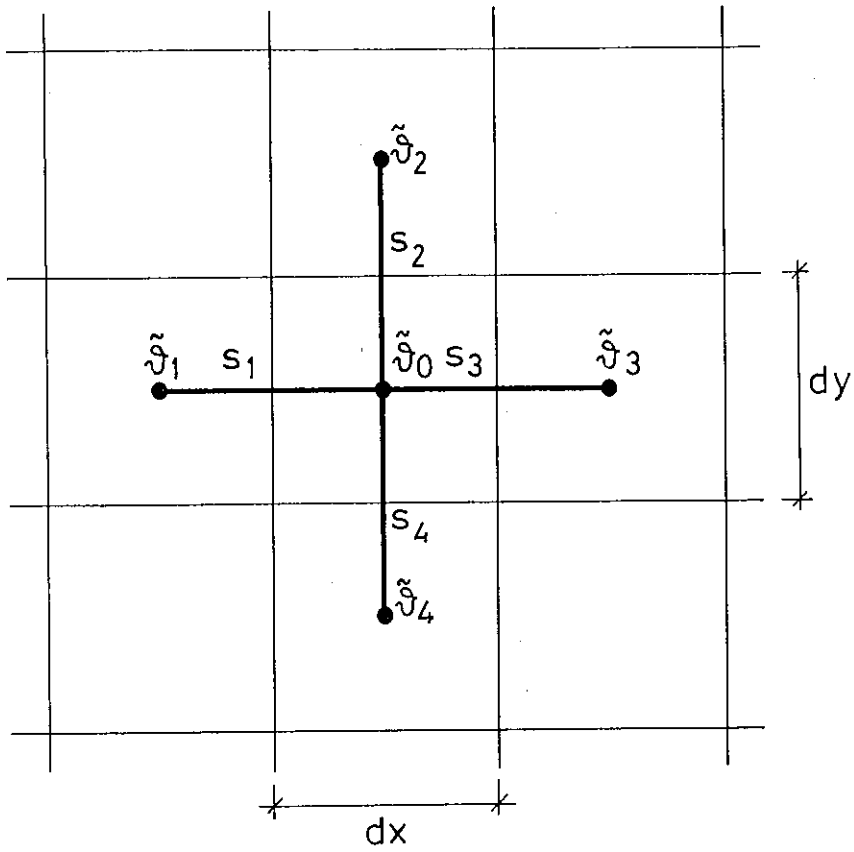

FIG. 4.5. Discrete representation of the two-dimensional non-steady heat flow problem.

$$s_{ab} = \frac{Q_{ab}}{\vartheta_a - \vartheta_b} = \frac{2\ dy}{\frac{dx_a}{\lambda_a} + \frac{dx_b}{\lambda_b}} \tag{4.46}$$

A heat balance for the cell in figure 4.5 gives

$$s_{10}(\vartheta_1 - \vartheta_0) + s_{20}(\vartheta_2 - \vartheta_0) + s_{30}(\vartheta_3 - \vartheta_0) + s_{40}(\vartheta_4 - \vartheta_0) =$$
$$= dydx\ \rho c \frac{\partial \vartheta_0}{\partial t} \tag{4.47}$$

Using equation (4.13) for the time derivative of ϑ, writing the temperature as

$$\tilde{\vartheta}_j = u_j + i\ v_j \tag{4.48}$$

and substituting into equation (4.47) gives two equations, one for the real and one for the imaginary part. The resulting equation system for the cell numbered 0 becomes in matrix form

$$\begin{bmatrix} \sum_1^4 s_{j0} & -\,dxdy\omega\rho c \\ -\,dxdy\omega\rho c & \sum_1^4 s_{j0} \end{bmatrix} \begin{bmatrix} u_0 \\ v_0 \end{bmatrix} = \begin{bmatrix} \sum_1^4 s_{j0}\, u_j \\ \sum_1^4 s_{j0}\, v_j \end{bmatrix} \qquad (4.49)$$

The 2 x 2 matrix on the left side can be inverted to give explicit expressions for u_0 and v_0.

This solution is very similar to the solution for steady state heat flow with heat sources. Two different temperature fields have to be solved simultaneously since the real part of the solution depends on the imaginary part of the adjacent solution and vice versa. The additional data needed are the imaginary temperatures at the boundaries, density and specific heat for each cell, and the angular velocity.

The calculation procedure sketched above has been implemented in a computer program developed by Andersson (1980) in which the two-dimensional temperature field is solved with relaxation. The implementation work was not very time-consuming and the solution converges within computation time which is of the same order of magnitude as for the steady state solution. Similarly to the steady state problem, the elements can have different material data and the surface heat transfer can be introduced by a fictitious material layer with thickness and thermal conductivity adjusted to give an equivalent thermal resistance.

The above analysis is given for two-dimensional heat flow problems but it can be extended to solve three-dimensional heat flow problems.

An advantage of the relaxation method compared to directly inverting the transport matrix of the system with some routine available, is that if the heat transfer data are slightly modified between two runs the new solution converges very fast if the resulting temperature field of the first run is used as an initial field for the second run. This is

especially useful when studying the frequency response for a construction in a large frequency interval. By altering stepwise the angular velocity ω from zero, giving the steady state solution, towards higher frequencies, the response for each new frequency demands minimal computation time.

As discussed in connection with the equations (4.4) and (4.5), any problem for which the boundary conditions can be expressed as a sum of a finite number of frequency components has a solution that is given with the same number of frequencies. This means that the response to different curve-forms can be estimated by the application of Fourier analysis.

4.2 SOLUTION BY LAPLACE TRANSFORM AND RELATED PROCEDURES

The Laplace transform of a function f(t) is given by the integral equation

$$L\{f(t)\} = \int_0^\infty f(t)e^{-st}dt = g(s) \tag{4.50}$$

An important property is that the Laplace of a derivative of a function is given simply by multiplying the transform by a factor s

$$L\left\{\frac{\partial f(t)}{\partial t}\right\} = sg(s) - f(0) \tag{4.51}$$

Applying the transform on the equation (4.1) for non-steady heat conduction but excluding the source term ϕ/λ and writing θ for the Laplace transform of ϑ this gives in one dimension

$$a\,\frac{\partial^2\theta(x,s)}{\partial x^2} = s\,\theta(x,s) \tag{4.52}$$

if $\vartheta(x,0)$ is put equal to 0.

The solution to this equation for one homogeneous layer of thickness l is similar to the solution given for harmonic temperature variations and is given by Carslaw and Jaeger (1959) in matrix form as

$$\begin{bmatrix} L\{\vartheta_1\} \\ L\{q_1\} \end{bmatrix} = \begin{bmatrix} A(s) & B(s) \\ C(s) & D(s) \end{bmatrix} \begin{bmatrix} L\{\vartheta_0\} \\ L\{q_0\} \end{bmatrix} \tag{4.53}$$

in which

$$A(s) = \cosh l \sqrt{s/a} \tag{4.54}$$

$$B(s) = - \frac{\sinh l \sqrt{s/a}}{\lambda \sqrt{s/a}} \tag{4.55}$$

$$C(s) = - \lambda \sqrt{s/a} \sinh l \sqrt{s/a} \tag{4.56}$$

$$D(s) = \cosh l \sqrt{s/a} \tag{4.57}$$

The directions of the heat flows are the same as given in figure 4.2.

The main difference between the matrix relating the harmonic quantities in equation (4.16) and the matrix in equation (4.53) is that the former consists of numerical values while the latter consists of algebraic expressions. A successive multiplication of the matrices for different layers of a multilayer wall therefore produces a matrix with increasing complexity of the elements. The inverse transform of the resulting matrix is therefore a complicated and tedious process and a further discussion of the technique is beyond the scope of this text.

The response factor method as presented by Mitalas and Stephenson (1967) is a procedure making systematic use of the Laplace transform for a unit triangular pulse. The solutions for different inputs in a linear system can be summarized to give the solution for the sum of the inputs. The input values are given as a super-position of triangular pulses with constant base but of different height as shown in figure 4.5 and the output values are given as a sum of their responses. This is sometimes referred to as convolution. The main advantage of this procedure is that the re-

sponse funtions relating heat flows and temperatures on both sides of a given construction have to be calculated only once within each run and they can also be stored for use in later runs. The amount of data necessary to describe the pulse responses is of the order of magnitude 30 - 50 real values.

Aittomäki (1973) proposed a procedure for calculating pulse responses with Fourier analysis. Muncey (1979) gives a detailed description of the procedure together with a computer program. He claims that only 18 frequency components are necessary to get an adequate description of the pulse response.

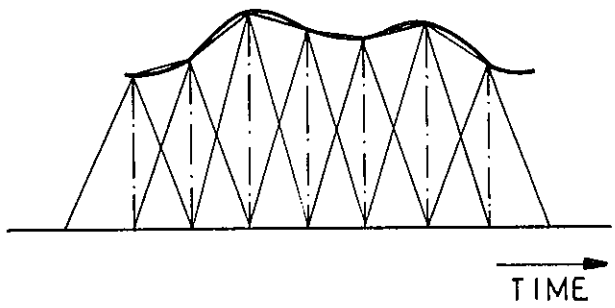

FIG. 4.6. Superposition of triangular pulses.

4.3 FINITE-DIFFERENCE METHODS - RC MODELS

In section 4.1.3 the technique of finite elements has already been introduced to give the solution for steady periodic two-dimensional heat-flow problems. The construction is divided into elements of finite dimensions and the heat balance for each element is calculated assuming that the total thermal capacity of the element is condensed into one point and the heat transfer between those points of adjacent elements is linearly dependent on the temperatures of the points. The construction is, in this way, transformed into a network of resistances and capacitances.

For a multilayer construction with homogeneous layers and one-dimensional flow the network becomes simply a series of resistances and capacitancies. Each layer is divided into one or more sublayers which are represented by an equivalent RC network according to figure 4.7 in which the capacitance C is given by

$$C = \Delta x \cdot \rho \cdot c \qquad (4.58)$$

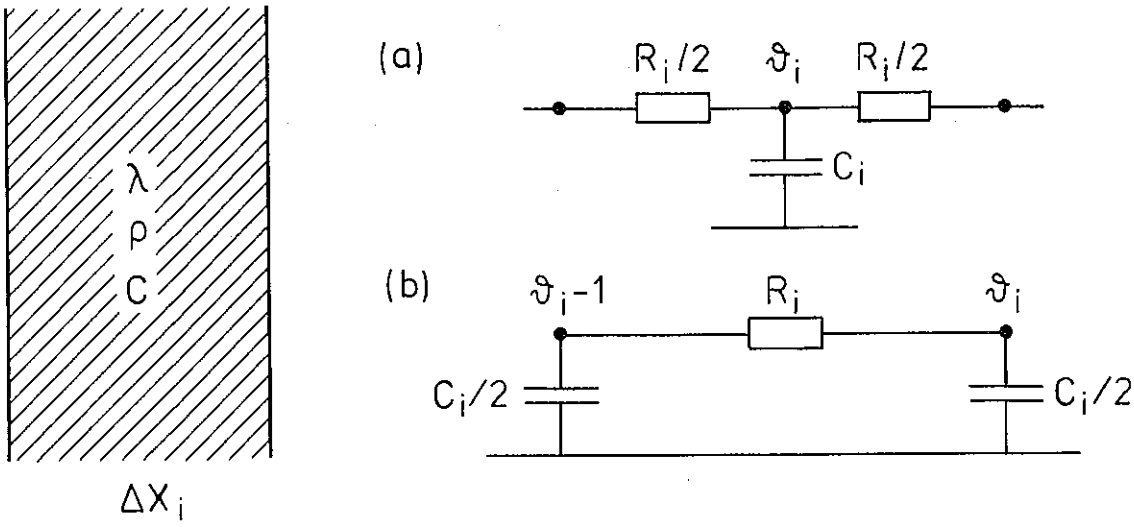

FIG. 4.7. A material layer of thickness Δx transformed into a network of capacitances and resistances.

and the resistance R is given by

$$R = \Delta x / \lambda \tag{4.59}$$

assuming that both those quantities are related to 1 m^2 area.

The two transforms, a and b, of figure 4.7 are both valid since the total thermal resistance and capacitance of the layer are represented in both cases. We shall, however, show that they give different results at high frequencies.

The thermal response of the resulting network for the whole construction can of course be solved both in the frequency domain and by the Laplace transform. The discretization is, however, usually carried out to make way for numerical calculations using finite time steps.

There exists a great number of procedures for calculation of the change of state of the resulting network during one time step. An explicit method known as the forward difference method is based on the assumption that the heat flows generated by the temperatures in the network remain constant during the time step. A heat balance for the nodal point i of figure 4.8 therefore gives the change of temperature during the time step as

$$\vartheta_i^{t+1} = \frac{\Delta t}{C_i}\left[Q_1 + \frac{1}{R_i}\vartheta_{i-1}^t + \frac{1}{R_{i+1}}\vartheta_{i+1}^t + \left(\frac{C_i}{\Delta t} - \frac{1}{R_i} - \frac{1}{R_{i+1}}\right)\vartheta_i^t\right] \tag{4.60}$$

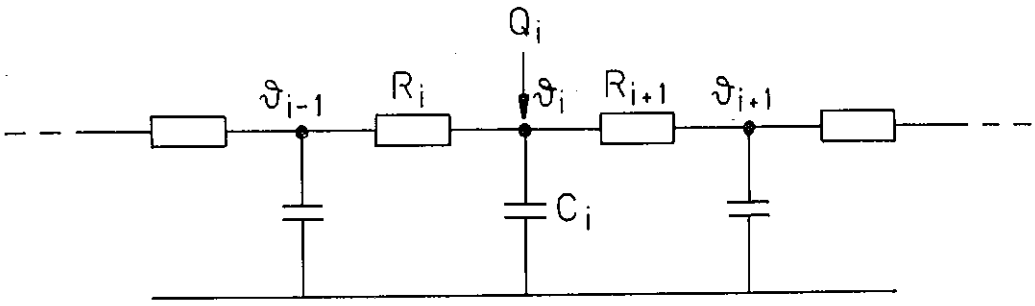

FIG. 4.8. RC network for one-dimensional heat flow.

ϑ_i^{t+1} is the temperature at point i after one time step, and Q_i is the heat flow generated at point i during the time step.

It is easily shown by studying the growth of a small increment that a necessary condition for stability is that the length of the chosen time step does not exceed the maximal time step given in equation (4.61).

$$\Delta t_{max} = \frac{C_i}{\frac{1}{R_{i+1}} + \frac{1}{R_i}} \tag{4.61}$$

It is of interest that the maximal time step increases with the thickness of the chosen sublayers. The calculation work decreases since the number of nodal points is reduced. Those advantages gained are obviously in conflict with the discretization error.

The limited time step for the calculation according to equation (4.61) occurs due to the inadequate description of the heat flow during the time step. In order to describe the heat flow better the temperatures are said to vary linearly during the time step.

$$\vartheta_i(t) = \vartheta_i + b_i \cdot t \qquad 0 < t < \Delta t \tag{4.62}$$

The total heat flow during one time step between the points i-1 and i of figure 4.8 is given by the expression

$$Q_{i-1 \to i} = \frac{1}{R_i} (\vartheta_{i-1} - \vartheta_i) \cdot \Delta t + \frac{1}{R_i} \int_0^{\Delta t} (b_{i-1} - b_i) \cdot t \, dt =$$

$$= \frac{1}{R_i} (\vartheta_{i-1} - \vartheta_i) \cdot \Delta t + \frac{\Delta t^2}{2 R_i} (b_{i-1} - b_i) \qquad (4.63)$$

The constant b_i which changes for each time step is then defined by the equation

$$b_{i-1} \frac{1}{2 R_i} - b_i \left(\frac{1}{2 R_i} + \frac{1}{2 R_{i+1}} + \frac{C_i}{\Delta t} \right) + b_{i+1} \frac{1}{2 R_i} =$$

$$= \frac{1}{\Delta t} \left[\vartheta_i \left(\frac{1}{R_i} + \frac{1}{R_{i+1}} \right) - \vartheta_{i-1} \frac{1}{R_i} - \vartheta_{i+1} \frac{1}{R_{i+1}} - Q_i \right] \qquad (4.64)$$

For each time step the b's are only known at the boundary, and the equations for all unknown temperatures have to be solved simultaneously. The resulting temperatures after one time step are calculated from equation (4.65).

$$\vartheta_i^{t+1} = \vartheta_i^t + b_i \cdot \Delta t \qquad (4.65)$$

The method is an implicit one and in principle the same as the method often referred to as the Crank-Nicholson method. Crank (1975) claims that the procedure remains stable for an arbitrary choice of Δt while other authors, such as Sandberg (1973), seem to have some doubts on this, based on their practical calculation work. Crank gives an example where the implicit methods give the same stability and accuracy as the explicit method even if the time step is increased by a factor 10.

The optimum choice between the two methods above depends mainly on the smallest time step that can be applied to give a satisfactory representation of input data. For both methods, however, it is essential that the number of nodes is kept as low as possible. The problem is then to transform the multilayer construction into a network of as few nodes as possible and still meet some predefined specifications on applicability and accuracy.

5 SIMPLIFIED MODELS FOR SURFACE HEAT EXCHANGE - CONSTRUCTION CHARACTERISTICS

Referring to the methods given in Chapter 4 the non-steady heat transfer within a building component can be accurately calculated in almost every application concerning building climate. The complexity of the methods, however, requires fresh calculations for each set of boundary conditions.

In this chapter possible ways of describing the important characteristics of constructions with simple models and parameters are discussed.

5.1 MODEL SPECIFICATIONS

In order to derive simplified models it is necessary to define limitations both in generality and applicability. This means that one has to decide which quantities and types of boundary conditions are of greatest interest. For the parameters derived one also has to bear in mind that for practical purposes they must have a physical interpretation and an algebraic form that is understood by many different users.

In this section different model and parameter specifications are proposed. In order to compare different simplified models the Bode diagram, well known from the theory of automatic control, is introduced.

5.1.1 Quantites of interest for calculating the room climate

Regard the wall construction in figure 5.1.

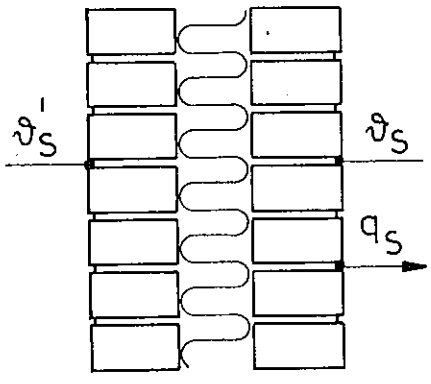

FIG. 5.1. A wall facing the room.

ϑ_s is the temperature of the wall surface facing the room, q_s is the net heat flow rate from the surface and ϑ_s' is the temperature of the external surface.

The heat flow rate q_s is a result of three different processes: The convective heat transfer between the surface and the room air, the long wave radiation between the surface and surrounding surfaces and the short wave radiation absorbed at the surface. A heat balance at the surface implies that the heat flow rate from the interior of the construction to the surface has to equal the net heat flow rate q_s. From Chapter 4 we know that this quantity can be expressed in terms of the surface temperatures, ϑ_s and ϑ_s'.

$$q_s = f(\vartheta_s, \vartheta_s') \tag{5.1}$$

The temperature distribution within the wall and the heat flow at the external surface are of no particular interest. For partitions the boundary conditions can in some cases be considered as symmetric. For insulated exterior constructions the heat flow variations due to changes in the external temperature are dominated by the heat flow generated by the internal loads. Examples of this will be shown below.

The relation of greatest importance that has to be regarded is therefore

$$q_s = f(\vartheta_s) \tag{5.2}$$

5.1.2 Limits to generality and applicability

There are various ways of limiting generality and applicability of the simplified model for a construction. One way is to limit the types of constructions and materials that the model is applied to. Another is to restrict the boundary conditions.

The models developed below will be applicable to all structures and materials normally present in buildings. For exterior walls some minimal thermal resistance will be assumed.

The model parameters will be adjusted for given boundary values. These are defined in the frequency domain and the boundary values on both sides of the construction will be defined at the same reference angular velocity ω.

The optimum choice of the reference angular velocity ω is different for each one of the three following groups of processes.

High frequency processes

For building climate processes high frequencies are those corresponding to a period down to 1 min. Such small periods are of interest only when studying automatic control processes. A simple model for the thermal response of rooms at such high frequencies has been derived by Jensen (1978). His model is based on the assumption that a normal room surface can be regarded as semi-infinite at frequencies corresponding to periods below 20 min.

Medium frequency processes

The most important variations in the heating or cooling load are those given by the day and night cycle with its overtones. Solar radiation, outdoor temperatures, internal heat load and ventilation are for natural reasons in the frequency domain most heavily represented at the 24 hour period. Figure 5.2 gives the approximation of typical outdoor variations by Fourier series with a different number of harmonics.

As is seen in figure 5.2 the daily influence of the elements is described fairly well by frequency components in an interval corresponding to periods between 5 h and 24 h. This applies to standard climatic conditions. If the climatic variables are studied for days with real weather data with abrupt changes in cloudiness, components with higher frequencies may be of importance. As the climatic data are usually given by hourly values the Nyqvist interval gives the shortest period represented to be 2 h.

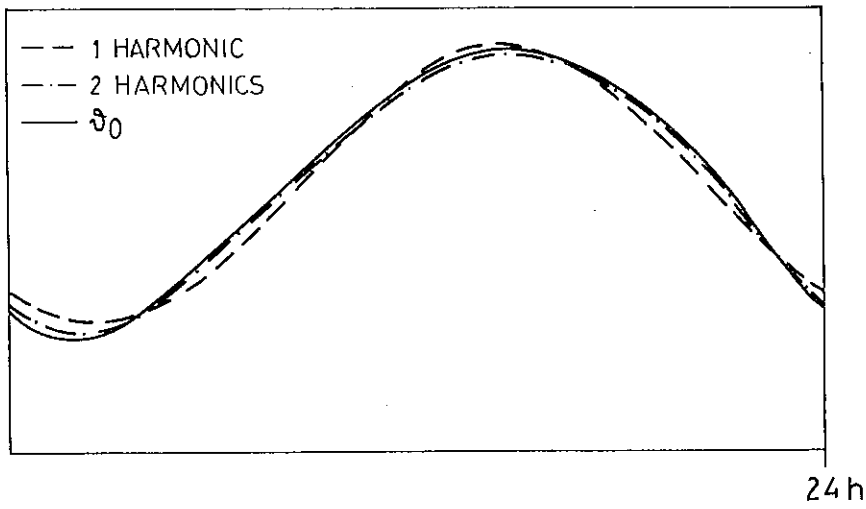

FIG. 5.2.a. Outdoor temperature variation approximated with truncated Fourier series. (From Aittomäiki (1974)).

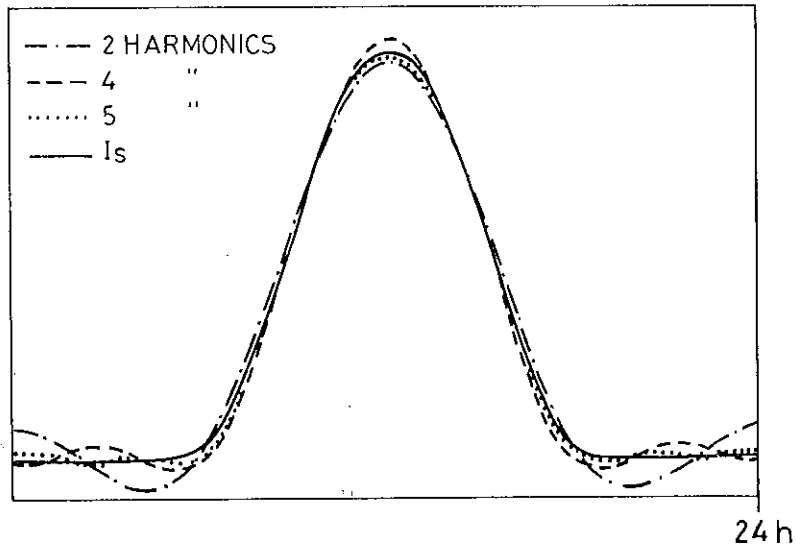

FIG. 5.2.b. Solar radiation approximated with truncated Fourier series. (From Aittomäiki (1974)).

Many internal steady-periodic processes can be regarded as on-off processes. Machines and lighting in a factory producing a constant amount of heat during working hours are examples of such processes. Here the importance of higher frequency components is greater; see figure 5.3. The process is still distorted using periods down to 24/5 hours and the relative distortion is greatest around the time for shift.

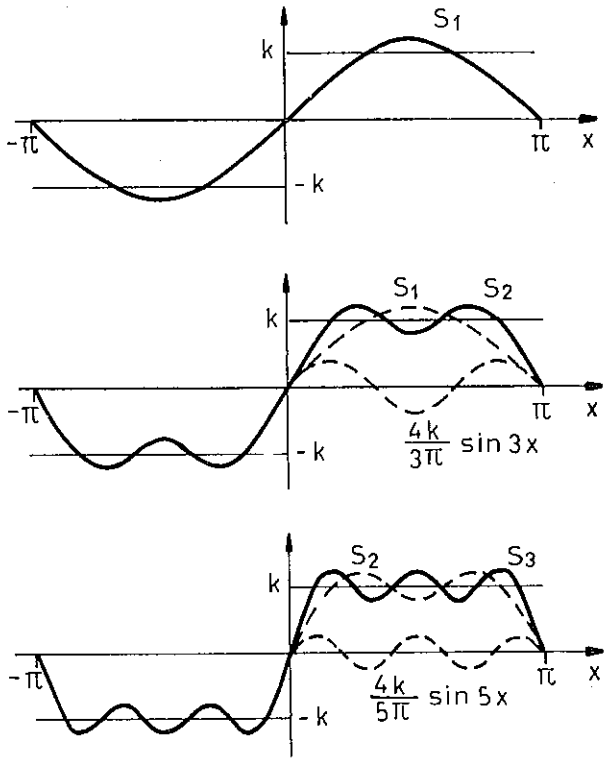

FIG. 5.3. The first three partial sums of the Fourier series corresponding to a periodic on - off function.(From Kreyszig (1967)).

An important factor that will be illustrated later on is that the influence of the heat generating processes on the resulting indoor temperature is greatly reduced at increasing frequencies. The following is therefore postulated.

When studying steady periodic building heat transfer processes with the fundamental period 24 hours, the parameters of a simplified model should be adjusted to give the best fit for the fundamental frequency and the model should be designed to give as close an approximation as possible to the response at higher frequencies.

Low frequency processes

Even if most non-steady calculations are done for steady periodic processes within a period of 24 h there are often reasons for extending the calculation to longer periods e.g.

Calculation of energy consumption based on weather data over longer periods.

The transient cooling down or warming up phase of a building.

Calculation of power load based on distribution of extreme boundary conditions.

The response of the models, should be investigated at periods from 24 h to the limit where the response is given by the steady state relations.

5.1.3 Presentation and evaluation of model characteristics - the Bode diagram

In section 5.1.2 the performance of a model is specified in the frequency domain. The comparison and evaluation of different models are also carried out at different frequencies. For this purpose we use the Bode diagram commonly used in automatic control theory for graphical representation of the transfer function of a system.

Referring to equation (4.53) the relations between temperatures and heat flows at both sides of a construction are given by a matrix of four transfer functions A(s), B(s), C(s), D(s). Rewriting the equation in order to form explicit equations for the heat flows defined in figure 5.1 gives

$$L\{q_s\} = E(s)\, L\{\vartheta_s\} + F(s)\, L\{\vartheta'_s\} \qquad (5.3)$$

According to equation (5.1) the transfer functions E(s) and F(s) are sufficient for this purpose to describe the heat transfer of the wall.

$$E(s) = \frac{L\{q_s\}}{L\{\vartheta_s\}} \quad \text{if } \vartheta'_s = 0 \tag{5.4}$$

$$F(s) = \frac{L\{q_s\}}{L\{\vartheta'_s\}} \quad \text{if } \vartheta_s = 0 \tag{5.5}$$

If the boundary temperatures are harmonic quantities $\tilde{\vartheta}_s$ and $\tilde{\vartheta}'_s$, according to section 4.1.2 the surface heat flow can be written as

$$\tilde{q}_s = r_1 \, e^{i\theta_1} \, \tilde{\vartheta}_s + r_2 \, e^{i\theta_2} \, \tilde{\vartheta}'_s \tag{5.6}$$

The definition of the Laplace transform in equation (4.51) gives the frequency function $E(i\omega)$

$$E(i\omega) = \frac{\int_0^\infty r_1 \cdot e^{i\theta_1} \cdot \tilde{\vartheta}_s \cdot e^{-st} \, dt}{\int_0^\infty \tilde{\vartheta}_s \cdot e^{-st} \, dt} \tag{5.7}$$

$$E(i\omega) = r_1 \, e^{i\theta_1} \tag{5.8}$$

and in the same manner

$$F(i\omega) = r_2 \, e^{i\theta_2} \tag{5.9}$$

If a transfer function $G(s)$ is known the amplitude and phase of the corresponding frequency function is calculated by

$$r = |G(i\omega)| \tag{5.10}$$

$$\theta = \arg G(i\omega) \tag{5.11}$$

This provides a simple means of comparing solutions given by the Laplace transform to solutions in the frequency domain.

A typical Bode diagram for a wall construction is shown in figure 5.4. The frequency axis is scaled as log ω but with markings at doubled fre-

quencies labelled with the corresponding periods in hours. The log r and the angle θ in degrees are plotted versus ω. At low frequencies the amplitudes r_1 and r_2 equal the steady state thermal transmittance k defined in section 3.1.1. Observe that in this context the thermal transmittance means the reciprocal of the thermal resistance of the construction as it is specified and does not necessarily include the effect of surface heat transfer.

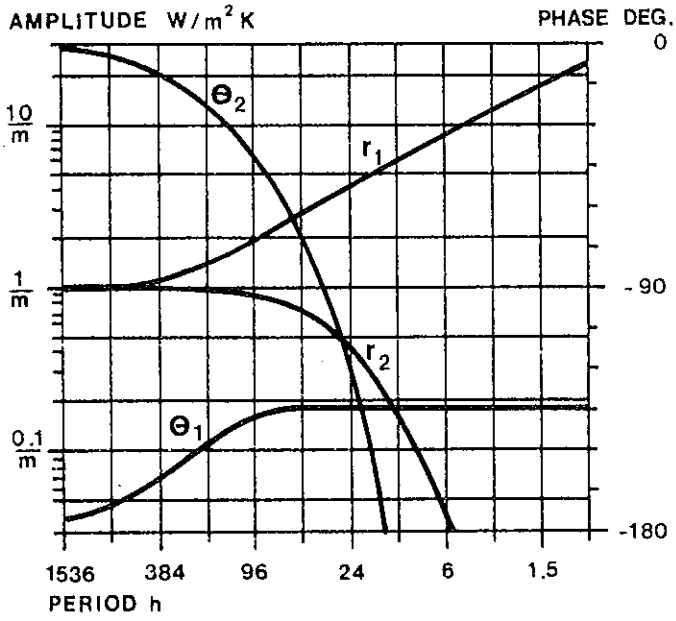

FIG. 5.4. A Bode diagram for a one-layer construction. The construction consists of 30 cm aerated concrete with thermal conductivity 0.2 W/m^2, density 510 kg/m^3 and specific heat capacity 1050 J/kg K. r_1 and θ_1 are the amplitude and phase of a heat flow oscillation generated by a temperature oscillation with unit amplitude at the inner surface with constant external surface temperature. r_2 and θ_2 are the amplitude and phase of a heat flow oscillation at the inner surface when the external surface temperature oscillates and the inner surface temperature is zero.

The Bode diagram for a construction or a model of a construction can be achieved both by calculations in the domain of complex numbers as given in section 4.1 or directly from a known transfer function. It is a convenient tool for indicating the validity of assumptions and simplified models within a wide frequency range.

A technique for estimating the transfer function from a known Bode diagram is described in Åström (1968).

5.2 INTRODUCTION AND EVALUATION OF DIFFERENT MODELS AND PARAMETERS

Different simplified models and parameters for describing the thermal performance of building components are treated in this section. In table 5.1 a set of constructions is given which will later illustrate the influence of certain assumptions and simplifications made, and to indicate the validity of the models. The material constants used in the examples come from several sources such as Nevander and Bankvall (1968), the Swedish Building Code (1975), Halldorsson (1978) and Tye and Spinney (1978). The thermal conductivities mostly follow the practically applicable values according to the Swedish Building Code except for concrete. The thermal conductivity for dry concrete is approximately 0.9 W/mK while the practically applicable value according to the code is 1.7 W/mK. This value includes the influence of high moisture content and reinforcing steel. At the surfaces facing the room the concrete layer is fairly dry and the reinforcing steel content is more important to the lateral heat transfer. Therefore the thermal conductivity for concrete suitable for this purpose has been set at 1.2 W/mK. Also an externally ventilated cavity has been given a thermal resistance which is not the case in the Swedish Building Code.

TABLE 5.1. A set of constructions. The layers are given from the outside of the room towards the inside. Layers that are of minor importance to the heat conduction through the wall, such as vapour barriers, are excluded. The heat flow is treated as one dimensional which means that the influence of thermal bridges such as studs is neglected.

		l, m	λ, W/mK	ρ, kg/m^3	c, J/kgK	m, m^{2}K/W
External walls						
1	brick	0.120	0.60	1500	840	
	cavity	0.020	(0.133)	1.2	1000	0.15
	impr. board	0.012	0.065	400	1350	
	mineral wool	0.150	0.040	23	750	
	plaster board	0.013	(0.216)	740	840	0.06
2	concrete	0.100	1.2	2400	880	
	cellular plastics	0.15	0.040	20	1400	
	concrete	0.100	1.2	2400	880	
3	boarding	0.020	0.140	500	2300	
	impr. board	0.012	0.065	400	1350	
	mineral wool	0.150	0.040	23	750	
	plaster board	0.013	(0.216)	740	840	
Roofs						
4	roofing felt	0.004	0.26	1100	1500	
	mineral wool	0.120	0.040	200	750	
	concrete	0.040	1.2	2400	880	
5	roofing felt	0.001	0.26	1100	1500	
	aerated concrete	0.250	0.12	600	1050	
6	roofing felt	0.004	0.26	1100	1500	
	mineral wool	0.120	0.040	200	750	
	sheet metal	0.001	50.0	7800	460	

	l, m	λ, W/mK	ρ, kg/m^3	c, J/kgK	m, m^{2}K/W
Internal walls					
7 plaster board	0.013	(0.216)	740	1090	0.06
cavity	0.075	(0.5)	1.2	1000	0.15
plaster board	0.013	(0.216)	740	1090	0.06
8 concrete	0.15	1.2	2400	880	
Ceilings/floors					
9 plastic covering	0.003	0.175	1300	1500	
concrete	0.160	1.2	2400	880	
10 chipboard	0.022	0.13	1000	2100	
cavity	0.200	(1.333)	1.2	1000	0.15
plaster board	0.009	(0.225)	850	1090	0.04

5.2.1 Frequency response - the admittance procedure

In section 4.1.2 it was shown that the time-dependent temperatures and heat flows on both sides of a construction can be related by a matrix of four complex numbers as long as these quantities vary sinusoidally in time with the same angular velocity. It is therefore tempting to characterize the thermal behaviour of the construction by the elements of the matrices given in equation (4.16) and (4.28), and at a reference frequency corresponding to the 24 h period.

As seen in section 5.7 the time-dependent heat exchange at the construction surface is given as the sum of the heat flow generated by the inner surface temperature at zero external temperature, and the heat flow generated by the external temperature at zero inner surface temperature.

The ratio between the surface heat flow and the surface temperature is called the admittance of the wall denoted Y. Using equation (4.28) this ratio is defined by the matrix element E if the external temperature is zero.

$$Y = \frac{\tilde{q}_s}{\tilde{\vartheta}_s} = E \; (\vartheta'_s = 0) \qquad (5.12)$$

The ratio between the surface heat-flow and the external temperature when the surface temperature equals zero is defined by the matrix element F of equation (4.28). This ratio will be referred to as the dynamic thermal transmittance or the transmittance, T_D.

$$T_D = \frac{\tilde{q}_S}{\tilde{\vartheta}'_S} = F \quad (\tilde{\vartheta}_S = 0) \tag{5.13}$$

The decrement factor f as given by Danter (1960) is given by

$$f = F \cdot m \tag{5.14}$$

in which m is the thermal resistance between the surface and the external temperature.

At this stage one notes a discrepancy between this presentation for the admittance and transmittance for a construction and that given by Danter (1960). Since the surface heat transfer coefficients should not affect the construction characteristics the heat transfer is considered to be generated by the surface temperatures. Danter considers the heat flow generated by environmental temperatures when the surface heat transfer is included in the calculation of the matrix elements E and F. For constructions with a thermal resistance dominating the surface resistances the transmittance is only slightly affected while the admittance behaves differently at higher frequencies.

In addition to the admittance and the decrement factor Milbank and Harrington Lynn (1974) define three other important factors: the impedance Z, the surface factor F and the modified admittance Y'.

The impedance Z at the surface of the construction is defined as

$$Z_S = \frac{\tilde{\vartheta}_S}{\tilde{q}_S} \tag{5.15}$$

$$Z_S = \frac{1}{E} \tag{5.16}$$

The surface factor F_S is defined as the ratio between the heat flow generated at a surface and the heat flow to some environmental temperature over a resistive surface layer. This factor depends on the surface heat transfer coefficient and is, according to the specifications above, not to be regarded as a construction characteristic.

$$F_S = \frac{\alpha}{\alpha - E} \tag{5.17}$$

For internal walls and when the boundary values can be assumed to be symmetric the modified admittance, Y', is defined as the ratio between the surface heat flow and temperature when the external temperature equals the surface temperature.

$$Y' = \frac{\tilde{q}_S}{\tilde{\vartheta}_S} \qquad (\tilde{\vartheta}_S' = \tilde{\vartheta}_S) \tag{5.18}$$

From the matrix equation (4.28) the modified admittance is given as

$$Y' = E + F \tag{5.19}$$

The parameters described above are the basis of the admittance procedure developed by Danter and Loudon at the Building Research Institute in Watford in the sixties and later included in the I.HVE Guide (1970). It is a technique for the calculation of temperatures and power loads within buildings for steady periodic diurnal climatic loads. The admittances at frequencies higher than the one corresponding to the 24 h cycle are assumed to equal the 24 h admittance, that is with the same amplitude and the same time lag given in hours. It is easy to show this in the Bode diagram since the amplitude of the admittance and transmittance are given as straight lines cutting the real amplitudes r_Y and r_T at 24 hours. Suffix Y stands for admittance and suffix T for transmittance. The phase is similarly set at 24 h and then doubled for each doubling of the frequency

$$\theta(\omega) = \theta(24\ h) \cdot 2^{(1 - \omega/\omega(24\ h))} \quad (T \leq 24\ h) \tag{5.20}$$

(1)

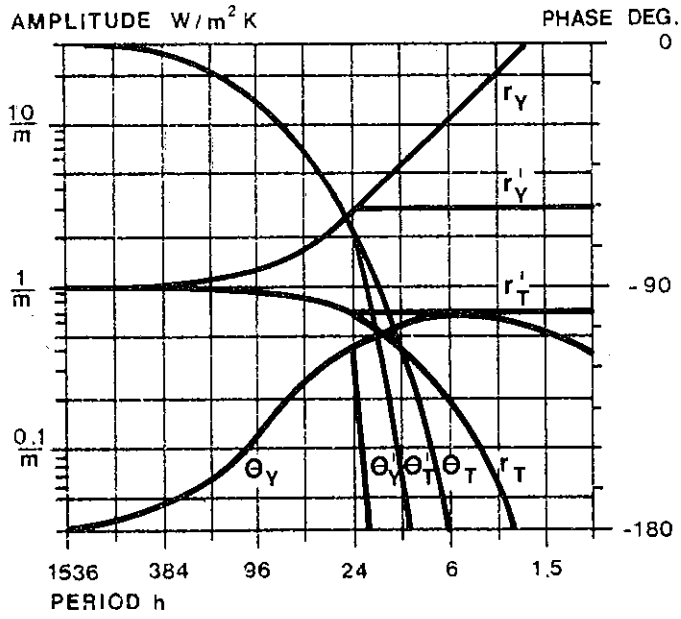

(4)

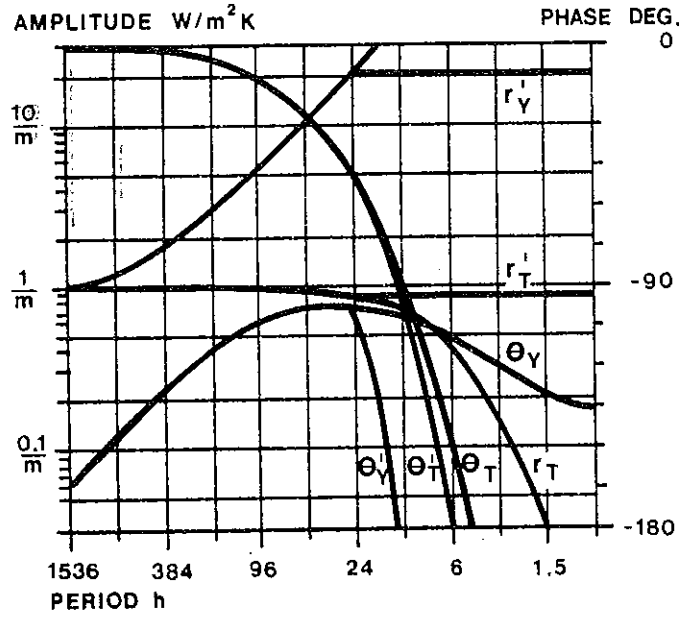

FIG. 5.5. The consequence of the assumptions for the derivation of the admittance procedure. Construction 1 and 4 of table 5.1 without surface resistances. Suffix Y stands for admittance and suffix T for tansmittance. r' and θ' illustrate the assumption that the 24 h amplitude and the phase in hours are valid at higher frequencies.

(1)

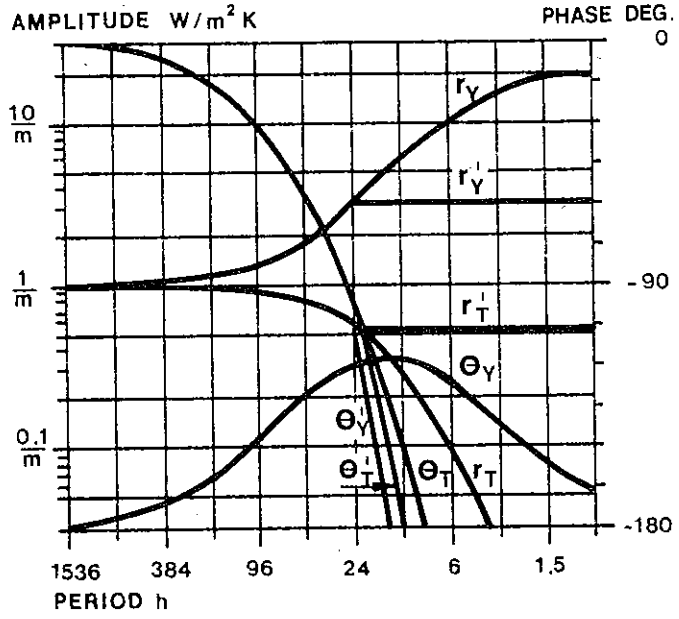

(4)

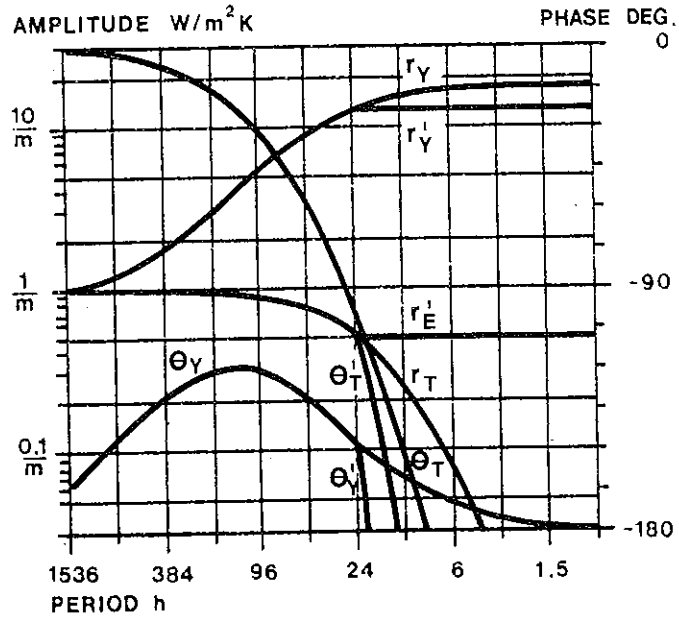

FIG. 5.6. Illustration of the frequency response of constructions 1 and 4 in table 5.1 when the surface resistances m_I = 0.2 m^2K/W and m_0 = 0.05 m^2K/W are included in the calculations.

In figure 5.5 the Bode diagrams for the construction alternatives 1 and 4 in table 5.1 are given. The necessary assumptions for the admittance procedure have been introduced by the quantities r_Y', θ_Y', r_T' and θ_T'.

Although the assumptions made seem to be of poor validity there are two things that must be considered. The admittance procedure is meant to describe day and night cycles where the content of higher frequency components is small. The admittance procedure also implies that the construction characteristics are calculated including the surface heat transfer on both sides. Figure 5.6, similarly to figure 5.5, shows the real frequency functions for constructions 1 and 4 together with the assumed model. In this case, however, the surface resistances are included in the calculations. On the inside m_I is 0.2 m^2K/W and on the outside m_0 is 0.05 m^2K/W.

Comparing figures 5.5 and 5.6 one sees that the heat flow through the wall expressed in terms of r_T and θ_T is only slightly affected by the surface resistances, while the surface heat exchange behaves differently. The amplitude r_Y in figure 5.5 increases linearly at higher frequencies while in figure 5.6 it has an upper limit given by the surface heat transfer coefficient. The phase θ_Y in figure 5.5 is assymptotically approaching -135 degrees or $-3/4\,\pi$ while in figure 5.6 the high frequency assymptote is -180 degrees.

To give a qualitative explanation of the heat transfer phenomena at the surface the four assymptotes of the admittance are defined:

I <u>The steady state transmittance</u>. The assymptote of r_Y at low frequencies is given by the thermal transmittance between the surfaces as defined in the calculations.

$$r_Y = \frac{1}{m} \qquad (\omega \to 0) \tag{5.21}$$

$$\theta_Y = -\pi = -180 \text{ degrees} \tag{5.22}$$

II <u>The simple mass response</u>. In the case of a heavy surface layer with high thermal conductivity next to an insulating layer, the surface

layer will, in a certain frequency interval behave isothermically and the heat exchange via the insulating layer is negligible. The admittance is then given by the formula

$$Y = -i\omega \cdot C \tag{5.23}$$

and this gives the amplitude assymptote in the Bode diagram as

$$\log r_Y = \log C + \log \omega \tag{5.24}$$

that is, a straight line with the slope 1:1.

The phase is given by a constant value

$$\theta_Y = -\pi/2 = -90 \text{ degrees.} \tag{5.25}$$

III <u>The semi-infinite solid response</u>. With increasing frequency the temperature oscillations are to a great extent damped out in the surface layer. The admittance approaches the one for a semi-infinite solid with the same material data as the surface layer. The admittance at the surface of a semi-infinite solid is derived from the equations (4.18), (4.20) and (4.29) when l goes to infinity.

$$Y = -\lambda \frac{\omega}{2a} (1 + i) \tag{5.26}$$

$$= -\lambda\rho c \cdot \omega \cdot e^{-\frac{i\pi}{4}} \tag{5.27}$$

$$= \lambda\rho c \cdot \omega \cdot e^{-\frac{i\,3\pi}{4}} \tag{5.28}$$

The amplitude of the admittance approaches a straight line with the slope 1:2 in the Bode diagram.

$$\log r_Y = \tfrac{1}{2} \log (\lambda\rho c) + \tfrac{1}{2} \log (\omega) \tag{5.29}$$

The phase is given by a constant value

$$\theta_Y = -\frac{3\pi}{4} = -135 \text{ degrees} \tag{5.30}$$

IV <u>The surface heat transfer coefficient</u>. If the admittance for a construction is calculated including a purely resistive surface layer, an upper limit to the admittance is given by the steady state transmittance of the surface layer. When the angular velocity goes to infinity the temperature amplitude of the underlying layer is zero and the admittance is given as $-\alpha$.

The amplitude r_y equals α and the phase equals $-\pi$ or -180 degrees.

The limiting function of the α value is seen by comparing r_Y at higher angular velocities in the figures 5.5. and 5.6.

To illustrate the assymptotes I, II and III, they are in figure 5.7 implemented in the Bode diagram for construction 2 uninfluenced by surface heat transfer. The insulation layer is reduced to the thickness of 1 cm which only affects the admittance ratio. The amplitude of the admittance and the phase are fairly well approximated by the assymptotes at high and low angular velocities.

The validity of the admittance procedure is best for constructions where the amplitude of the 24 hour admittance is close to the surface α value, as for construction 4 in figure 5.6. This means that it is best suited to describe the heat flow processes within buildings with heavy surface layers towards the room. It can also be noted that the amount of the internal load absorbed by the room surfaces will be underestimated while the heat flow from outer surface to the room will be overestimated when components of frequencies higher than the reference frequency are present.

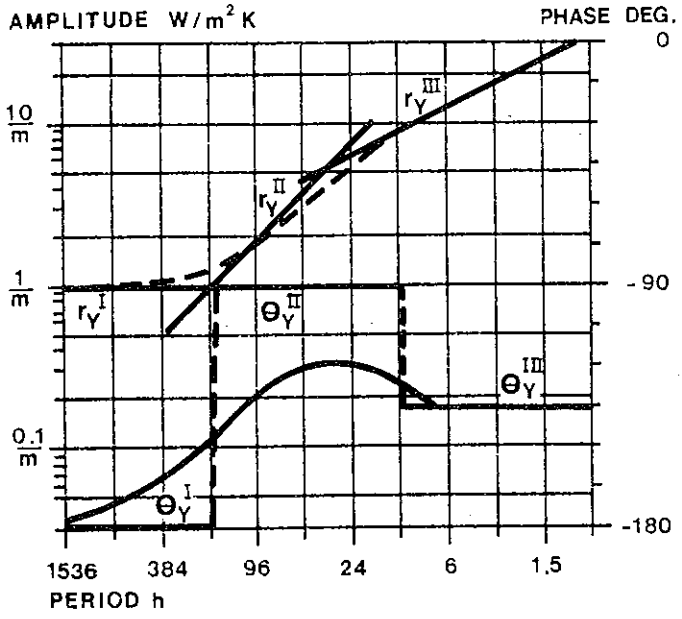

FIG. 5.7. Bode diagram for construction 2 with assymptotes defined in the text. The insulation thickness is reduced to 1 cm.

5.2.2 The ω-RC transform

Section 4.3 gives a calculation method for non-steady heat transfer through building components by representing the construction as a series of resistances and capacitances. The thermal response for the network can be solved for finite time differences, see section 4.3, or in the frequency domain by successive use of the equations (4.26-27). The thermal response of the chosen network can thus be compared to the analytical solution in a big frequency interval. The transfer matrices of equation (4.25) and (4.28) will also prove useful to find the optimum network for a limited number of nodes.

Since the number of possible models is infinite the study starts by introducing two different cases, figure 5.8. The models C and RC are only useful for those constructions for which the surface heat exchange, the admittance, dominates the heat flow through the construction.

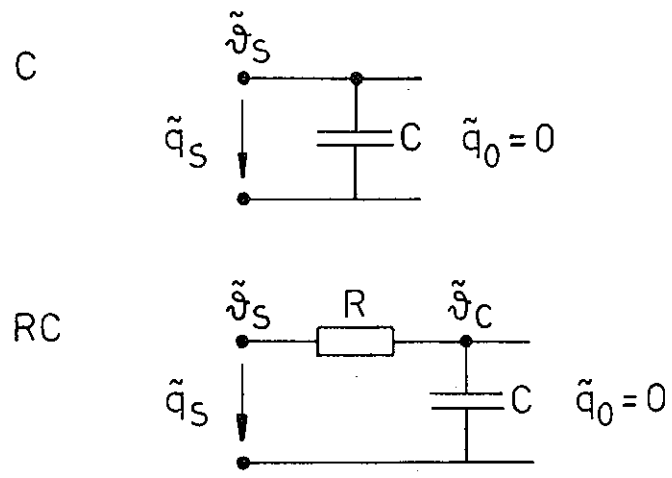

FIG.5.8. Two models to describe the heat exchange at the surface. of a building component exposed to symmetrical boundary conditions.

This is the case for inner walls with symmetric boundary conditions and for the non-steady part of the heat flow through exterior constructions. This means that the construction is modelled towards a limit for zero heat flow. The non-steady transmittance for the constructions is therefore neglected and the characteristics of the construction are fully described by the admittance.

The admittance for a single thermal storage C is given together with its interpretation in the Bode diagram, in equation (5.23-5.25). The constant C can be identified from the modified admittance of the construction for the 24h period.

$$- i\omega C = E + F \quad (T = 24h) \tag{5.31}$$

The quantity C resulting from this would in some cases have a complex component. Since C has a physical interpretation in the real space only and the resulting phase of the model is constant, the best choice of C is

$$C = \left|\frac{E + F}{\omega}\right| \quad (T = 24h) \tag{5.32}$$

The admittance of the RC-model in figure 5.8 can be achieved from a heat balance for the temperature $\tilde{\vartheta}_C$.

$$\frac{1}{R}(\tilde{\vartheta}_S - \tilde{\vartheta}_C) = C \cdot \frac{\partial \tilde{\vartheta}_C}{\partial t} = i\omega C\tilde{\vartheta}_C \tag{5.33}$$

$$\tilde{\vartheta}_S = \tilde{\vartheta}_C(1 + i\omega RC) \tag{5.34}$$

The surface heat flow is given by

$$\tilde{q}_S = - \frac{1}{R}(\tilde{\vartheta}_S - \tilde{\vartheta}_C) = - i\omega C\tilde{\vartheta}_C \tag{5.35}$$

and the admittance is then

$$Y = \frac{\tilde{q}_S}{\tilde{\vartheta}_S} = \frac{-1}{R + \frac{1}{i\omega C}} \tag{5.36}$$

The amplitude and phase of the admittance for the 24 hour cycle can be represented exactly by the RC-model since the real and imaginary part of the admittance can be varied independently through R and C.

$$R = -\mathrm{Re}\left(\frac{1}{E + F}\right) \tag{5.37}$$

$$C = \frac{1}{\mathrm{Im}\left(\frac{1}{E + F}\right) \cdot \omega} \tag{5.38}$$

Before going further to more complex models let us look at the results achieved so far. The modified admittance has been primarily defined as a property of interior constructions. In figure 5.9 the admittance for the models C and RC as defined in figure 5.8 and the equations (5.32), (5.37) and (5.38), is compared to the modified admittance for construction number 8, a 15 cm thick homogeneous concrete wall.

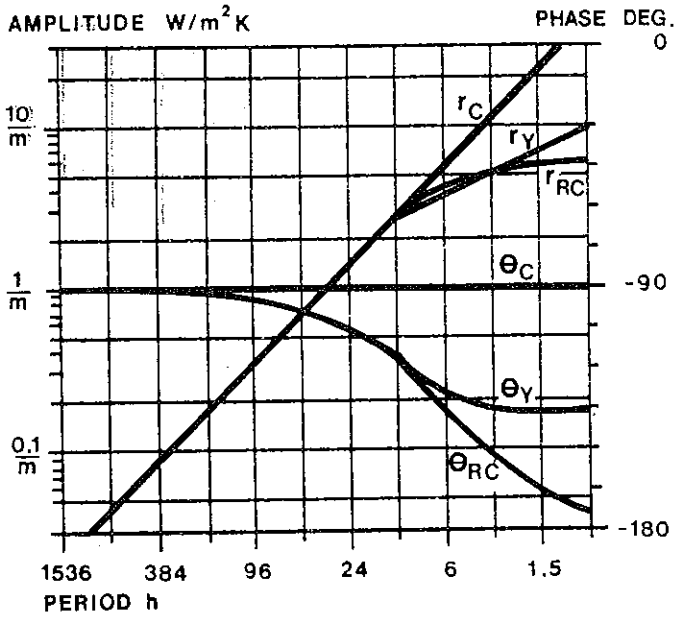

$C_C = 1.524 \cdot 10^5$ J/K

$R_{RC} = 0.0208$ K/W

$C_{RC} = 1.566 \cdot 10^5$ J/K

FIG. 5.9. The admittance for models C and RC of figure 5.8 compared to the modified admittance of construction number 8, a homogeneous concrete wall. The thermal capacity of the C-model is C_C and the resistance and capacity for the RC-model are given by R_{RC} and C_{RC} respectively. They are all calculated for 1 m^2 surface area.

The thermal capacity C for the C-model is $1.524 \cdot 10^5$ J/K and the resistance and thermal capacity for the RC-model are 0.0208 K/W and $1.556 \cdot 10^5$ J/K respectively. As might be expected the RC-model gives better agreement to the real admittance both for the amplitude and phase. If a criterion for the phase difference is chosen as 15 degrees this is exeeded for the C-model at periods a little less than 24h but, for the RC-model, at periods less than 3 hours. If a criterion for the amplitude difference is set at 20%, this, for the C-model, is exeeded at periods less than 6 hours, and for the RC-model at periods less than 1.5 hours.

The thermal capacity per square meter of the construction is $1.584 \cdot 10^5$ J/K for each surface so that the thermal capacity of both models is very close to the maximum available. The thermal resistance of the slab is 0.195 m^2K/W which means that the RC-model can be seen as the thermal capacity C being concentrated at a distance of 2.5 cm from the surface.

For a light weight construction, e.g. the interior wall number 7 of table 5.1, the admittance is less sensitive to the choice of model, especially when the biggest part of the thermal capacity of the construction is concentrated near the surface. In this case the amplitude of the admittance is in good agreement for both models down to a period of 0.75 hours as can be seen in figure 5.8. The phase for the C-model is shifted more than 15 degrees at periods less than 1.5h.

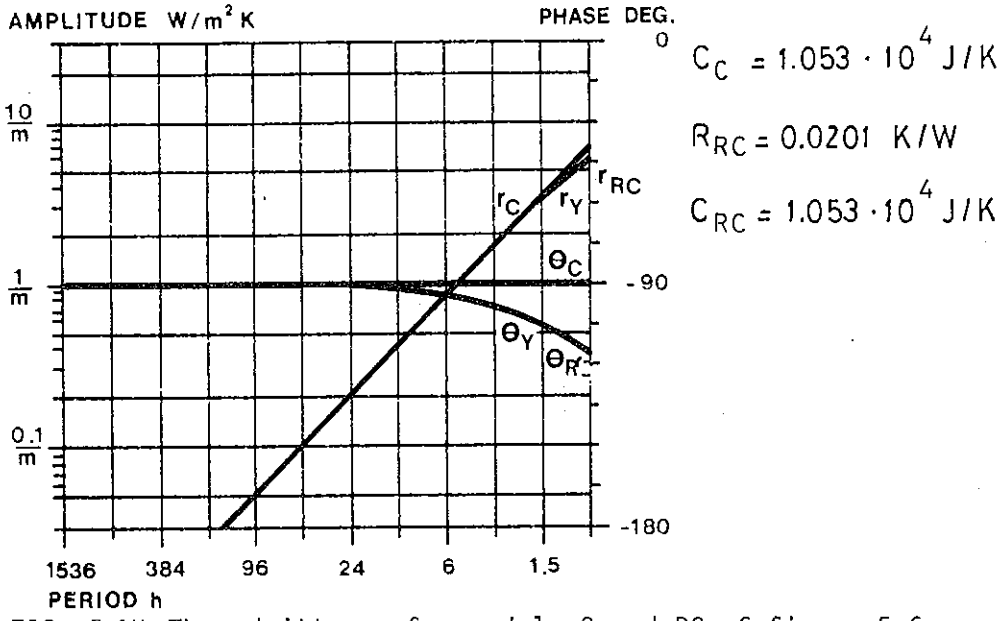

FIG. 5.10. The admittance for models C and RC of figure 5.6 compared to the modified admittance of construction 7 of table 5.1.

The two constructions studied above are symmetrical. The floor construction 10 of table 5.1 consists, on the upper side, of a chipboard with five times as high a thermal capacity per unit area as the plaster board below. The modified admittances for both sides are given in figure 5.11.

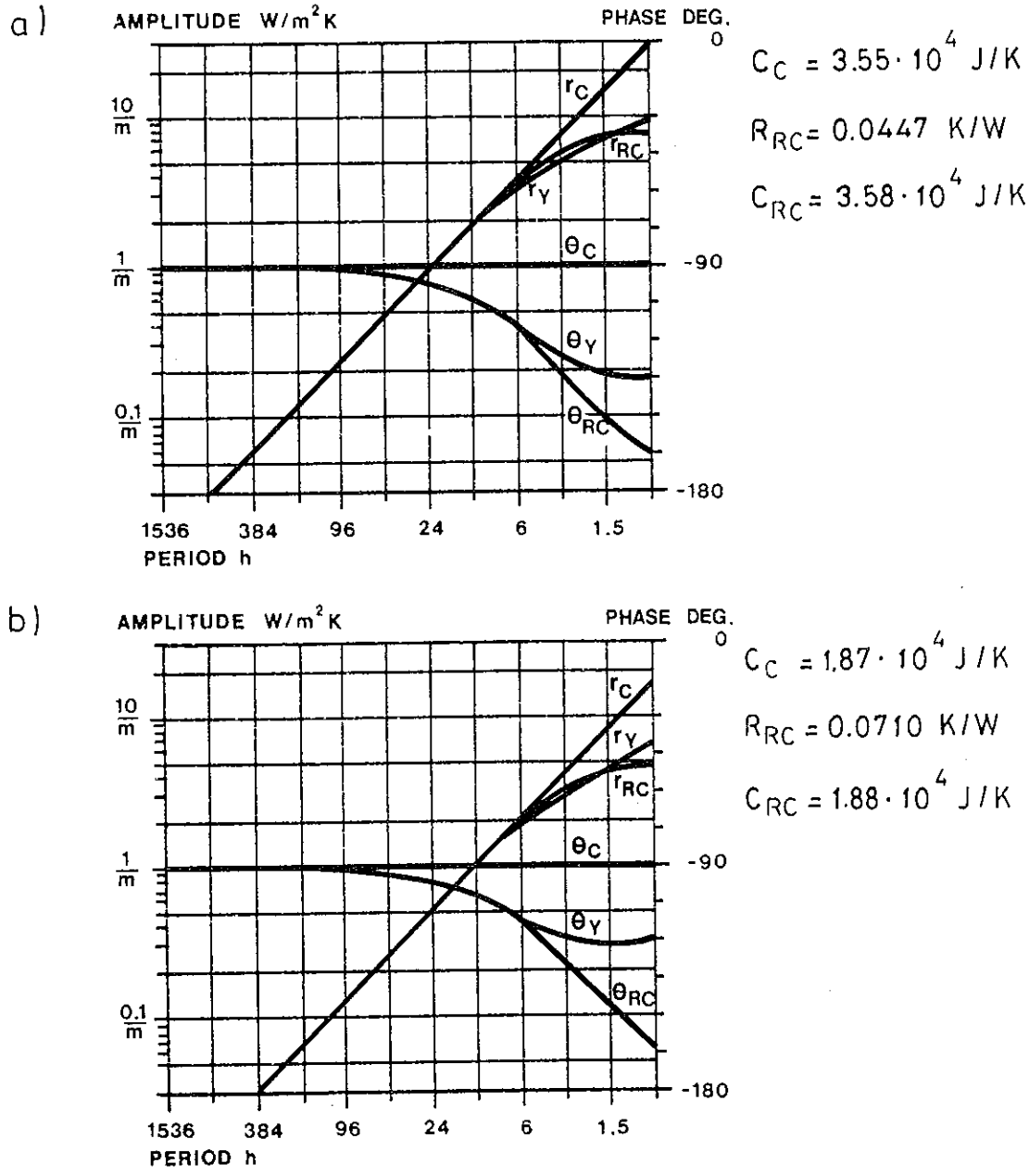

FIG. 5.11. The admittance for models C and RC of figure 5.6 compared to the modified admittance of construction 10 of table 5.1. In (a) the admittance is calculated at the upper side and in (b) at the lower side of the construction.

The agreement between the admittances for the three different models is similar to the results for the heavy concrete construction, figure 5.9. It is interesting to note that the participating capacitances for both models are about $3.6 \cdot 10^4$ J/K on the upper side and $1.9 \cdot 10^4$ J/K on the lower side while the thermal capacity per square meter of the chipboard is $4.6 \cdot 10^4$ J/K and for the plasterboard $0.8 \cdot 10^4$ J/K. Simplified methods to esimate the participating thermal capacity related to a surface will be treated below, and one problem is to locate the adiabatic central line of the construction.

The examples in figures 5.9 to 5.11 all have the amplitude of the admittance around the 24h period as a straight line with the slope 1:1 that is corresponding to the simple mass response. It is useful to test the models against mode III constructions - those behaving as a layer of infinite thickness - or mode IV constructions with resistive surface layer. Mode III is effected through increased total thickness of the concrete wall number 8 of the table 5.1 to 30 cm. See figure 5.12.

The interesting change from the constructions in figures 5.9 and 5.11 is that the low frequency admittance is different for the different models. The accuracy is better for the RC-model than the C-model but the error for the admittance amplitude of the RC-model is more than 20% for periods less than 6 hours while the corresponding limit for the 15 cm wall is 1.5 hours.

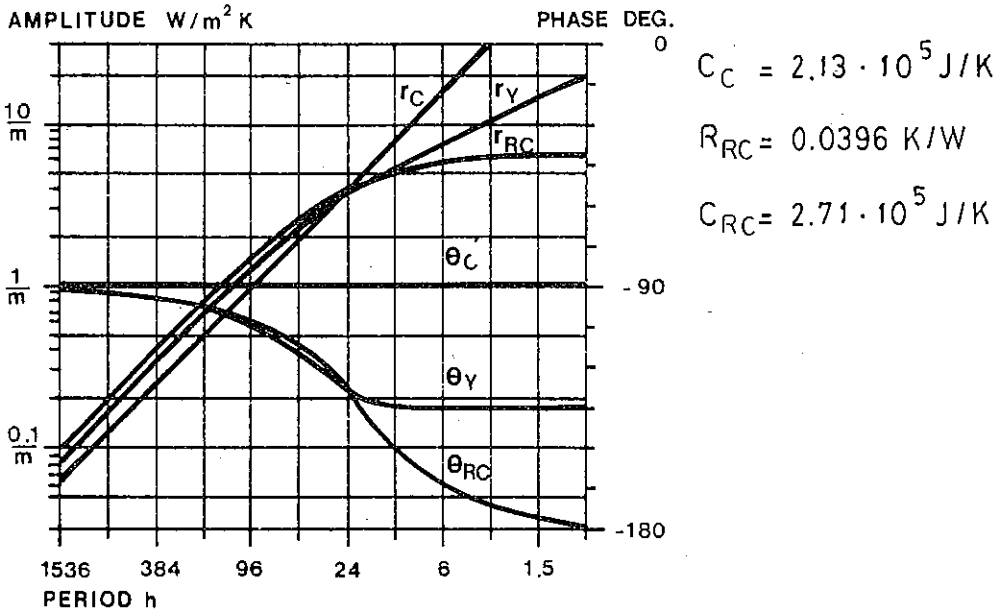

$C_C = 2.13 \cdot 10^5$ J/K

$R_{RC} = 0.0396$ K/W

$C_{RC} = 2.71 \cdot 10^5$ J/K

FIG. 5.12. The admittance for the models C and RC of figure 5.8 compared to the modified admittance of construction 8 of table 5.1 where the total thickness of the construction is increased to 30 cm.

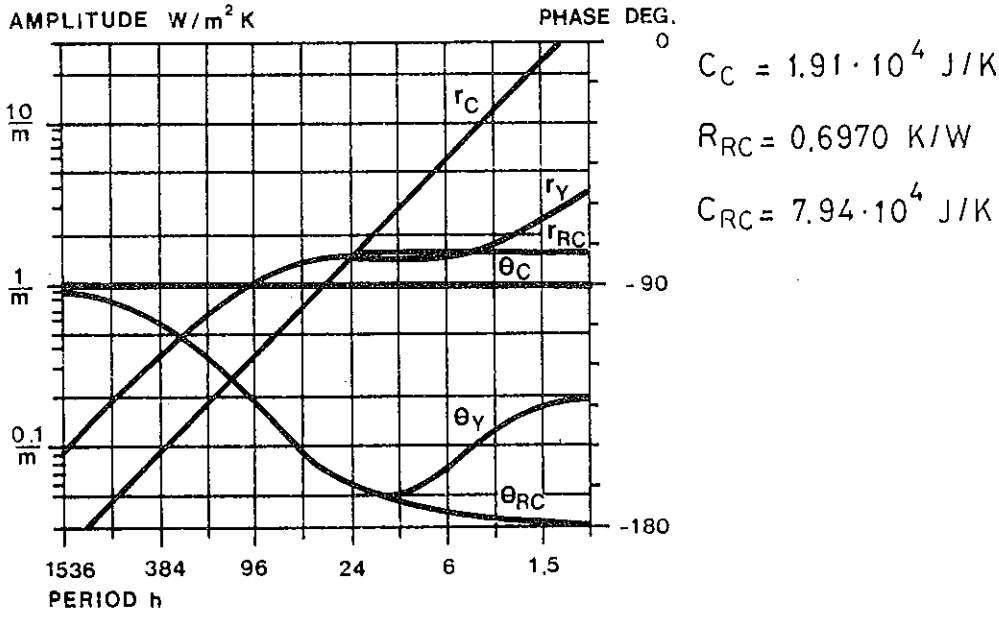

$C_C = 1.91 \cdot 10^4$ J/K

$R_{RC} = 0.6970$ K/W

$C_{RC} = 7.94 \cdot 10^4$ J/K

FIG. 5.13. The admittance for the models C and RC of figure 5.8 compared to the modified admittance of the construction of figure 5.12 covered with 3 cm of an acoustical absorbent.

To realise mode IV the construction of figure 5.12 is covered with 3 cm of light weight mineralwool as an acoustical absorbent on the surface closest to the room. The resulting admittances are shown in figure 5.13. The RC-model is in good agreement down to periods of 3 hours while the C-model is rather insufficient.

(a)

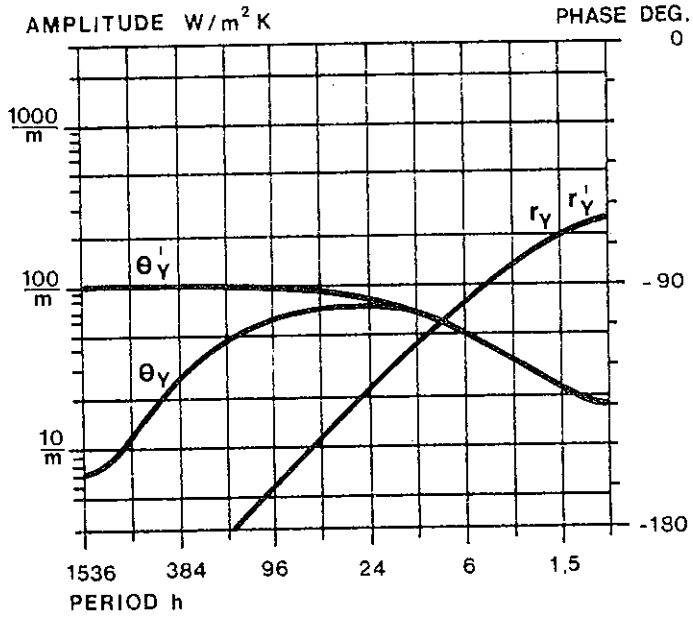

(b)

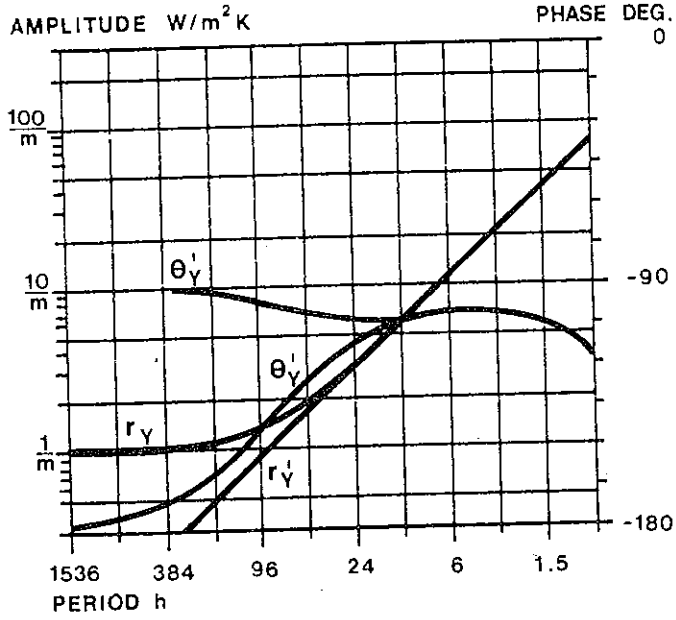

FIG. 5.14. Comparison between the modified admittance r_y', θ_y' and the admittance r_y, θ_y for the construction 1 (a) and 4 (b) of table 5.1.

Two models to describe the surface heat exchange for symmetrical conditions at the surface boundaries have already been treated and their parameters have been adjusted to give the best possible representation of the admittance for the 24h period. The next step is to give a model which can be used to calculate the admittance and the transmittance for a construction with the same chosen parameters. Figure 5.14 shows a comparison between the admittance and the modified admittance for the constructions 1 and 4 of table 5.1. Since the amplitude and the phase are not significantly different for the 24h period one concludes that the capacitances and resistances calculated with symmetrical boundary values remain valid even for asymmetrical constructions. The problem then is to give a model which represents the coupling between the existing model for the admittance, and the external surface.

The total resistance of the model has to equal the total resistance of the construction to provide for a correct steady state solution. Some possible combinations are given in figure 5.15.

Sonderegger (1977) treats the transform of a multilayer wall into a model of the type RCR in figure 5.15. For the identification of the components he uses the transfer functions given in section 4.2. This implies immense mathematical exercises even when the analysis is limited to simple constructions.

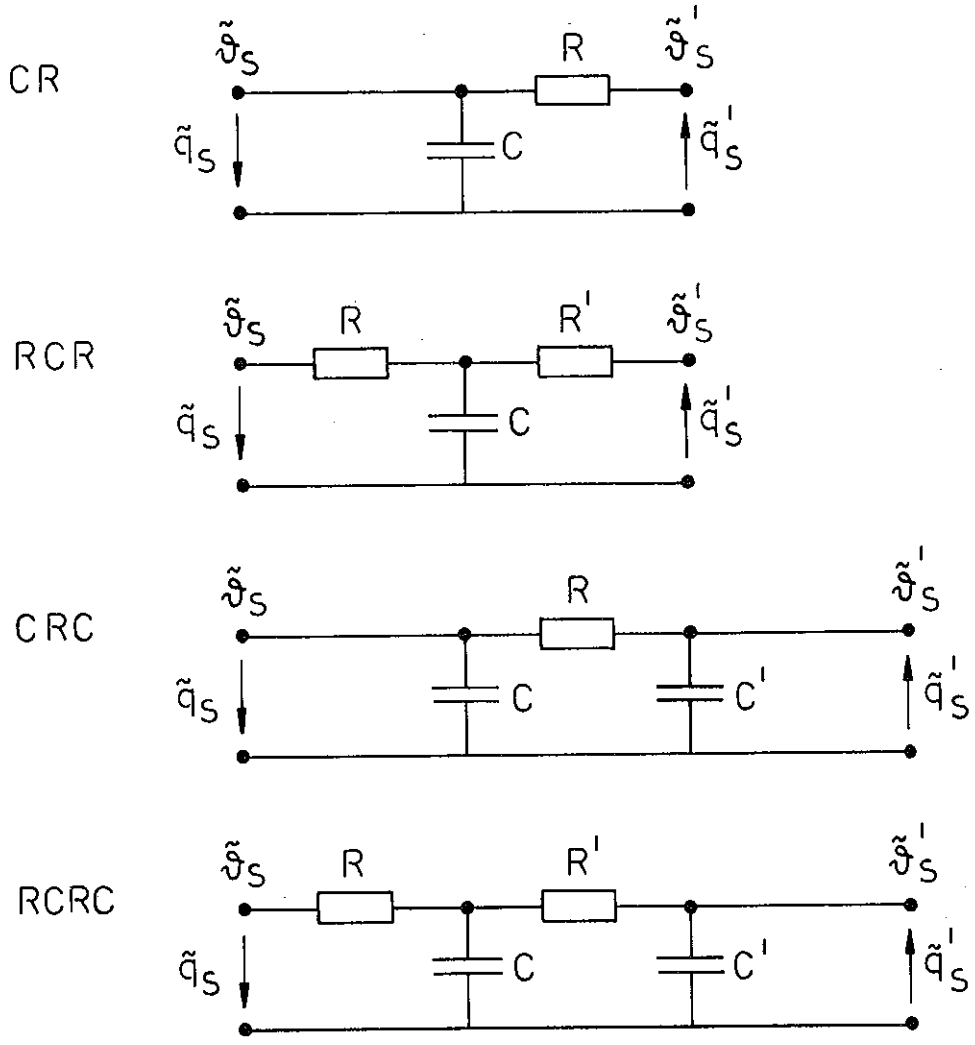

FIG. 5.15. Possible modifications of the models in figure 5.8. The models should also give the transmittance characteristics for the constructions.

In the two first models CR and RCR parameters are fixed by the specification on the steady state transmittance. In the two latter models of figure 5.15 CRC and RCRC the resistances are fixed for the same reason but the external capacity C' can be varied.

The choice of the models in figure 5.15 has been made considering various aspects. The number of nodes has to be kept at a minimum. A simplified model with more than 3 nodes is not meaningful. The thermal capacity C has been calculated assuming an adiabatic boarder along the construction.In order not to distort the surface admittance a high thermal resistance between C and C' is necessary in the models CRC and RCRC. These two aspects motivate the placing of C' at the exterior surface. As most modern insulated constructions are built of high density surface layers with low density insulation in between, the chosen models are realistic.

To meet the specifications given above, C' of the models CRC and RCRC is calculated to give the correct transmittance for the 24 hour period. Since only one parameter can be varied this only applies to the amplitude of the transmittance. To estimate the constant C', the follwing assumptions are made. If the surface temperature $\tilde{\vartheta}_S$ is kept at zero, this means that the temperature of C in both models is practically zero since in the RCRC model R'>>R. For the same reason since the resistance R' of the RCRC model is close to the total resistance, the thermal capacity C' for both models can be estimated at the same time using the total resistance of the construction.

The thermal transmittance of a construction is defined in equation (5.13).

$$T_D = \frac{\tilde{q}_S}{\tilde{\vartheta}'_S} \qquad (\tilde{\vartheta}_S = 0) \qquad (5.39)$$

The thermal transmittance of the networks CRC and RCRC, figure 5.15, would att all frequencies equal the steady state transmittance since fixing the external surface temperature implies a fixed temperature for the thermal capacitance C'. Instead the ratio between the heat flows $\tilde{q}_S$ and $\tilde{q}'_S$ with constant surface temperature is chosen. This ratio for which the letter ξ is used can from equation (4.24) be calculated as

$$\xi = \frac{\tilde{q}_S}{\tilde{q}'_S} = D - \frac{CB}{A} \tag{5.40}$$

The equivalent network, based on the above assumptions, for the constructions transmittance is shown in figure 5.16.

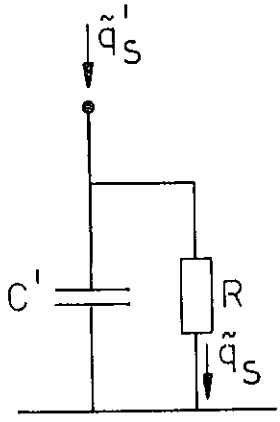

FIG. 5.16. Equivalent network for construction transmittance.

The ratio ξ' between $\tilde{q}_S$ and $\tilde{q}_S$ of figure 5.16 is

$$\xi' = \frac{1}{1 + i\omega RC'} \tag{5.41}$$

The magnitude of C' is then calculated from the equation

$$C' = \frac{1}{\omega R} \left| \frac{1}{\xi} - 1 \right| \qquad (T = 24h) \tag{5.42}$$

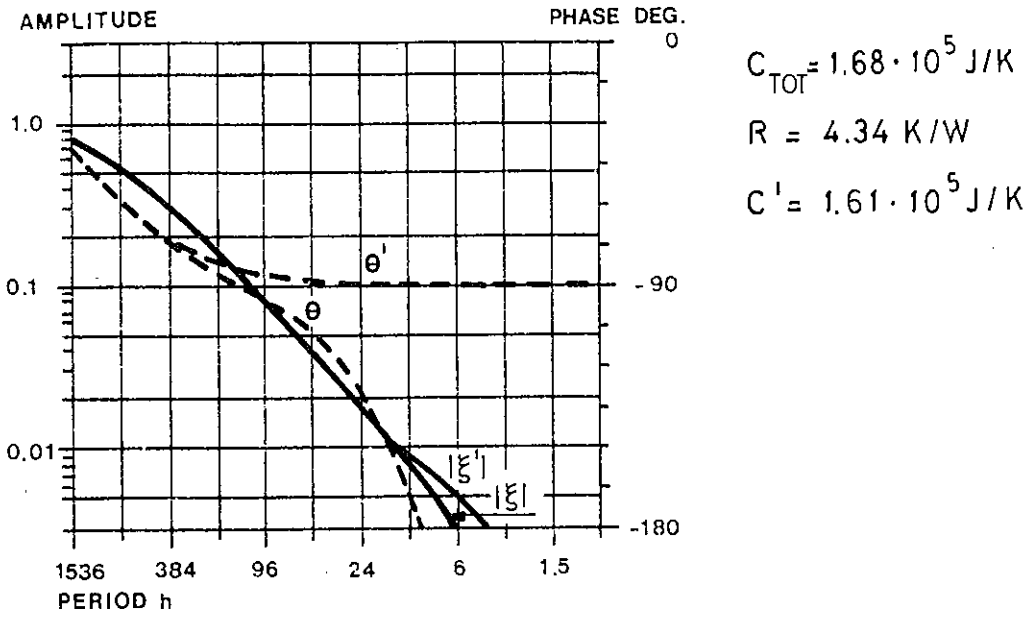

FIG. 5.17. The heat flow ratio according to equation (5.40), (ξ , θ) and equation (5.41), (ξ' , θ') for construction 1 of table 5.1.

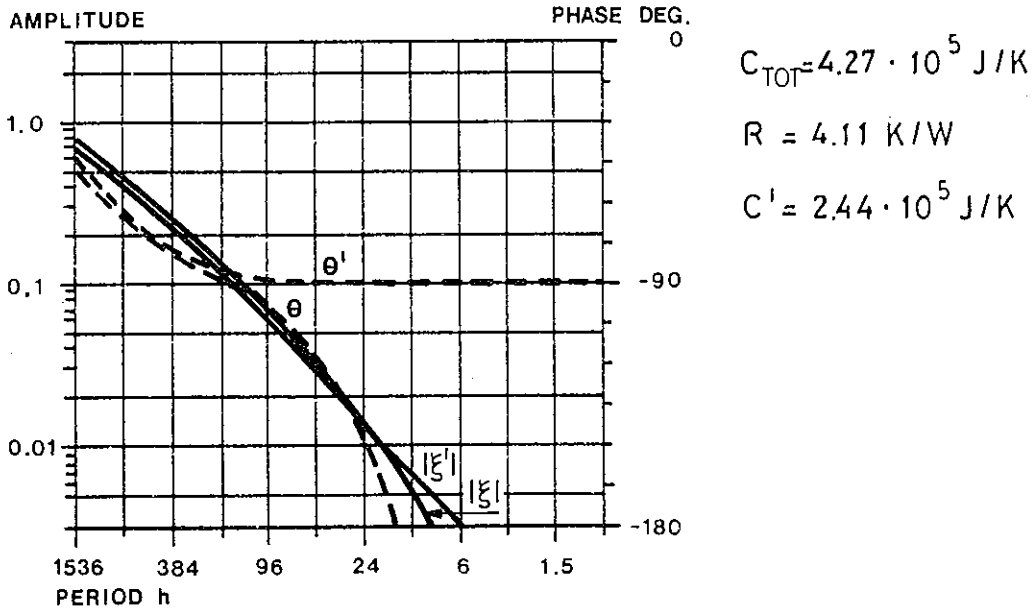

FIG. 5.18. Same as in figure 5.17 for construction 2 of table 5.1.

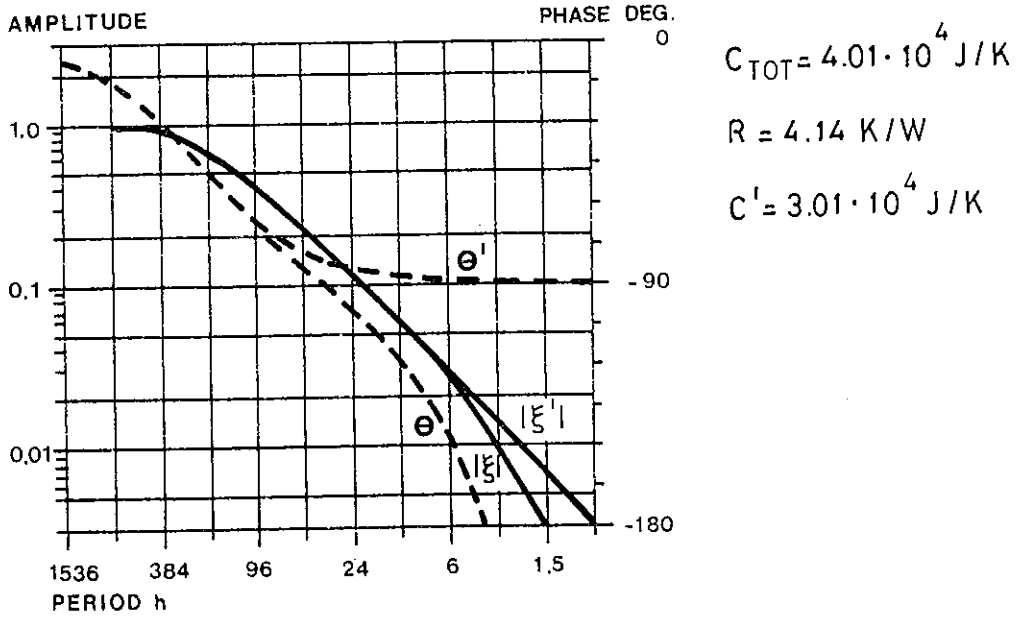

FIG. 5.19. Same as in figure 5.17 for construction 3 of table 5.1.

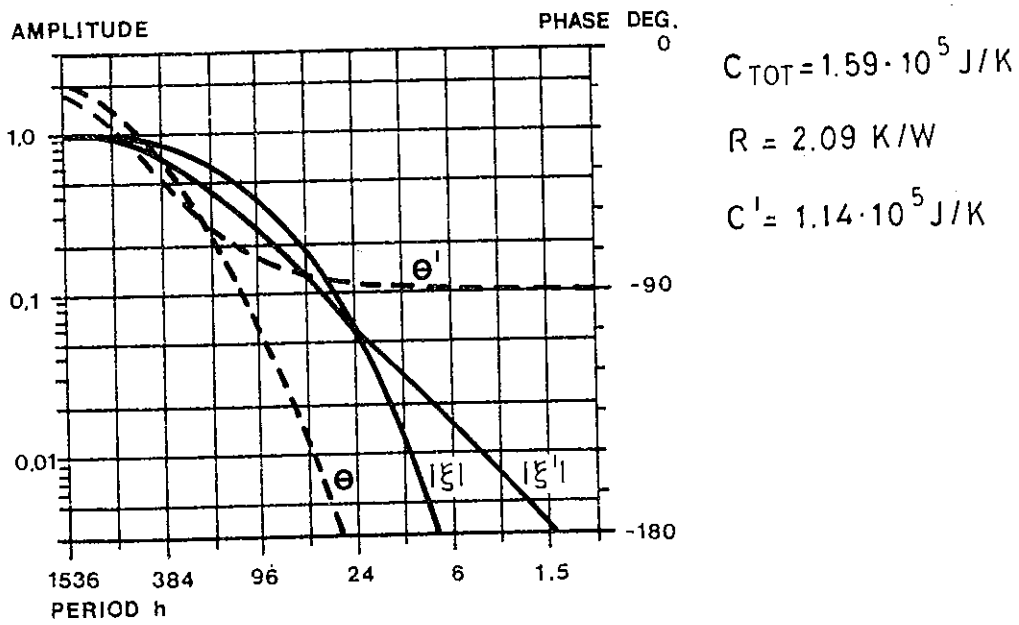

FIG. 5.20. Same as in figure 5.17 for construction 5 of table 5.1.

In figures 5.17 - 5.20 the heat flow ratios calculated according to equation (5.40) and equations (5.41-42) are compared for the construction alternatives 1, 2, 3 and 5 of table 5.1. For the constructions 1, 2 and 3 the magnitudes of the heat flow ratios are in good agreement for the simplified model down to periods of 3 or 6 hours. At these periods the heat flow wave is damped to such a degree that a deviation has no practical significance. The phase shift varies between 1 and 3 hours at the 24 hour period. These rather favourable results, bearing in mind the simplicity of the model, stem from the fact that the distribution of the thermal capacity within the construction corresponds very well to the assumed model. A construction with uniform mass distribution, a roof made of aerated concrete, is studied in figure 5.20. Here the magnitudes of the heat flow ratios are separated at frequencies lower than the reference frequency and the deviations both in magnitudes and phase are considerably greater than for the constructions 1, 2 and 3.

The conclusion is that the accuracy provided by a model of type RCRC, with the described parameters, is sufficient for quantitative calculations of indoor climate processes, that is, if the processes can be represented by discrete hourly values, and the non-steady conduction through the external constructions is a relatively small part of the time dependent thermal load. Introducing a single capacitance to represent the surface admittance generally implies reduction of the validity at higher frequencies. However as will be shown later on fairly accurate calculations of the room climate can be carried out using the simple C-model. It also has the advantage that the construction admittance can be characterized with one single parameter, a thermal capacity, that has a simple interpretation. A problem that will be studied in the next chapter is the combination of surface admittances to estimate the admittance for a whole enclosure. The solution is simple if based on the C-model.

5.3 THE PROPOSED PARAMETER

In this section a suitable parameter for the description of the non-steady state performance of a construction, "Active heat capacity", is presented. A simplified procedure to estimate the active heat capacity with the aid of two diagrams is also given, together with a strict mathematical definition based on the results of section 5.2.

The choice of the parameter proposed below has been made to fullfill the specifications in section 5.1. Consequently the parameter is to describe the admittance of the construction rather than the non-steady transmittance. In section 5.2 three different models to describe the admittance at a surface of a construction have been studied, i.e. constant admittance given by the 24h value, the C-model and the RC-model.

The RC-model is valid in a larger frequency interval than both the constant admittance model and the C-model. The use of two parameters R and C to describe the admittance would make comparison of different constructions rather complex. The choice between the C-model and the admittance is not difficult since a heat capacity placed at the surface has a clearer physical interpretation than the admittance and is, as shown above valid in a larger frequency interval for most constructions. An interesting difference between the two models is that, at higher frequencies, the amount of heat absorbed by the constructions, will always be overestimated by the C-model while it is underestimated by the admittance. Another thing that has to be pointed out is that the C-model gives better agreement than the admittance only when the surface resistances are excluded. These are included in the calculation of the admittances as they are given in the IHVE guide (1970) and by Milbank and Harrington Lynn (1974).

5.3.1 Active heat capacity

The active heat capacity is a property given to the surface of a construction. Physically it can be described as a heat storage per square meter concentrated at the surface that gives the same amplitude ratio between surface temperature and heat flow generated at the surface as the real construction when the temperatures at both surfaces are oscillating with the same amplitude and phase and with period 24 hours. Mathematically the active heat capacity is defined by equation (5.32). From the definition of the active heat capacity it is obvious that an asymmetric construction is described by two different active heat capacities, one for each surface. For external constructions the characteristics of the outer surface are of no importance while asymmetric partitions have to be described by two different values.

The active heat capacity below is denoted by C_A and has the unit J/m^2K.

An exact calculation of the active heat capacity can hardly be carried out manually for multilayer constructions while it is an easy task for a minicomputer. The calculation is started by forming the matrix element A_k, B_k, C_k and D_k given by the equations (4.17-22) for each layer k and ω corresponding to the 24 hour period or

$$\omega \simeq 7.27 \cdot 10^{-5} \quad \text{rad/s}$$

By successive multiplications of the matrices for the different layers as shown in equation (4.25) the overall matrix (A, B, C, D) is formed. Then the elements of the flow temperature matrix E and F are calculated from the equations (4.28 and 4.29) and finally the active heat capacity C_A is calculated as in equation (5.32).

$$C_A = \left| \frac{E + F}{\omega} \right| \qquad (5.43)$$

The active heat capacity could of course be defined assuming a constant temperature at the other side of the construction which would give

$$C'_A = \left| \frac{E}{\omega} \right| \qquad (5.44)$$

to be used for partitions against locals with constant temperature. Also if the structure can be considered as semi-infinite, as is the case for ground constructions, F equals zero.

5.3.2 A basis for an approximative method for calculation of the active heat capacity

Even if the active heat capacity has a clear mathematical definition it is of limited practical value since a user without access to some computing power would have to rely on pretabulated values. With the variety of materials and dimensions that may occur in building construction this would be a severe drawback. The admittance procedure as presented in the IHVE guide (1970) gives no simplified means for estimating construction admittances and this will, for many users, limit the applicability of the method to constructions identical or similar to those given in the enclosed set of tables.

The aim is to give a simple procedure to estimate the active heat capacity for the surface of a construction both for the reasons mentioned above and also to give the user a quantitative and qualitative knowledge of which parameters affect this important quantity.

The simplified method is based on two major observations.

1. The contribution of each layer to the active heat capacity cannot exceed the active heat capacity for a homogeneous wall with the same material data and twice the thickness of the layer. The contribution of each layer is thus calculated according to equation (5.45)which is derived from the definition of the active heat capacity, equation (5.43), the elements of the modified admittance in the equations (4.28, 4.29 and 4.30) and the elements of the frequency response matrix given by the equations (4.17-4.22).

$$C_A = \frac{1}{\omega} \left| - \lambda k \ (1 + i) \ \frac{\sinh kl \ (1+i)}{\cosh kl \ (1+i)} \right| \qquad (5.45)$$

l is the thickness of the layer, m.

In this way an upper limit to the contribution of each layer to the active heat capacity is found. Equation (5.45) is given graphically in figure 5.21 for a number of commonly used building materials. The effective thickness l_E corresponding to the calculated active heat capacity for the layer k is expressed as a function of the real thickness l. At small thicknesses the whole thermal capacity of the layer is accessible but as the thickness increases an upper limit to the active heat capacity is reached. Similar curves are given by Adamsson (1970) for the parameters of RC-models equivalent to homogeneous walls with symmetric boundary conditions.

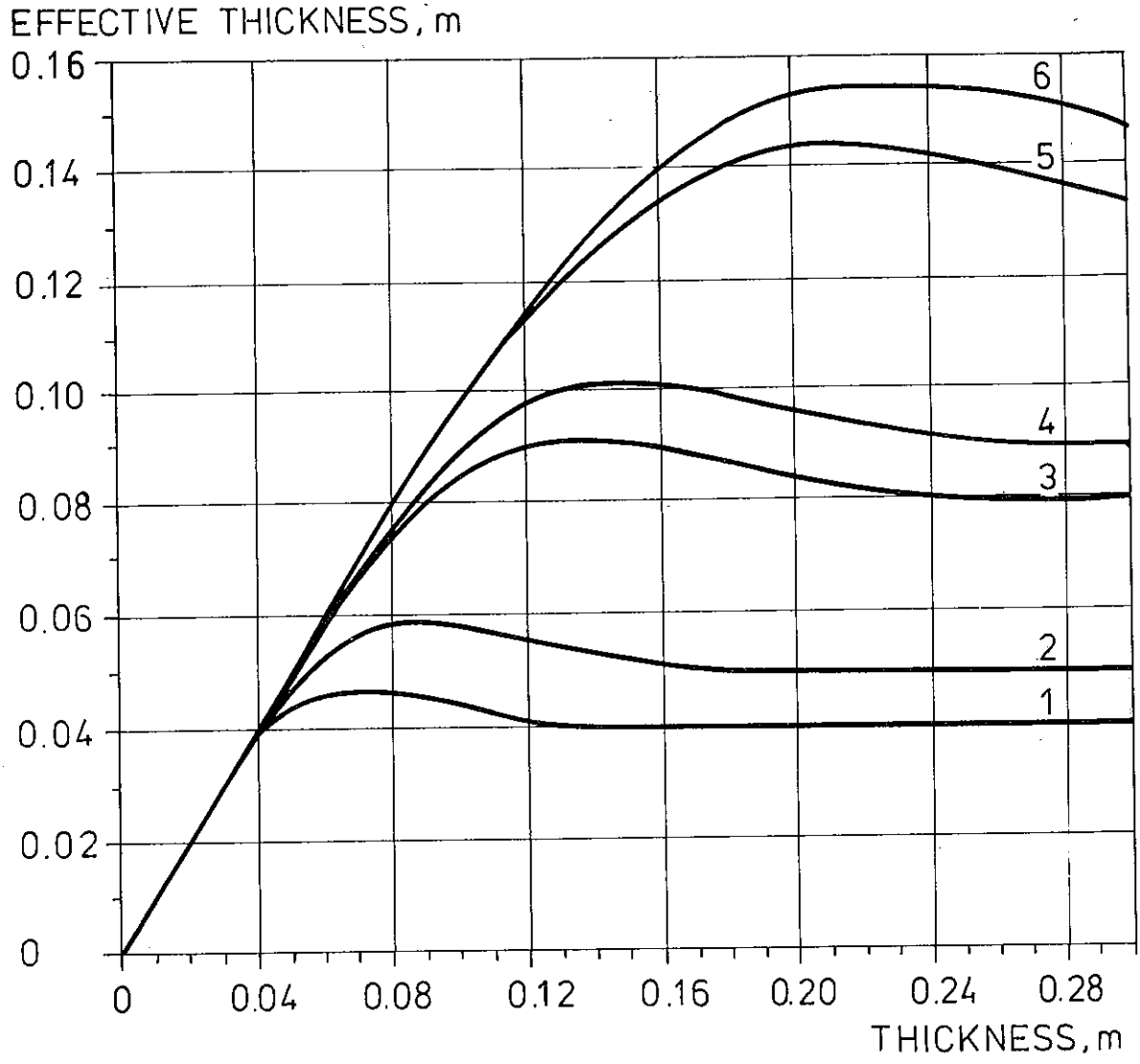

FIG. 5.21. Effective thickness for a homogeneous layer of different building materials.

Material	λ W/mK	ρ kg/m^3	C J/kgK
1. Wood	0.14	500	2300
2. Aerated concrete	0.12	600	1050
3. Brick	0.60	1500	840
4. Concrete	1.2	2400	880
5. Cellular plastic	0.04	25	1400
6. Mineral wool	0.04	30	1000

2. The contribution of each layer to the active heat capacity is limited by the thermal resistance between the layer and the surface. Figure 5.22 shows an idealized situation where a layer with heat capacity C', J/m^2K, and infinite thermal conductivity is covered by a layer with thermal resistance R, m^2K/W, but no heat capacity.

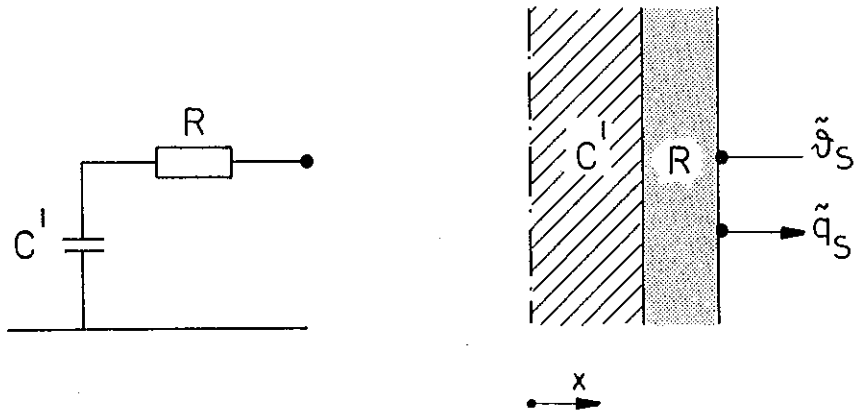

FIG. 5.22. Idealized wall construction.

The admittance for the construction is

$$Y = \frac{-1}{R + \frac{1}{i\omega C'}} \tag{5.46}$$

and as the construction is symmetrical Y also equals the modified admittance. Equation (5.43) gives the active heat capacity in terms of the modified admittance which in this case can be written

$$C_A = \frac{1}{\omega} \left| Y \right| \tag{5.47}$$

The corrected heat capacity is therefore calculated

$$C'' = \frac{1}{\sqrt{\omega^2 R^2 + \frac{1}{C'^2}}} \tag{5.48}$$

This relation is given graphically in figure 5.23. The heat capacity corrected with respect to the thermal resistance between the layer and the surface is given as a function of the original heat capacity for a set of thermal resistances.

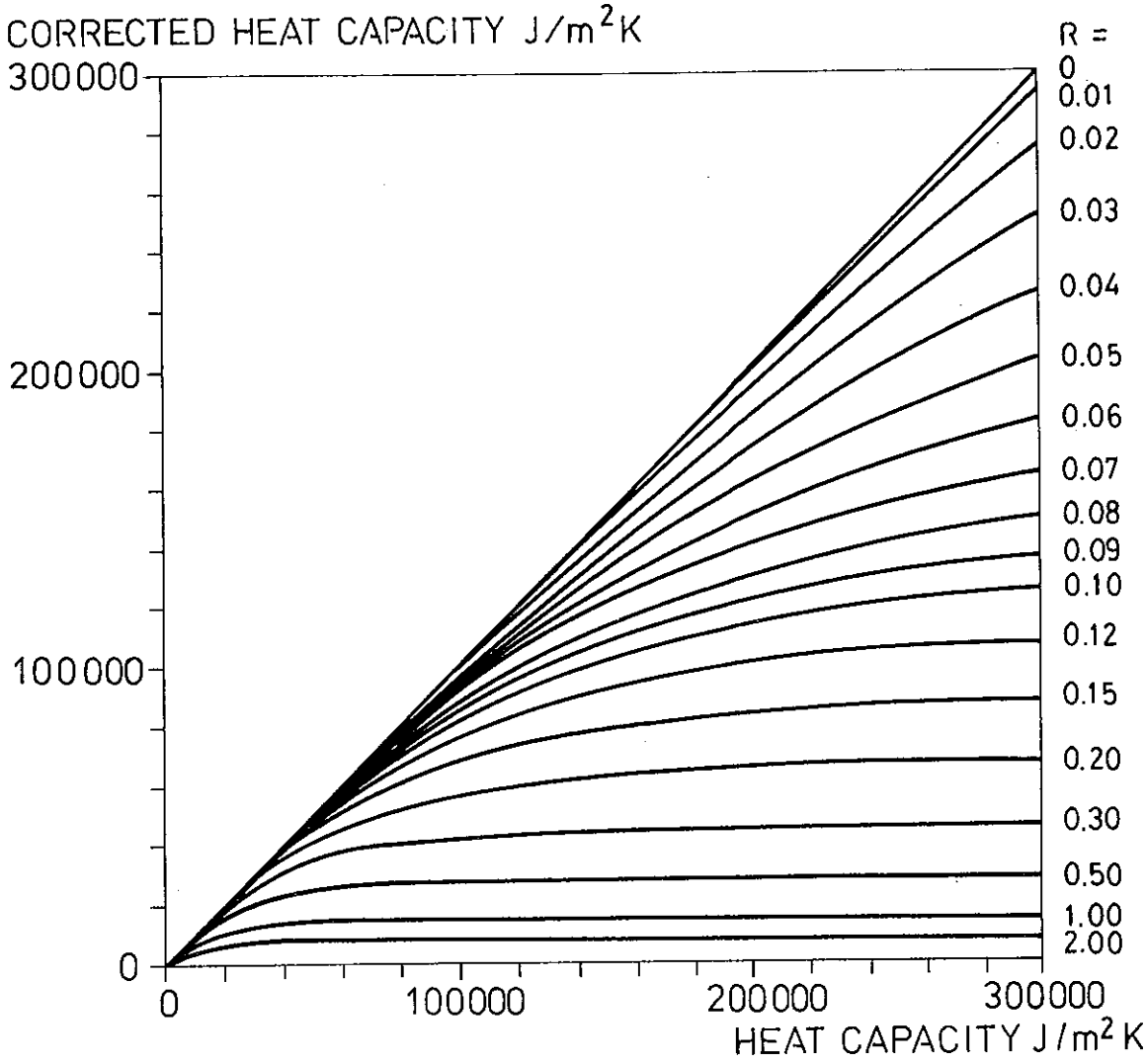

FIG. 5.23. Active heat capacity for a single layer corrected with respect to the thermal resistance between the layer and the surface.

The two relations, equations (5.45) and (5.48), or the corresponding diagrams, can be used to give an upper limit to the contribution of each layer to the active heat capacity.

In a construction that is exposed to symmetrical boundary conditions, in this case the surface temperature variations, the total capacity of the construction has to be divided between the two sufaces. For a symmetrical construction this is no problem since no heat flow crosses the line of symmetry. For well insulated constructions figure 5.23 shows that the heat capacity on the other side of an insulation layer with a thermal resistance 2.0 m^2K/W or more is of small significance. For asymmetrical constructions with low thermal resistance,

as construction 10 of table 5.1, there is no clear line of division. The only thing that can be said is that it is somewhere between the line where half of the thermal resistance is passed and the line where half of the total heat capacity is passed. If the part of the construction included in the calculation is chosen so that both those limits are passed this leads to an upper limit for the active heat capacity. Another limiting factor, which in some cases will prove useful, is that the sum of the active heat capacities for both sides of the construction can never exceed the total heat capacity.

In figure 5.21 the limit to the heat capacity is given in terms of an effective thickness rather than the accessible heat capacity. The reason for this is that the effective thickness is less sensitive to moderate changes in material data and this gives the user an opportunity, within reasonable limits, to apply different material data and still make use of the diagram. For concrete the differences in thermal conductivity used by different sources are too great.

A separate diagram for concrete is given in figure 5.24 for a set of four different thermal conductivities. Other data are the same as in figure 5.19.

In figure 5.22 the material layer between the surface and C' is assumed to be purely resistive. Another possibility is to calculate the admittance and the active heat capacity at the surface using real material data for the surface layer. The resulting equation for the active heat capacity then becomes, in terms of the matrix elements of equation (4.16) for the surface layer.

$$C_A = \frac{1}{\omega} \left| \frac{C - Di\omega C'}{A - Bi\omega C'} \right| \qquad (5.49)$$

The heat capacity calculated in this way is given graphically for concrete, brick, wood and aerated concrete in figures 5.25-5.28.

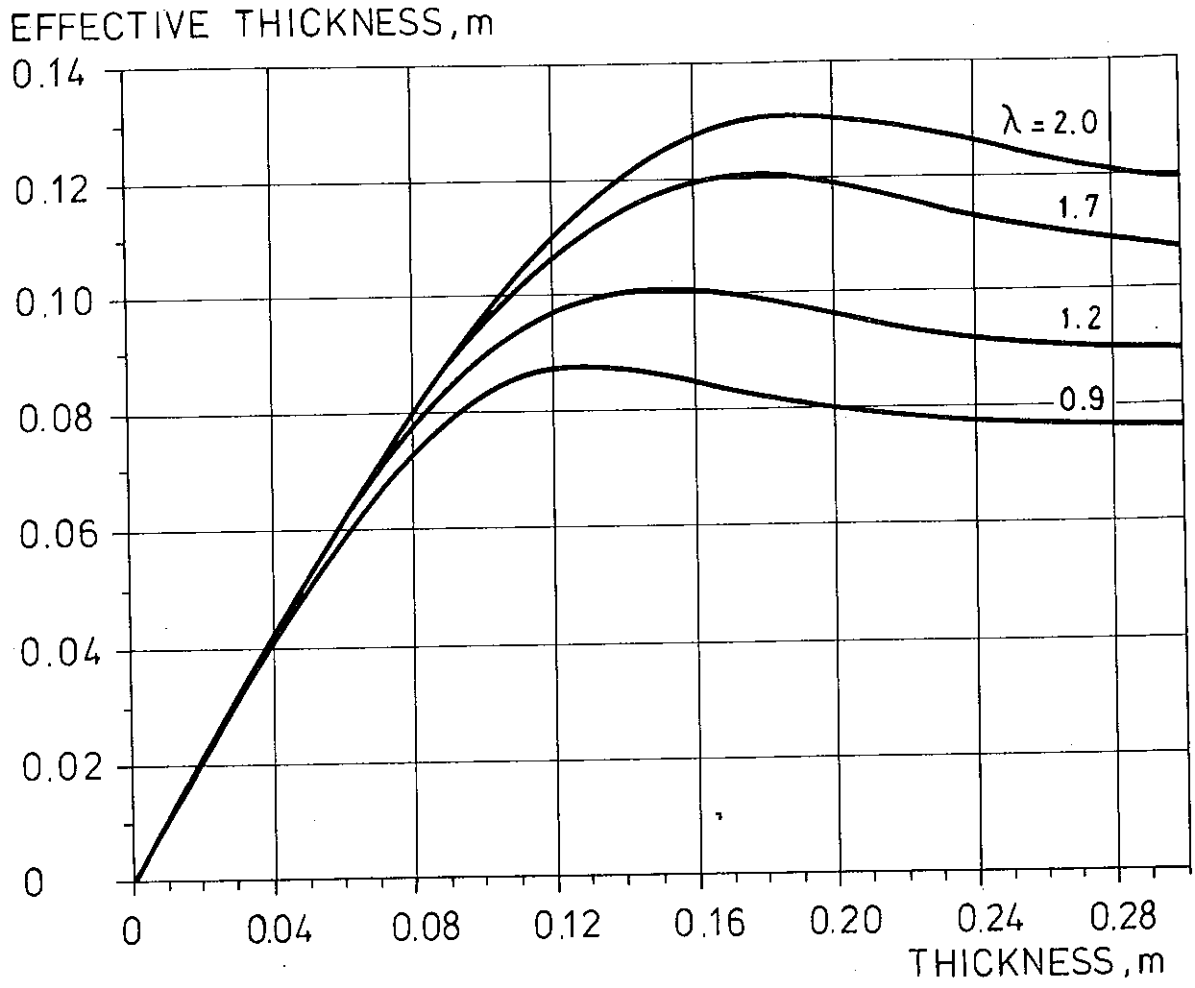

FIG. 5.24. Effective thickness for a homogeneous layer of concrete. The thermal conductivity, λ has four different values while density and specific heat capacity are the same as in figure 5.21.

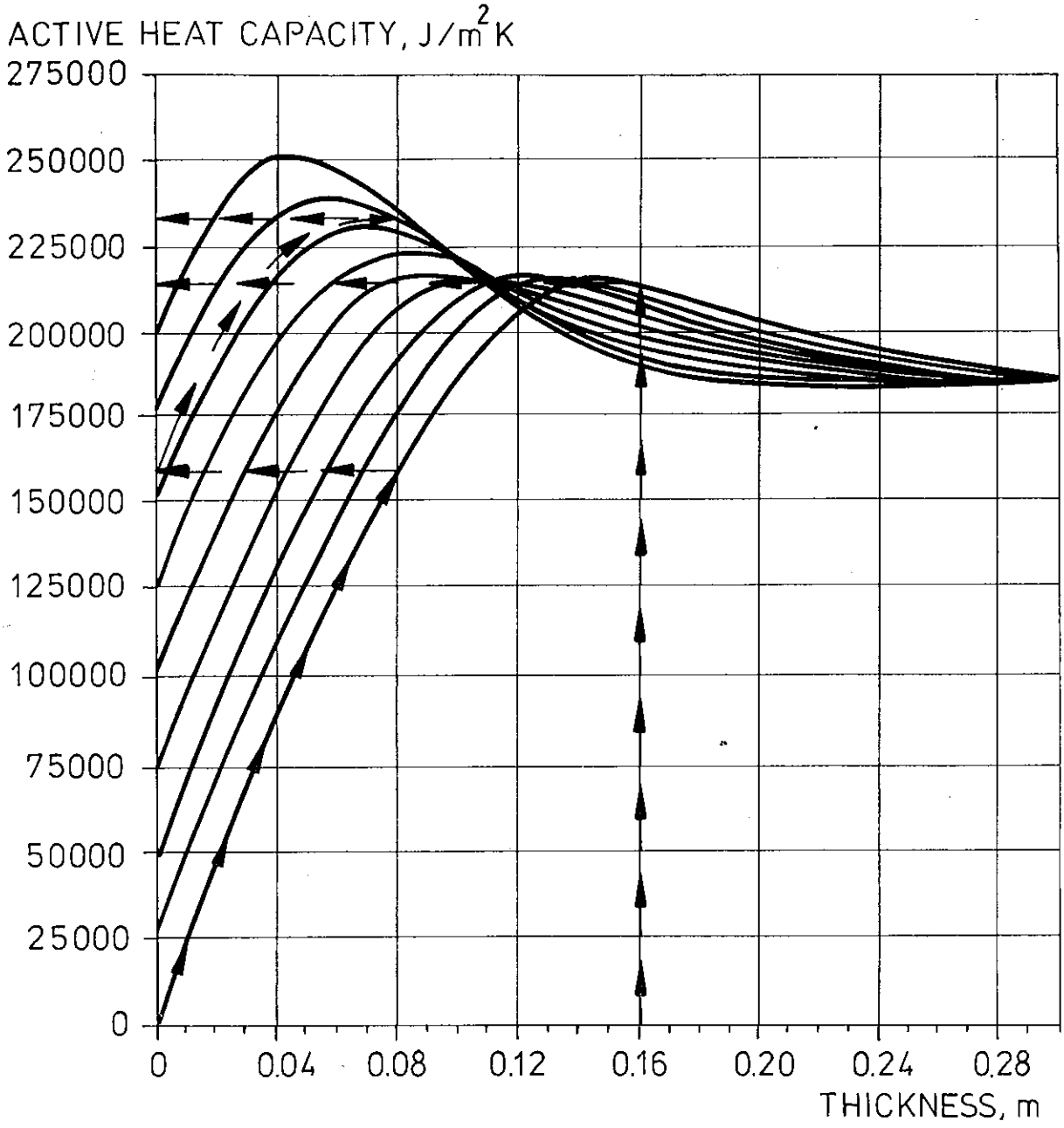

FIG. 5.25. Active heat capacity for the idealized construction of figure 5.22 if the surface layer consists of concrete with material data as given in figure 5.21. The curve for each value for the thermal capacity C' can be identified by the active heat capacity when the thickness equals zero. As an example we consider the active heat capacity for a 16 cm thick layer of concrete that is treated as two separate layers of thickness 8 cm. First we follow the curve for C'=0 to 8 cm resulting in an active heat capacity of 160000 J/Km^2. Starting again from zero thickness following the corresponding curve gives the the active heat capacity for both layers as 230000 J/Km^2. Direct use of the diagram for 16 cm gives 215000 J/Km^2.

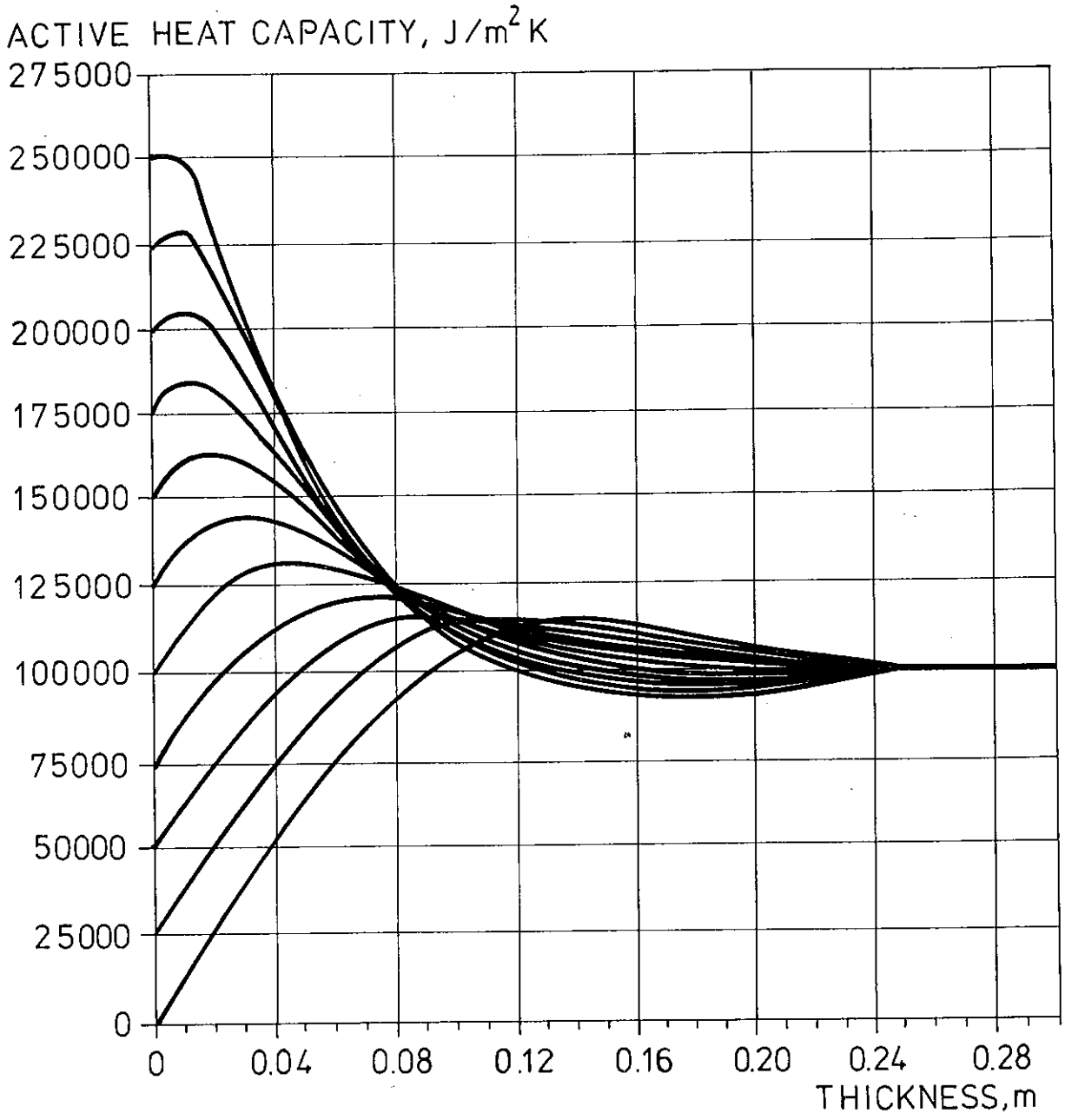

FIG. 5.26. Same as in figure 5.25 for brick.

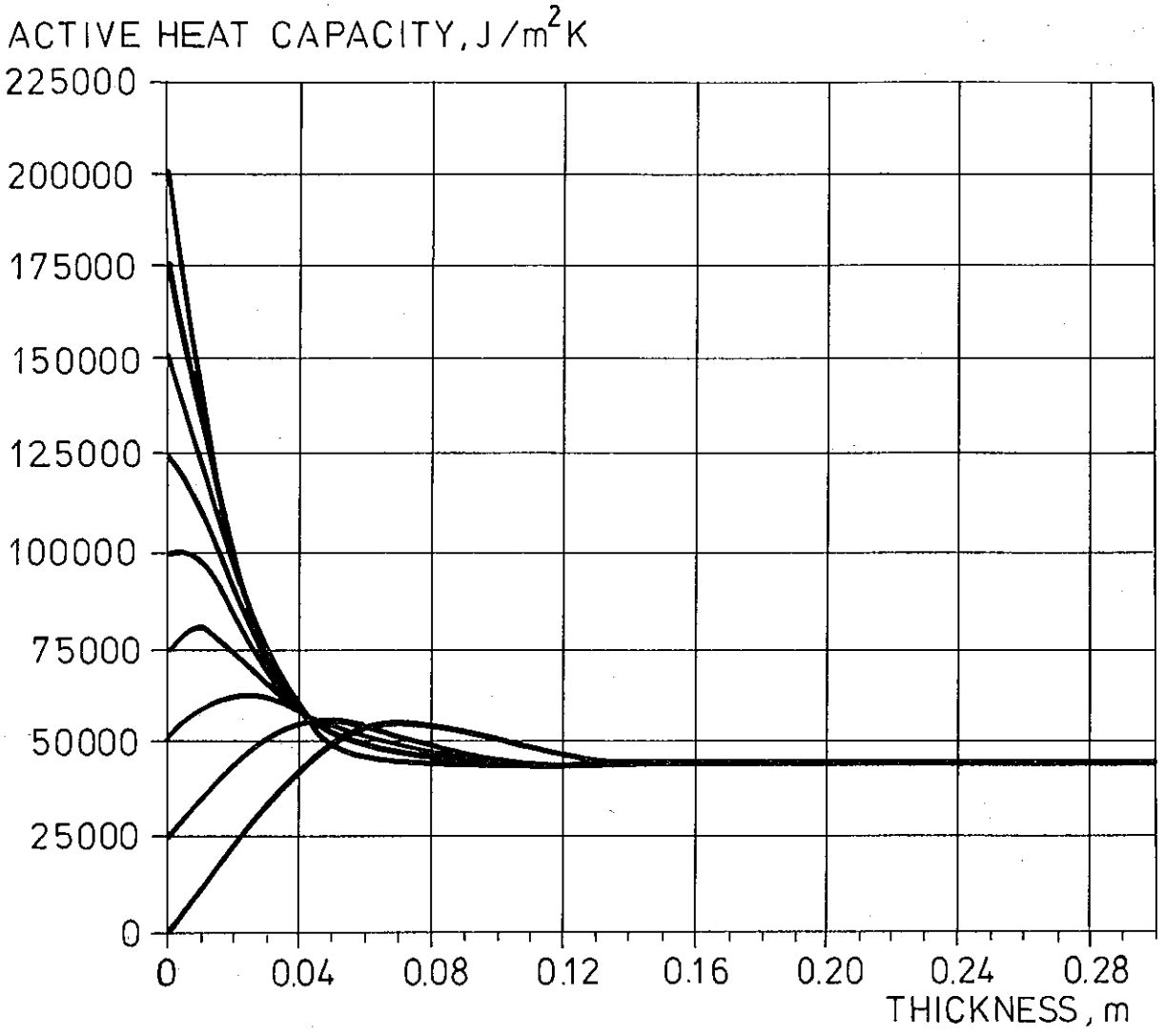

FIG. 5.27. Same as in figure 5.25 for wood.

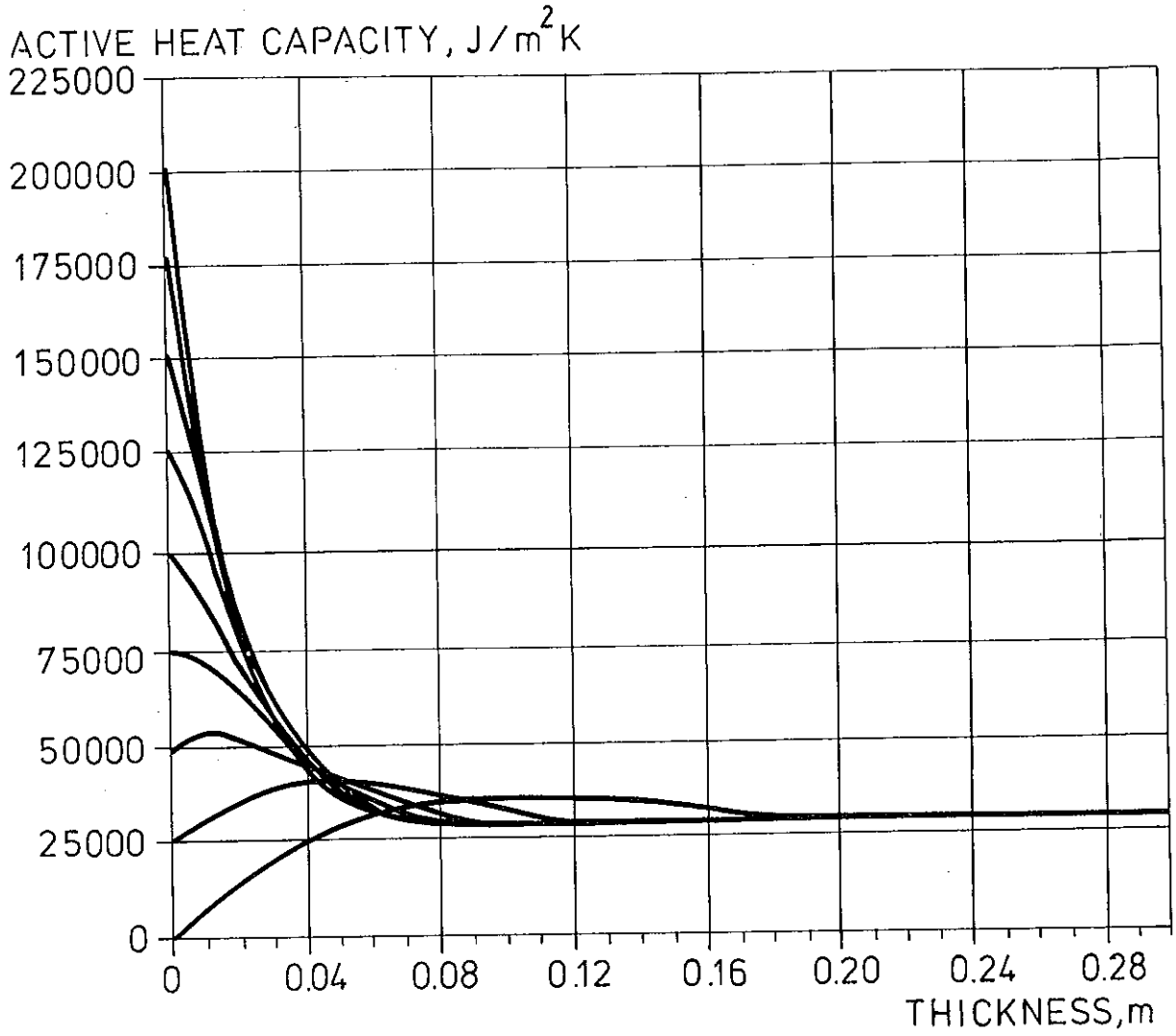

FIG. 5.28. Same as in figure 5.25 for aerated concrete.

5.3.3 An approximative calculation method to estimate the active heat capacity

Based on the principles and formulae discussed in the previous section a calculation procedure for the active heat capacity is formulated below.

For each homogeneous layer k from the very surface of the construction to the limit where half of the total thermal resistance and half the total heat capacity of the construction is reached proceed as follows:

Calculate the heat capacity for the layer k C'_k J/m^2K using figure 5.21 for the effective thickness or equation (5.45).

$$C'_k = l_E \rho c \qquad (5.50)$$

Correct the heat capacity C'_k with respect to the thermal resistance between the layer and surface using figure 5.23 or equation (5.48). The resulting heat capacity is called C''_k.

The active heat capacity for the surface is then calculated as

$$C_A = \sum_k C''_k \qquad (5.51)$$

If the sum of the active heat capacities for both surfaces exceeds the total heat capacity of the construction they are reduced proportionally.

The procedure given above has the advantage that it is at the same time fast as it covers all multilayer constructions and gives detailed information about the contribution of each layer, how it is limited and how the material layers should be arranged to make optimum use of the thermal capacity of the building materials. The procedure gives almost exact answers for homogeneous constructions while the inaccuracy is as a rule increased as the number of layers increases and in the presence of asymmetry. It is also of interest that the procedure comes up with a different answer if an internal material layer with a high thermal capacity is divided into two separate layers.

An improvement in accuracy and generality could be achieved by making successive use of the diagrams in the figures 5.25-28 together with figure 5.23, which still could be used for cavities and lightweight insulation. This however calls for a greater number of diagrams and one must also consider that layers of different heavy materials coupled in series are rather uncommon in modern constructions.

In table 5.2 the active heat capacity for the constructions of table 5.1 is compared to the active heat capacity estimated by the procedure above. The agreement is good even for the asymmetric construction nr 10. The estimated values are, as explained above, always expected to exceed the computed values. This is not so in all cases due to reading errors in the diagrams used. The procedure has been tested against a number of more complicated structures and the percentage error has proved greatest for lightweight constructions composed of many different material layers, up to +30%.

TABLE 5.2 Comparison between estimated and calculated active heat capacity for the constructions of table 5.1. The matrix elements E and F are also given.

	E		F		C_A J/m^{2}K	C_A J/m^{2}K
Alt	Re	Im	Re	Im	Calc	Est
1	-0.251	- 0.654	0.054	-0.155	11450	10500
2	-5.330	-12.559	0.032	-0.187	189790	190000
3	-0.256	- 0.647	0.220	-0.087	10100	10300
4	-0.901	- 6.401	0.199	-0.201	91290	93500
5	-1.663	- 1.659	-0.132	-0.066	34220	34000
6	-0.420	- 0.658	0.225	-0.180	11840	12600
7	-3.707	- 0.620	3.694	-0.146	10530	10500
8	-9.367	- 7.306	6.816	-3.479	152400	150000
9	-8.845	- 8.372	4.841	-3.689	174760	177000
10	-2.827	- 0.792	2.695	-0.565	18750	20300
10*	-2.994	- 2.000	2.695	-0.565	35590	34500

* from opposite side of the construction

5.4 MODELS FOR CONSTRUCTIONS WITH TWO-DIMENSIONAL HEAT FLOW

The solution of frequency response for two-dimensional heat flow problems given in section 4.1.2 can be applied to calculate the admittances for constructions with thermal bridges or non-planar geometry. Combined with the technique of section 5.2.2, this provides an opportunity to identify both the active heat capacity and the parameters of simple RC-models for such constructions.

A complication that has to be kept in mind is, however, that neither the surface temperatures or heat flows are constant along the boundaries. This means that the admittance for a surface cannot be calculated independent of the surface heat transfer characteristics.

The boundary conditions for the calculation are given by an ambient air temperature ϑ_A and a surface heat transfer coefficient α. The quantity calculated for each boundary with area A is the heat flow at the surface $\tilde{Q}_S$.

The average admittance for each boundary and if the surface heat transfer coefficient is included is then given as

$$Y_\alpha = \frac{\tilde{Q}_S}{A \cdot \vartheta_A} \tag{5.52}$$

To establish a relation for the surface admittance we make use of the relation

$$\tilde{Q}_S = A\alpha\,(\vartheta_S - \vartheta_A) \tag{5.53}$$

or

$$\vartheta_S = \frac{\tilde{Q}_S}{A\alpha} + \vartheta_A \tag{5.54}$$

The surface admittance is then given as

$$Y = \frac{\tilde{Q}_S}{A\vartheta_S} = \frac{\tilde{Q}_S}{\frac{\tilde{Q}_S}{\alpha} + A\vartheta_A} = \frac{\alpha Y_\alpha}{\alpha + Y_\alpha} \tag{5.55}$$

The construction alternatives given in table 5.1 are simplified to only consist of planar layers. For construction alternative 3 the insulation layer would in real constructions contain wooden studs 0.045 x 0.15 m^2 with a distance between the centres of 0.60 m.

In figure 5.29 are compared the solutions in one-dimension through different sections and the two-dimensional solution given in section 4.1.3.

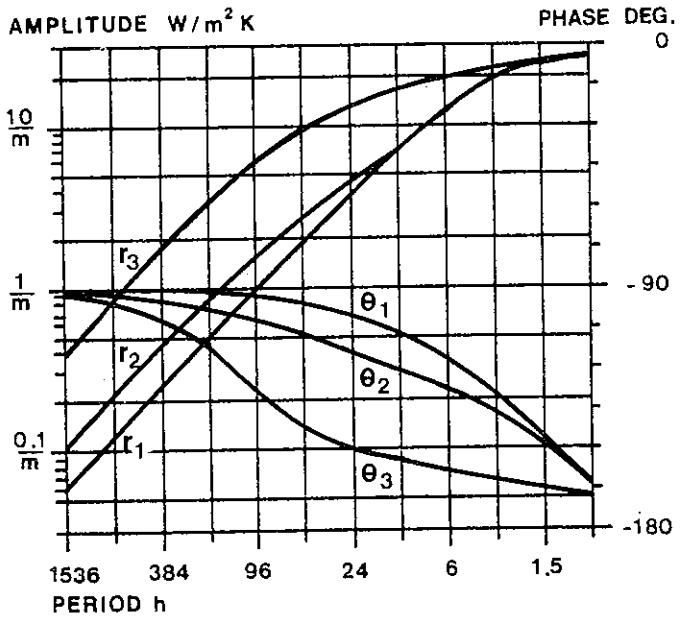

FIG. 5.29. The modified admittance for construction 3 calculated in three different ways: (1) for the construction as described in table 5.1, (2) for the two-dimensional heat flow problem and (3) for a section through the wooden stud. α equals 8 W/m^2K. The thermal resistance m is valid for alternative (1).

6 CALCULATION OF ROOM HEAT BALANCE

In this chapter models for thermal performance of room systems of the type presented in Chapter 2 are studied.

The heat transfer in building components is given above in terms of transfer operators which relate the heat flow at the inside surface of a construction to the temperature variations at the internal or external surfaces. These transfer operators can either be given as transfer functions as in equation (4.61) or complex numbers when only one frequency component is involved as in equation (4.28) or an equivalent RC-network as in figure 4.8. Simplified transfer operators are the 24h admittance and transmittance defined in section 5.2.1 and the RC-networks of varying complexity derived in section 5.2.2. The proposed construction parameter the active heat capacity C_A, can be regarded as a transfer operator relating temperature and heat flow variations at the surface of a construction.

The calculation of the heat balance within a room as in figure 2.1 leads to the solution of a system of linear equations where the unknown variables are the temperature of the air together with the different surface temperatures and in some cases the power needed to maintain these within certain limits. For each unknown quantity a heat balance equation is established. In each equation the time-dependent heat flow characteristics can be expressed with any one of the transfer operators given above. The choice of transfer operators will however affect the solution in various ways.

Simplified models for the balance of whole enclosures or room systems are derived below. According to the specification listed in chapter 1 and section 5.1 the simplest models and parameters given must not assume the use of computer power. Separate treatment of each surface of the room implies an equation system of at least 7 unknown variables and therefore the first step towards a simple model is to combine the heat transfer operators of the different surfaces. That is, to transform the system into a simplified model of the type shown in figure 2.2 or figure 2.3. The response of the simple model can then be solved manually in the time domain for different curveforms

and even for non-linear systems. That is, the ventilation can be varied.

The accuracy of the simplified solution is limited in the frequency plane by the accuracy of the heat transfer operators chosen for the time-dependent parts of the heat flow pattern. Another important source of error arises when all the surfaces of the room are combined. The heat exchange by convection and radiation within the room is also simplified due both to the fact that all surfaces are given the same temperature and that the convection heat transfer coefficient is given a constant value independent of the temperature difference.

6.1 MODELS FOR ROOM HEAT BALANCE

The heat balance for the room system can be regarded as a combination of the heat balances for the isothermal parts of the discretisized system. That is, the different surfaces and the room air. The heat flows generated within the system can either be expressed in terms of the momentaneous values of the variables involved or be dependent on the prehistory of the variables. The latter are a result of time-dependent processes treated in chapter 4 and the former result from processes dealt with in chapter 3 and referred to as steady state. Figure 6.1 is a modification of figure 2.3 where a distinction is made between purely resistive heat transfer and heat transfer operators that can be realized as a network of resistances and capacitances. Figure 6.1 gives a system with only two isothermal surfaces. Each additional surface would be resistively coupled to the room air and other surfaces, and to an external temperature by a heat transfer operator.

The thermal capacity of the room air is not taken into account in figure 6.1. As will be shown below this is valid for most medium and low frequency processes. The influence of the air can be realized by a single thermal storage. It does not increase the calculation work considerably but can in some cases give rise to stability problems in finite difference solutions of the system.

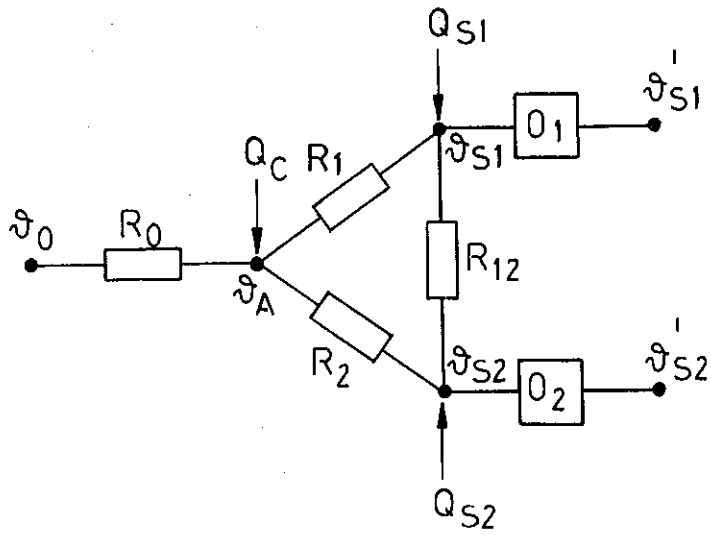

FIG. 6.1. Model of the room system with two different surface temperatures showing which heat transfer operators are resistive.

The resistance R_0 normally represents two heat transfer processes, that is the ventilation loss and transmission loss through windows. If the room is ventilated with outside air only and if the convective solar power gain is treated separately as shown in equation (3.42) R_0 is calculated

$$1/R_0 = k_W \cdot A_W + \frac{n \cdot \rho \cdot c \cdot V}{3600} \qquad (6.1)$$

If the convective heat transfer coefficient α_C is given a constant value for each surface the resistance between the room air and each separate surface k is calculated

$$1/R_k = \alpha_{Ck} \cdot A_k \qquad (6.2)$$

A_k is the area of surface k, m^2.

The resistances between each pair of surfaces represent the radiative heat exchange between the surfaces. The resistance has a physical interpretation if the process is linearly approximated and if there

are only two surfaces involved in the process. In this case R_{12} is calculated from the equation

$$1/R_{12} = A_1\alpha_S \tag{6.3}$$

if α_S is defined as in section 3.2.2.

In other cases the resistances would change with every new set of temperatures. The heat flows at the surfaces due to the radiation exchange are therefore calculated directly using the resulting radiosities of equation (3.11) and the resistances are only there to symbolize that the process is not time-dependent. Since the resulting heat flows in turn affect the surface temperatures the calculation process becomes iterative. Kreith (1965) gives an equivalent resistance network for linearized radiation exchange within a room which implies that an extra node is added to the model for each surface. Brown (1964) claims that for rooms with normal surfaces the long wave reflection can be neglected. If so the heat exchange between each pair of surfaces can be treated independently.

The transfer operators for the solid parts have been discussed in Chapter 4. The convective and radiative power gains are discussed in Chapter 2 and 3.

6.1.1 Alternative ways to simplify the model for room heat balance.

The division of the room system into a limited number of isothermal surfaces and air volumes is a simplification common for all present works in this field. Many authors of computer programs introduce further simplifications in order to reduce programming work and the computer time and capacity needed to solve each case. The complexity of the system is due to two main processes that is, the time-dependent heat flow through the opaque walls and the heat exchange between the surfaces and the room air. A simplified approach to the former process is treated in Chapter 5 and in this section different ways to simplify the internal heat exchange are discussed. It has been stated above that a practical limit for a model to be solved manually or by a programmable desk calculator is a model with not more than two or three unknown variables.

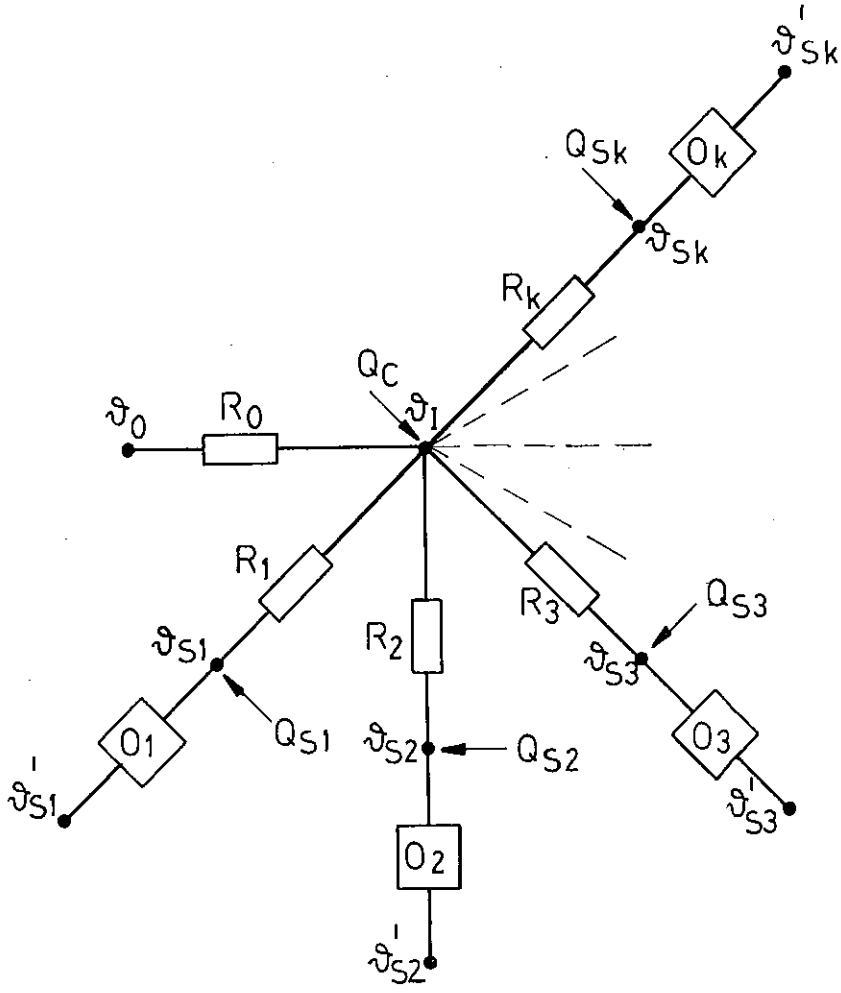

FIG. 6.2. Resulting model for a room system when the radiation exchange between the surfaces is neglected.

A simplification used and justified by many authors such as Mitalas (1965), Hauser (1977) and Muncey (1979) but rejected by others as Aittomäiki (1974), is to neglect the long wave radiation exchange between the surfaces. At the same time the convective heat transfer coefficients are modified so that the heat transfer from the surface to the surrounding surfaces equals the total heat transfer for convection and radiation. In the model in figure 6.1 this would imply that coupling between the surfaces via R_{12} no longer exists and the resistances R_1 and R_2 are reduced. The resulting model becomes a star network as shown in figure 6.2. The confusion over the validity of this simplification can partly be explained by the fact that the authors are referring to different modes of operation and partly by the fact that some authors treat this simplification together with another one: namely the assumption that all power supplied to the room is fed into the room air. The following aspects of the first simplification are discussed assuming that convective and radiative heat gains are treated separately.

Assume that all constructions of the room enclosure are the same, having identical external boundary conditions and that the radiative power gain Q_S is uniformly distributed over the surfaces. Consider the following cases:

o Constant air temperature

The ratio between the heat flow generated at a surface and the heat flow to the air is given by the surface factor defined in equation (5.17). Using $-i\omega C_A$ for the admittance, the amplitude ratio is given by

$$\frac{\hat{Q}_{S\to A}}{\hat{Q}_S} = \frac{1}{\sqrt{1 + \frac{\omega^2 C_A^2}{\alpha^2}}} \qquad (6.4)$$

This ratio is given in figure 6.3 for two different values for the active heat capacity C_A.

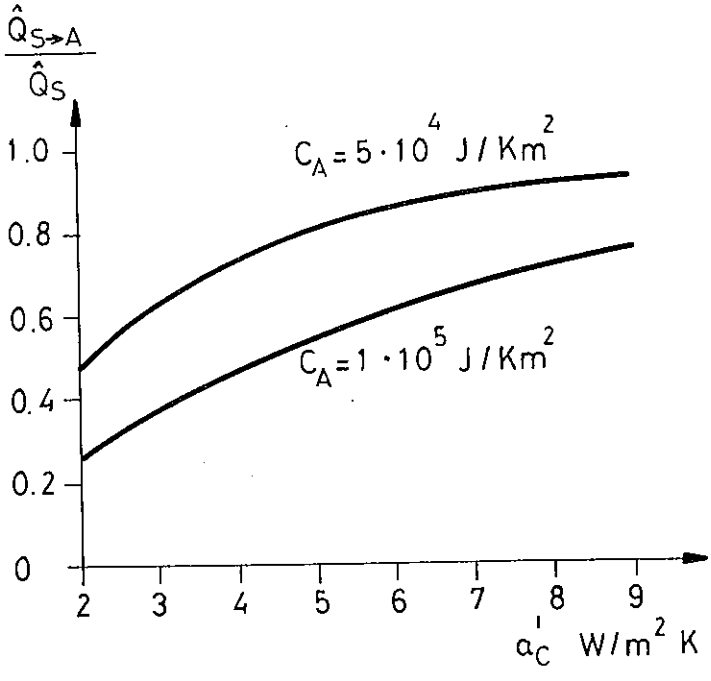

FIG. 6.3. Ratio between heat flow to the air at constant temperature and heat flow generated at the surfaces of a room depending on convective α value.

o Floating air temperature

In this case the resulting thermal resistance between the air and the surfaces R_C has to be put in relation to the resistance R_0 between the room air and the outside air.

$$\frac{R_C}{R_0} = \frac{k_W \cdot A_W + \frac{n \cdot \rho \cdot c \cdot V}{3600}}{A \cdot \alpha_C} \qquad (6.5)$$

A is the sum of the areas for all opaque surfaces, m^2.

For a room of normal dimensions and with a ventilation rate 0.5-1.0 h^{-1} this ratio is of the order of magnitude 0.1. If α_C is increased by a factor of 2 or 3 the resulting air temperature is increased by about 0.5 K under normal summertime conditions.

In the case of forced ventilation, if n equals 5 á 10 h^{-1}, the ratio of equation (6.5) is considerably larger. The order of magnitude is 0.5. The modification of α_C then has a relatively larger effect on the resulting air temperature which also implies that the ventilation loss is overestimated by the order of magnitude 30%.

o Convective power input

Assume that a 24 hour power wave is fed into the room air. If no heat is generated at the surfaces the active heat capacity can be corrected with respect to the surface thermal resistance in order to estimate its contribution to the damping of the air temperature oscillation. The influence of the surface resistance on this correction can be studied in figure 5.23. If the active heat capacity is 10^5 J/m^2K and the surface resistance is 0.5 m^2K/W the corrected active heat capacity is found to be about $0.27 \cdot 10^5$ J/m^2K. If the surface resistance is now reduced to 0.15 m^2K/W the corrected heat capacity is increased to $0.67 \cdot 10^5$ J/m^2K and the resulting amplitude of the air temperature variation is underestimated by 50%.

The conclusion that can be drawn from these observations is that for a normally ventilated enclosure under summertime conditions where a dominating part of the energy entering the room is absorbed by the surfaces, the inaccuracy introduced by the transform in figure 6.2 is limited to the calculation of the equivalent resistances. With increasing ventilation rate or convective power gain the inaccuracy increases due to the erroneous coupling between the room air and the surfaces.

One way to simplify the internal heat exchange without disturbing the convective surface heat transfer is to regard two or more surfaces as isothermal. Or, formulated otherwise, to assume that the resistance representing the long wave radiation heat transfer between each pair of surfaces is zero. To study the consequences of this assumption on the resulting air temperature for a room the response of the model of figure 6.4 is calculated. The model includes two different isothermal surfaces for which the admittances are given in terms of the active heat capacity. Surface 1 is plane and surrounded by surface 2 and consequently the resistance connecting the surfaces is given by equation (6.3). If the heat flows to the surfaces and the outside air temperature are sinusoidal with an angular velocity ω the resulting temperatures for the room air and the surface temperatures can be solved from the equation system in equation (6.6).

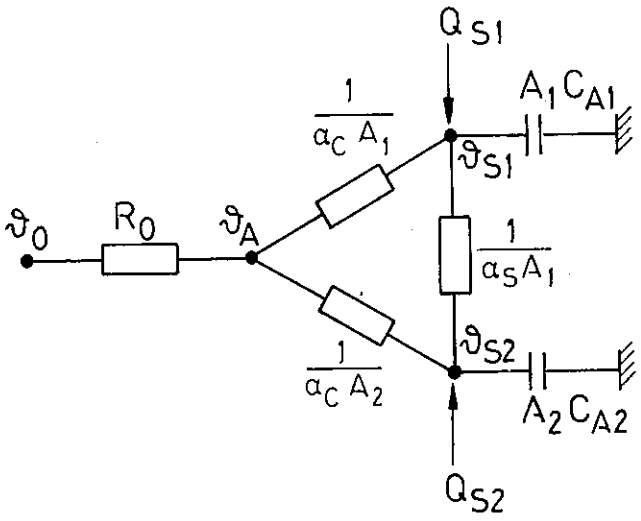

FIG. 6.4. Model of a room with two isothermal surfaces. Surface 1 is plane and surrounded by surface 2. Surface admittances are given in terms of the active heat capacities C_{A1} and C_{A2}. No heat is transmitted through the opaque surfaces.

$$\begin{bmatrix} \frac{1}{R_0} + \alpha_C(A_1+A_2) & -\alpha_C A_1 & -\alpha_C A_2 \\ -\alpha_C A_1 & i\omega A_1 C_{A1} + A_1(\alpha_S+\alpha_C) & -\alpha_S A_1 \\ -\alpha_C A_2 & -\alpha_S A_1 & i\omega A_2 C_{A2} + \alpha_S A_1 + \alpha_C A_2 \end{bmatrix} \begin{bmatrix} \vartheta_A \\ \vartheta_{S1} \\ \vartheta_{S2} \end{bmatrix} = \begin{bmatrix} \frac{\vartheta_0}{R_0} \\ \dot{Q}_{S1} \\ \dot{Q}_{S2} \end{bmatrix} \tag{6.6}$$

The amplitude of the room air temperature for a typical room is given in figure 6.5. The solution for $\alpha_S = \infty$ is compared to two cases with normal α_S. In one case the distribution of the thermal capacity varies from all being at surface 2 to all being at surface 1 while the generated heat flow is uniformly distributed over both surfaces. The second case is similar exept that all the flow is generated at surface 1.

The validity of the simplification is best when the admittances of the involved surfaces are similar. In the worst case when most of the thermal capacity is gathered at the smaller surface the amplitude of the room temperature is underestimated by about 40%. This error can, to a certain extent, be compensated for by a sophisticated combination of the admittances. This will be discussed in section 6.1.2.

An uneven distribution of the generated power has a limited effect if the admittances are similar. If a greater portion of the power is absorbed at the surface with higher thermal inertia this compensates for the uneven distribution of the thermal capacity.

If the two simplifications studied above are compared it can be concluded that the first is sensitive to convective power loads while for the latter the error increases if the admittances for the surfaces are greatly different. The latter also leads to a model for the room with two unknown variables which according to the specifications given above is an upper limit for a manual calculation method.

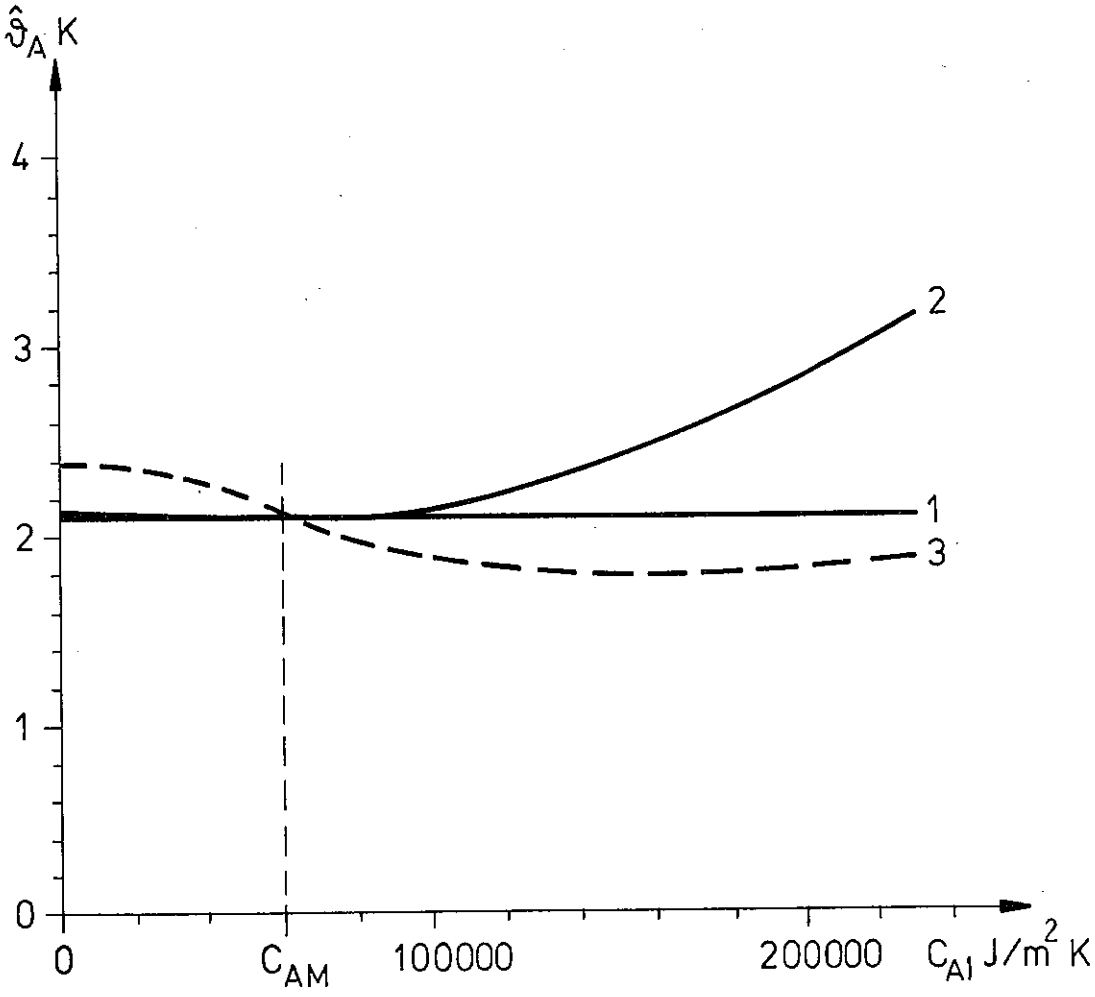

FIG. 6.5. Room air temperature amplitude calculated from equation (6.6). In curve 1 $\alpha_S = \infty$, in curve 2 α_S is 5 W/m^{2}K and in curve 3 α_S is 5 W/m^{2}K and all power is generated at surface 1.

$A_W = 4\ m^2$	$A_1 = 20\ m^2$
$k_W = 2\ W/m^2K$	$A_2 = 67\ m^2$
$V = 55\ m^3$	$\alpha_C = 3\ W/m^2K$
$n = 1\ h^{-1}$	$C_{AM} = 60000\ J/m^2K$
$\tilde{Q}_{S1} + \tilde{Q}_{S2} = 870\ W$	$\tilde{\vartheta}_0 = 0$
$\omega = 7{\cdot}27{\cdot}10^{-5}$ rad/s	

6.1.2 Principles for combination of surface admittances.

In this section an approximate method for estimating an equivalent surface admittance for a room is worked out. This will be used together with the simplification that all surfaces of the room are isothermal.

If the admittances for all the surfaces in the room are coupled in one point the resulting average admittance Y_m is calculated as

$$Y_m \cdot A_{TOT} = \sum_k A_k Y_k \tag{6.7}$$

If the admittances are expressed in terms of the active heat capacities this is written

$$i\omega C_{AM} \cdot A_{TOT} = i\omega \sum_k A_k \cdot C_{Ak} \tag{6.8}$$

If the admittances are expressed in terms of a thermal capacity and a thermal resistance as the RC model of figure 5.8, the expression for the admittance is given by

$$Y_m A_{TOT} = \sum \frac{-A_k}{R_k + \frac{1}{i\omega C_k}} \tag{6.9}$$

if R_k and C_k are related to 1 m^2.

It is seen from figure 6.5 that a straight forward addition of the surface admittances gives erroneous results in cases where the thermal inertia of the room is unevenly distributed over the surfaces. It is therefore necessary to establish addition rules for the surface admittances which take into account the limits to radiative heat exchange between the surfaces.

To establish such relations the simplified model of figure 6.2 can be used. In the previous section it has been stated that this model is suitable for cases with low convective heat flow to the room air.

Assume that Q_C equals zero, R_0 is infinitely large, the generated heat flow at the surfaces is uniformly distributed, and the modified convective surface heat transfer coefficient α'_C is equal for all surfaces. The surface heat transfer operator for each surface k is given by an admittance Y_k.

A heat balance for the internal temperature ϑ_I gives

$$\vartheta_I = \frac{1}{A_{TOT}} \sum_k A_k \cdot \vartheta_{Sk} \tag{6.10}$$

Heat balance for each surface temperature ϑ_{Sk} gives

$$\vartheta_{Sk} = \frac{\tilde{Q}_S}{A_{TOT}(\alpha'_C - Y_k)} + \vartheta_i\left(\frac{\alpha'_C}{(\alpha'_C - Y_k)}\right) \tag{6.11}$$

Input of equation (6.11) into equation (6.10) gives the resulting internal temperature ϑ_I as

$$\vartheta_I = \frac{\tilde{Q}_S}{A_{TOT}} \frac{\sum_k A_k\left(\frac{1}{\alpha'_C - Y_k}\right)}{\left(A_{TOT} - \sum_k A_k\left(\frac{\alpha'_C}{\alpha'_C - Y'_k}\right)\right)} \tag{6.12}$$

The average effective admittance is defined as the ratio between the surface heat flow $\tilde{q}_S$ and internal temperature ϑ_I. If the admittance and surface heat flow are uniformly distributed this can be done since all surface temperatures and the internal temperatures are equal.

$$Y^*_m = - \frac{\tilde{Q}_S}{A_{TOT}\vartheta_I} \tag{6.13}$$

This, together with equation (6.12) gives an explicit equation for the average effective admittance.

$$Y_m^* = \frac{-1}{\sum_k \frac{A_k}{A_{TOT}} \left(\frac{1}{\alpha'_C - Y_k} \right)} + \alpha'_C \qquad (6.14)$$

If each admittance is expressed in terms of an active heat capacity as in equation (6.8) the effective mean active heat capacity is expressed as

$$C_{AM}^* = \frac{1}{\omega} \left| \frac{1}{\sum_k \frac{A_k}{A_{TOT}} \left(\frac{1}{i\omega C_{Ak} + \alpha'_C} \right)} - \alpha'_C \right| \qquad (6.15)$$

The above analysis is based on the assumption that the modified α'_C value is equal for each surface. From equation (3.34) it is seen that even if the convective heat transfer coefficient α_C is set equal for all surfaces this is not the case since α'_C also depends on the ratio between the surface area and the area of the surrounding surfaces. It can be shown using figure 5.23 that the relative importance of α'_C is greatest for surfaces with high active heat capacity and consequently the α'_C should be calculated for the surface with highest thermal inertia. It can also be shown that an increase in α'_C brings C_{AM}^* closer to C_{AM}.

The solution of equation (6.15) implies the use of complex arithmetics. In figure 6.6 the solution is given graphically for a room with two different surfaces. Eight different graphs are given. Each graph represents a constant value for C_{A1}, C_{A2} is given on the x-axis and the capacity ratio

$$n = \frac{C_{AM}^*}{C_{AM}} \qquad (6.16)$$

can be decided from the curves given for the ratio between the area A_2 and the sum of the areas A_1 and A_2.

For enclosures with more than two different surfaces the graphs of figure 6.5 can be used to estimate C_{AM}^* by successive combinations of pairs of surfaces. For best results surfaces with similar active heat capacity should be combined first.

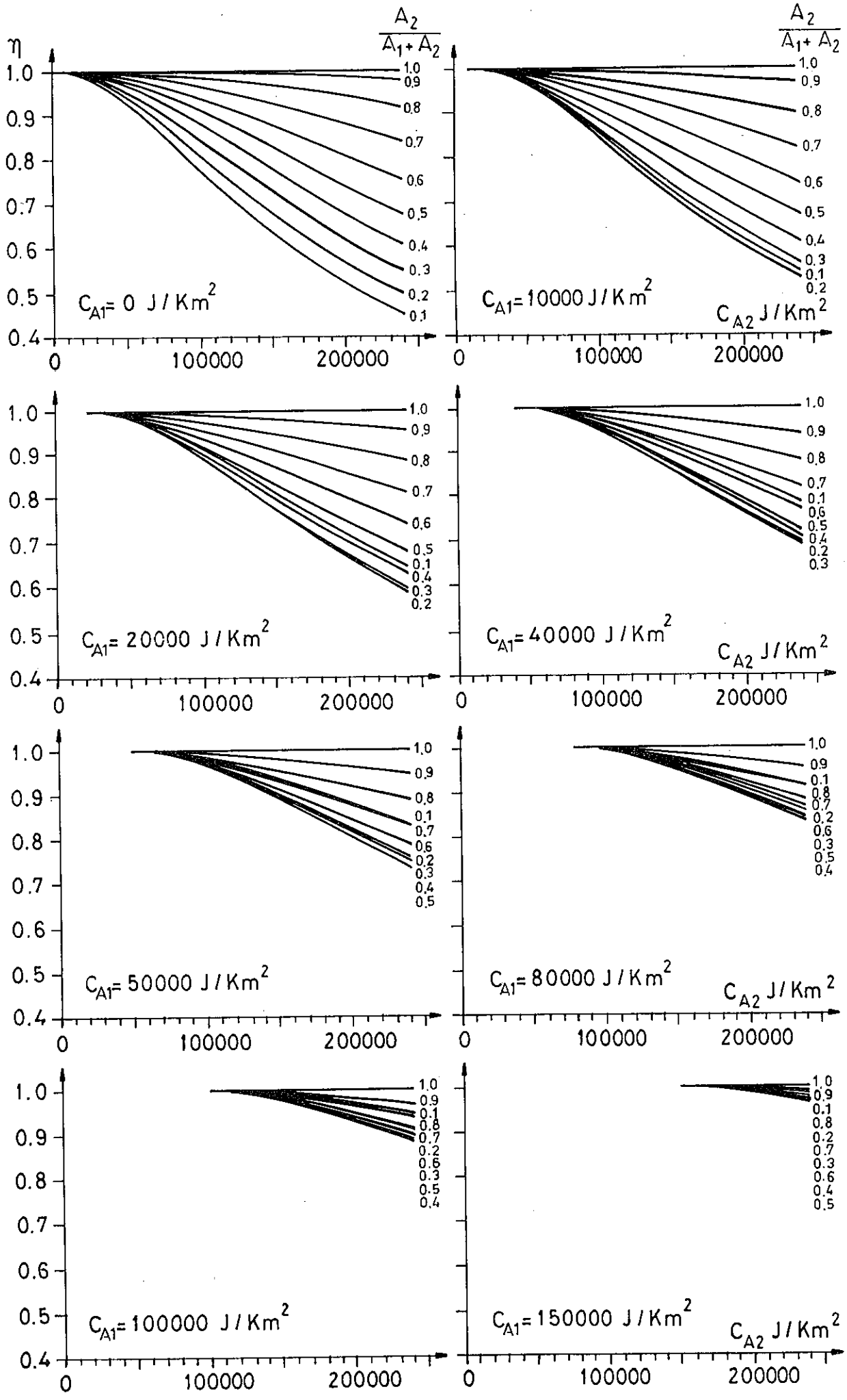
η
$\frac{A_2}{A_1+A_2}$
1.0
0.9
0.8
0.7
0.6
0.5
0.4
0
100000
200000
C_{A1}= 0 J / Km²
C_{A1}= 10000 J / Km²
C_{A1}= 20000 J / Km²
C_{A1}= 40000 J / Km²
C_{A1}= 50000 J / Km²
C_{A1}= 80000 J / Km²
C_{A1}= 100000 J / Km²
C_{A1}= 150000 J / Km²
C_{A2} J / Km²

In figure 6.5 the resulting temperature amplitude for the two-surface model of figure 6.4 was given for a specified room configuration. This was compared to the solution for a corresponding one-surface model using an average active heat capacity C_{AM} as in equation (6.8). In figure 6.7 the solution for the two-surface model is compared to the solution for a one-surface model when the active heat capacities are combined according to equation (6.15) and with two different values for α'_C, 8.0 and 9.5 W/m^2K. The former value is the same as used in figure 6.6 while the latter is calculated for the surface A_1 from equation (3.34). In the most extreme case. C_{A1} = 230000 J/m^2K the amplitude is overestimated by 10 and 20% respectively. To fit the two-surface solution a value of 12 W/m^2K would have to be used for α'_C in equation (6.15).

FIG. 6.6. The ratio η for a combination of two different active heat capacities.

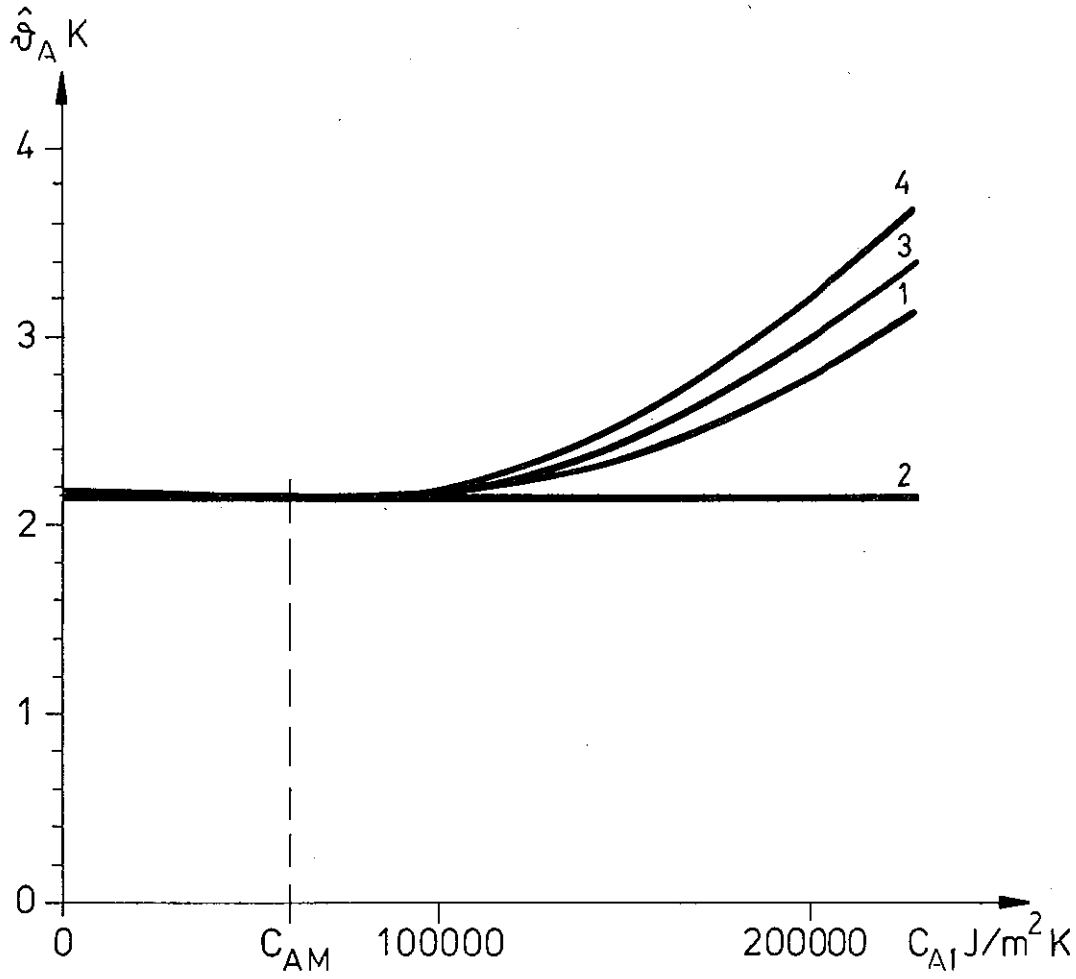

FIG. 6.7. The temperature amplitude for the same case as in figure 6.5. Curve 1 gives the amplitude for a model with two isothermal surfaces with radiative coupling between them. Curves 2-4 give the amplitude for a model with one isothermal surface. In curve 2 the active heat capacities are combined as in equation (6.8). In curve 3 and 4 the active heat capacities are combined as in equation (6.5) when α_C' equals 9.5 and 8.0 W/m^{2}K respectively.

6.1.3 Influence of heat capacity of the room air.

In previous sections the heat capacity of the room air has been neglected in the models derived for room heat balance. In this section a possible inaccuracy due to this simplification is studied in the frequency domain.

From figure 6.1 it is observed that room air is coupled to the outside air via the resistance R_0 defined in equation (6.1) and to opaque surface k of the room via the resistance R_k defined in equation (6.2). The study can be done by setting the adjacent temperatures equal to zero and then studying the response of the room air temparature to varying convective load $\tilde{Q}_C$.

A model of this simplified situation is given in figure 6.8. The thermal capacity C is calculated as

$$C = \rho c V \tag{6.17}$$

and if the convective surface heat transfer coefficient α_C is assumed to be equal for all surfaces the resistance R is given by

$$\frac{1}{R} = k_W A_W + \alpha_C A_{TOT} + \frac{n \cdot \rho c V}{3600} \tag{6.18}$$

The thermal response of the room air is calculated

$$\tilde{\vartheta}_A = \frac{\tilde{Q}_C}{i\omega C + 1/R} \tag{6.19}$$

and this can be related to the thermal response when the thermal capacity C is set equal to zero.

$$\tilde{\vartheta}_A' = R\tilde{Q}_C \tag{6.20}$$

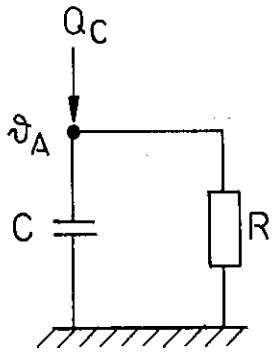

FIG. 6.8. Model for thermal response of the room air.

The amplitude ratio between these two quantities is denoted by ξ

$$\xi = \frac{\hat{\vartheta}'_A}{\hat{\vartheta}_A} \tag{6.21}$$

and expressed in terms of R and C

$$\xi = 1 + \omega^2 R^2 C^2 \tag{6.22}$$

The error increases with RC. The key to a general conclusion is therefore to find an upper limit to RC and then study the growth of ξ as the angular velocity ω is increased.

Combining equations (6.17) and (6.18) gives

$$RC = \frac{\rho c V}{k_W A_W + \alpha_C A_{TOT} + \frac{n \rho c V}{3600}} \tag{6.23}$$

For normal rooms the areas can be related to the floor area A_F in the following way

$$V \approx 3A_F \tag{6.24}$$

$$A_W \approx 0.15A_F \tag{6.25}$$

$$A_{TOT} > 2A_F \tag{6.26}$$

If $\rho c = 1200\ J/m^3K$, $k_W = 2\ W/m^2K$, $\alpha_C = 2\ W/m^2K$ and $n = 0.5\ h^{-1}$ then

$$RC \gtrsim 700\ s$$

In figure 6.9 the amplitude ratio is given as a function of the angular velocity in a Bode diagram. The approximation holds down to a period of 2 hours which is quite sufficient if input data are given by hourly values.

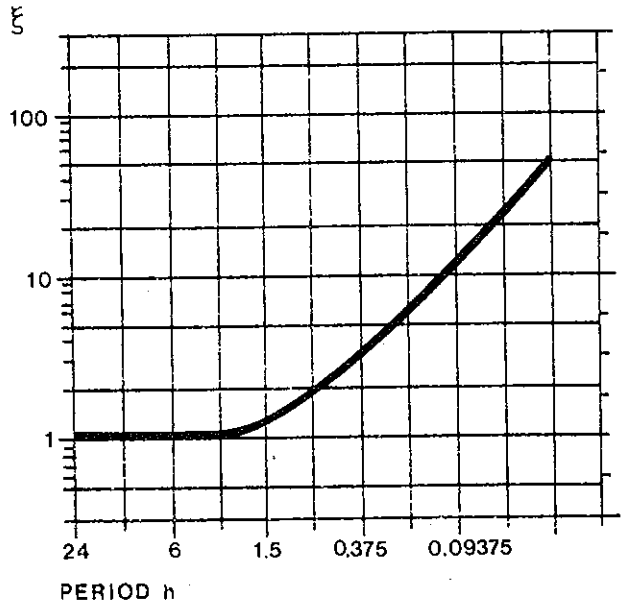

FIG. 6.9. Bode diagram showing the ratio between the amplitudes of the room air temperature when the thermal capacity of the room air is neglected and when it is not.

It is of interest to compare these results with the stability criterion for the forward-difference method given in equation (4.59). For the model of figure 6.8 this becomes

$$\Delta t_{max} = RC \tag{6.27}$$

which for the case discussed above gives a maximum time-step of about 10 min.

6.1.4 The two-node model for room heat balance.

Based on the principles for the combination of surface admittances given in section 6.1.2 a two-node model for the room heat balance can be established. The model is shown in figure 6.10.

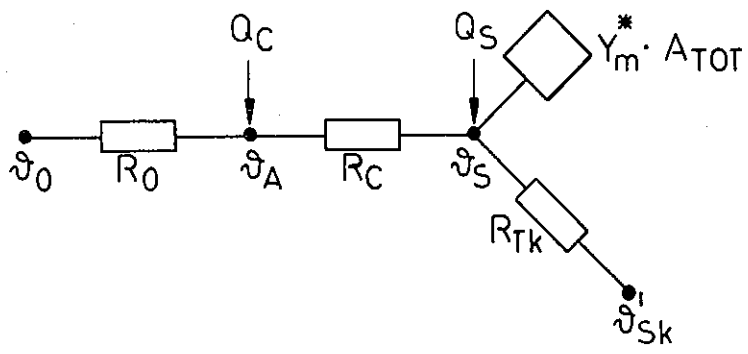

FIG. 6.10. A two-node model for the room heat balance.

The only time-dependent heat transfer operator is the surface admittance Y_m*. The part of the surface heat gain due to transmission through the opaque surfaces is included by a simple resistance between the surface and an external temperature. Normally the transmitted heat flow would only influence the daily mean average of the internal temperatures. If so the external temperatures for the surfaces could be given a constant value, equal to its daily mean value. Since the temperature ϑ_S is not known a priori it is not possible to weigh together different external temperatures if the thermal resistances for the involved constructions are not equal. This

means that for each surface k, for which the boundary conditions are not assumed to be symmetrical, the external temperature is coupled to the surface temperature via a resistance R_{Tk}.

Heat balance for ϑ_A gives

$$\vartheta_A = \vartheta_S \frac{R_0}{R_0 + R_C} + (\vartheta_0 + R_0 Q_C) \frac{R_C}{R_0 + R_C} \tag{6.28}$$

and for ϑ_S

$$C_{TOT} \frac{\partial \vartheta_S}{\partial t} + \vartheta_S \left(\frac{1}{R_C} + \sum_k \frac{1}{R_{Tk}}\right) = Q_S + \frac{1}{R_C} \vartheta_A + \sum \frac{\bar{\vartheta}'_{Sk}}{R_{Tk}} \tag{6.29}$$

By input of (6.28) into (6.29) the result is a differential equation for ϑ_S

$$C_{TOT} \frac{\partial \vartheta_S}{\partial t} + \vartheta_S \left(\frac{1}{R_C + R_0} + \sum \frac{1}{R_{Tk}}\right) = \frac{\vartheta_0 + R_0 Q_C}{R_C + R_0} + \sum \frac{\bar{\vartheta}'_{Sk}}{R_{Tk}} + Q_S \tag{6.30}$$

6.2 CALCULATION METHODS FOR ONE-SURFACE MODELS

In section 6.1 a two-node model for the room heat balance was derived. The only time-dependent heat transfer operator is the surface admittance which can be expressed in terms of a single heat capacity. The complexity corresponds to the specifications given in Chapter 2 for a model to be solved manually. The resulting temperatures of the model are for the surface temperature solved from the differential equation (6.30). The air temperature is solved from equation (6.28) when the surface temperature is known. There are different modes of operations to be considered such as when convective load is supplied to keep the air temperature fixed or within certain limits. In this section solutions will be given both for the steady state and for the frequency response of the model.

A finite different method is also derived which can handle the non-linearity due to changes in ventilation rate ind input variables expressed as time series during the calculated period.

6.2.1 The steady state solution.

If the heat transfer parameters in the system are constant the solution can be divided into a steady state solution where the average temperatures $\bar{\vartheta}_S$ and $\bar{\vartheta}_C$ are calculated from the average values of the input variables $\bar{Q}_C$, $\bar{Q}_S$, $\bar{\vartheta}_0$ and $\bar{\vartheta}_{Sk}$, and a non-steady solution. The final solution comes from a superposition of the two solutions.

For the steady state solution the time derivative of ϑ_S equals zero and the average surface temperature is explicitly solved from equation (6.30).

$$\bar{\vartheta}_S = \frac{\dfrac{\bar{\vartheta}_0 + R_0\bar{Q}_C}{R_0 + R_C} + \bar{Q}_S + \sum_k \dfrac{\bar{\vartheta}_{Sk}}{R_{Tk}}}{\left(\dfrac{1}{R_C + R_0} + \sum \dfrac{1}{R_{Tk}}\right)} \qquad (6.31)$$

The resulting air temperature is given by equation (6.28).

$$\bar{\vartheta}_A = \bar{\vartheta}_S \frac{R_0}{(R_0 + R_C)} + (\bar{\vartheta}_0 + R_0\bar{Q}_C) \frac{R_C}{(R_0 + R_C)} \tag{6.32}$$

If ϑ_A is fixed the average surface temperature $\bar{\vartheta}_S$ comes from a heat balance at the surface

$$\bar{\vartheta}_S = \frac{\frac{\bar{\vartheta}_A}{R_C} + \sum_k \frac{\bar{\vartheta}'_{Sk}}{R_{Tk}} + \bar{Q}_S}{\left(\frac{1}{R_C} + \sum_k \frac{1}{R_{Tk}}\right)} \tag{6.33}$$

and the convective heat load comes from rewriting equation (6.28).

$$\bar{Q}_C = \frac{1}{R_0}(\bar{\vartheta}_A - \bar{\vartheta}_0) + \frac{1}{R_C}(\bar{\vartheta}_A - \bar{\vartheta}_S) \tag{6.34}$$

6.2.2 The frequency response.

The response of the room system to harmonic power loads has been studied by several authors. Aittomäiki (1974) gives the complete solution for a room model with radiation heat exchange between the surfaces and where the heat transfer operators for the walls are given by the transfer matrix of equation (4.28). The solution for a network as in figure 6.2, where all power is supplied convectively, is given in Muncey (1979) together with a discussion on how the resulting internal temperature should be interpreted. The admittance procedure given by the IHVE guide (1970) is based on a similar solution. Since in figure 6.2 all branches of the network are coupled through ϑ_1 only, a total admittance for the room equals the sum of the admittances for each branch. If the construction admittances are calculated including the influence of α_C' the total admittance for the room system is given by

$$Y_{TOT} = \sum_k A_k \cdot Y_k - 1/R_0 \tag{6.35}$$

The resulting internal temperature swing is then calculated

$$\tilde{\vartheta}_I = \frac{-\tilde{Q}_C}{Y_{TOT}} \tag{6.36}$$

Equation (6.36) gives the response to convective loads only. Milbank and Harrington Lynn (1974) claim that the surface loads can be added to the convective loads if they are first multiplied by the surface factor F_S of equation (5.17).

$$\tilde{Q}_C{}' = \tilde{Q}_C + F_S\tilde{Q}_S \tag{6.37}$$

The response to convective loads, however, will still be erroneous as discussed in section 6.1.1.

From equation (6.28) and (6.30) and by using expression (3.14) for the derivative of a harmonic variable the response of the surface temperature is given by the expression

$$\tilde{\vartheta}_S = \frac{\dfrac{\tilde{Q}_C R_O}{R_O + R_C} + \dfrac{\tilde{\vartheta}_O}{R_O + R_C} + \tilde{Q}_S}{i\omega C_{TOT} + \dfrac{1}{R_C + R_O} + \Sigma\dfrac{1}{R_{Tk}}} \tag{6.38}$$

The resulting air temperature oscillation is solved from equation (6.28). From equation (6.38) the surface temperature variation can be solved separately for each of the variables $\tilde{Q}_C$, $\tilde{Q}_S$ and $\tilde{\vartheta}_O$ and a similar expression is given below for the air temperature variation. The expression is derived by input of equation (6.38) into equation (6.28).

$$\vartheta_A = \dot{Q}_C\left(\frac{R_0^2}{(R_0 + R_C)^2(i\omega C_{TOT} + \frac{1}{R_0 + R_C} + \sum_k \frac{1}{R_{Tk}})} + \frac{R_0 \cdot R_C}{R_0 + R_C}\right)$$

$$+ \vartheta_0\left(\frac{R_0}{(R_0 + R_C)^2(i\omega C_{TOT} + \frac{1}{R_0 + R_C} + \sum_k \frac{1}{R_{Tk}})} + \frac{R_C}{R_0 + R_C}\right)$$

$$+ \dot{Q}_S\left(\frac{R_0}{(R_0 + R_C)(i\omega C_{TOT} + \frac{1}{R_0 + R_C} + \sum_k \frac{1}{R_{Tk}})}\right) \qquad (6.39)$$

From equation (6.39) several ratios of interest can be defined which can be used to estimate the relative influence of the different parameters on the room air temperature amplitude.

The ratio between the air temperature and the convective heat load called the room air impedance to convective heat loads is denoted by Z_{AC}, K/W.

$$Z_{AC} = \frac{\vartheta_A}{\dot{Q}_C} \qquad (\vartheta_0 = 0,\ \dot{Q}_S = 0) \qquad (6.40)$$

The ratio between the air temperature and the surface heat load is similarly called the room air impedance to surface heat loads and denoted by Z_{AS}

$$Z_{AS} = \frac{\vartheta_A}{\dot{Q}_S} \qquad (\dot{Q}_C = 0,\ \vartheta_0 = 0) \qquad (6.41)$$

The ratio between the room air temperature and the outside air temperature can be expressed in terms of Z_{AS}, R_O and R_C.

$$\frac{\vartheta_A}{\vartheta_O} = \frac{Z_{AS}+R_C}{R_O + R_C} \qquad (\dot{Q}_S = 0,\ \dot{Q}_C = 0) \tag{6.42}$$

Of special interest is the ratio between a convective heat load and a surface heat load needed to maintain the same room air temperature variation.

This can be derived from the equality

$$\vartheta_A = \dot{Q}_S \cdot Z_{AC} = \dot{Q}_S \cdot Z_{AS} \tag{6.43}$$

The ratio is then given by

$$\frac{\dot{Q}_C}{\dot{Q}_S} = \frac{Z_{AS}}{Z_{AC}} \tag{6.44}$$

or in terms of the constants of the network being analysed

$$\frac{\dot{Q}_C}{\dot{Q}_S} = \frac{1}{1 + R_C(i\omega C_{TOT} + \frac{1}{\Sigma R_{Tk}})} \tag{6.45}$$

Analogous to the definition of a construction-surface factor given in equation (5.17), this can be called the room-surface factor F_{RS}. This relation is useful because the convective power needed to match a given surface load to maintain constant room air temperature is given by the equation

$$\dot{Q}_C = - F_{RS}\dot{Q}_S \qquad (\vartheta_A = 0) \tag{6.46}$$

The relations derived in this section are a powerful tool to analyse qualitatively the thermal performance of building enclosures. The response of the internal temperatures to three input variables are explicitly given in terms of the heat transfer parameters of the room model. The relations are based on the assumption that the surface admittance can be written in terms of a single thermal capacity C_{TOT}. The corresponding relations in terms of the admittance are easily established by replacing $i\omega C_{TOT}$ with $-A_{TOT} \cdot Y_m^*$.

For a quantitative calculation of the room heat balance the frequency response has its drawbacks. Each calculation handles only one frequency component of the input variables. Since the thermal loads as a rule consists of more frequency components this leads to two alternatives: either assume that the impedances Z_{AC} and Z_{AS} are constant for all frequencies larger than the fundamental frequency, or make a Fourier analysis of the input variables. The former alternative leads back to the principles of the admittance procedure and the latter would cost too much calculation work.

6.2.3 Solution with finite differences.

The solution for the model of figure 6.10 with finite differences is simple since the air temperature is linearly dependent on the surface temperature. The time dependent solution is therefore carried out with ϑ_S as the only unknown variable.

Below three modes of operation are treated

- o The thermal loads Q_C, Q_S, ϑ_0 and ϑ_{Sk} are known a priori as a time series during the calculated period.

- o The air temperature is to be kept constant during some parts of the calculated period. To achieve this, power from the plant is supplied to the room air or, in terms of the model parameters, added to Q_C.

- o The air temperature is allowed to float within some predefined limits.

TAB. 6.1. Constants for finite difference calculation of room temperatures according to equations (6.47) and (6.48).

	Forward diff. method	Crank Nicholsson method
K_1	$\frac{\Delta t}{C(R_0+R_C)}$	$\frac{1}{(R_C+R_0)(\frac{1}{2(R_C+R_0)} + \Sigma\frac{1}{2R_{Tk}} + \frac{C}{\Delta t})}$
K_2	$\frac{\Delta t}{C}$	$\frac{1}{\frac{1}{2(R_C+R_0)} + \Sigma\frac{1}{2R_{Tk}} + \frac{C}{\Delta t}}$
K_3	$\frac{\Delta t\ R_0}{C(R_0+R_C)}$	$\frac{R_0}{(R_0+R_C)(\frac{1}{2(R_C+R_0)} + \Sigma\frac{1}{2R_{Tk}} + \frac{C}{\Delta t})}$
K_4	$\frac{\Delta t}{C}(\frac{C}{\Delta t} - \frac{1}{R_0+R_C} - \Sigma_k\frac{1}{R_{Tk}})$	$\frac{\frac{C}{\Delta t} - \frac{1}{2(R_C+R_0)} - \Sigma\frac{1}{2R_{Tk}}}{(\frac{1}{2(R_C+R_0)} + \Sigma\frac{1}{2R_{Tk}} + \frac{C}{\Delta t})}$
K_5	$\frac{\Delta t}{C}\Sigma\frac{\bar{\vartheta}'_{Sk}}{R_{Tk}}$	$\frac{\Sigma\frac{\bar{\vartheta}'_{Sk}}{k_{Tk}}}{(\frac{1}{2(R_C+R_0)} + \Sigma\frac{1}{2R_{Tk}} + \frac{C}{\Delta t})}$
K_6	$\frac{R_0}{(R_0+R_C)}$	$\frac{R_0}{(R_0+R_C)}$
K_7	$\frac{R_0R_C}{(R_0+R_C)}$	$\frac{R_0R_C}{(R_0+R_C)}$
K_8	$\frac{R_C}{(R_0+R_C)}$	$\frac{R_C}{(R_0+R_C)}$

The thermal loads as a function of time are either steady-periodic or transient. For steady periodic loads the output variables are also steady periodic which means thar their values at the beginning of a period are to equal their values at the end. For transient loads the prehistory of the system has to be known if the initial values for the calculation are to be set correctly.

For the finite difference solution of equation (6.30) it is assumed that the surface temperature at a time t, ϑ_S^t, is known. The problem is to find the temperature ϑ_S^{t+1} after a time interval Δt. During the time interval the input variables Q_S^t, Q_C^t, ϑ_0^t and $\bar{\vartheta}'_{Sk}$ are assumed to be constant. As for the RC-models representing building constructions, equation (6.30) can be solved both with a forward difference method and the Crank-Nicholsson method. In this case both methods are explicit since there is only one unknown variable. The general form of the solution is given in equation (6.47) and the constants K_1 to K_5 are given in table 6.1 for both methods.

$$\vartheta_S^{t+1} = K_1\vartheta_0^t + K_2Q_S^t + K_3Q_C^t + K_4\vartheta_S^t + K_5 \qquad (6.47)$$

If the surface temperature is known the air temperature is calculated as

$$\vartheta_A = K_6\vartheta_S + K_7Q_C + K_8\vartheta_0 \qquad (6.48)$$

The constants K_6, K_7 and K_8 can be identified from equation (6.28). They are also given in table 6.1. Since the input variables Q_C and ϑ_0 are constant during each time interval the resulting air temperature will be discontinuous at each time point t.

The amount of work needed to calculate the constants K_1 to K_5 of table 6.1 is almost the same for both methods.

Since input data are often given by hourly values it is natural to use 1 h as a time step. Such a long time step will give instability problems if the forward difference method is used for enclosures with

low thermal inertia and high resistive heat loss. The Crank Nicholsson method is therefore preferable.

The equations (6.47 and 6.48) give the solution when the thermal loads are known a priori. If ϑ_A is restricted in some way the problem is to find the minimum additional convective load needed to keep ϑ_A within the given limits. From the equations (6.47 and 6.48) a relation between a change in the convective load ΔQ_C^t and the resulting change in air temperature at the end of the time interval $\Delta\vartheta_A^{t+1}$ is established

$$\Delta\vartheta_A^{t+1} = K_6\Delta\vartheta_S^{t+1} + K_7\Delta Q_C^t \tag{6.49}$$

$$\Delta\vartheta_A^{t+1} = (K_6K_3 + K_7)\Delta Q_C^t \tag{6.50}$$

If the air temperature does pass its limits by an amount $\Delta\vartheta_A^{t+1}$ the convective load is increased by

$$\Delta Q_C^t = - \frac{\Delta\vartheta_A^{t+1}}{(K_6K_3 + K_7)} \tag{6.51}$$

and the calculation for the actual time step is carried out once more.

If the air temperature is constant the calculation of the convective load can be simplified.

By setting R_0 equal to zero when the constants K_1 to K_5 are calculated and by replacing ϑ_0^t with ϑ_A^t in equation (6.47) the surface temperature ϑ_S^{t+1} is explicitly given and the heat load can be calculated from equation (6.48).

This analysis can be extended so that the room climate is controlled on basis of the surface temperature or some combination of the internal temperatures. The additional power load could also be partly generated at the surface.

One of the major advantages of the finite difference method given above compared with the frequency response solution is that the transfer coefficients of the system can vary during the calculated period. This makes it possible to study the influence of different ventilation patterns. For each new ventilation rate, however, a new set of constants K_1 to K_8 has to be calculated.

For steady periodic loads the initial guess about the surface temperature is of importance for the number of cycles that have to be calculated until the solution converges. It is, however, difficult to give any sophisticated rules for choice of the initial value except for the expected mean value. After the first period has been calculated the resulting difference in surface temperature over the period can be used to predict the final solution. Assuming that the system is linear a time constant for the surface is defined as

$$t^* = \frac{C_{TOT}}{\left(\frac{1}{R_C + R_0} + \Sigma\frac{1}{R_{Tk}}\right)} \tag{6.52}$$

An initial disturbance in surface temperature $\Delta\vartheta_S(0)$ would decay according to equation (6.53)

$$\Delta\vartheta_S(t) = \Delta\vartheta_S(0)e^{-\frac{t}{t^*}} \tag{6.53}$$

From the first period the difference

$$\Delta\vartheta_{SPER} = \Delta\vartheta_S(T) - \Delta\vartheta_S(0) \tag{6.54}$$

is known. T is the length of the period.

Putting the equation (6.53) into equation (6.54) the initial disturbance can be calculated

$$\Delta\vartheta_S(0) = \frac{-\Delta\vartheta_{SPER}}{(1 - e^{-T/t^*})} \tag{6.55}$$

This provides a new initial value

$$\vartheta_S(T) = \vartheta_S(0) - \Delta\vartheta_S(0) \tag{6.56}$$

which for linear systems is very close to the correct one. The practical consequence is that in most cases only two or three cycles are needed depending on the convergence criterion chosen.

For a non-linear system the time constant is altered during the period. If the period is divided into N time intervals t_k and if the corresponding time constant is t_k^* equation (6.55) becomes

$$\Delta\vartheta_S(0) = \frac{-\Delta\vartheta_{SPER}}{(1 - e^{-(\frac{t_1}{t_1^*} + \frac{t_2}{t_2^*} \cdots\cdots \frac{t_N}{t_N^*})})} \tag{6.57}$$

7. APPLICATIONS TO NON-STEADY HEAT TRANSFER PROCESSES IN BUILDINGS

The transform of the opaque constructions into single active heat capacities given in Chapter 5 and the combination of these to a single mass point provide a model for the enclosure which can be studied from the different ratios given in section 6.2.2 or by the finite difference solution given in section 6.2.3. To illustrate the applicability and relevance of this simplified approach some interesting modes of operation are treated below. These are: overheating in summertime, intermittent heating, and energy consumption during days with casual energy excess. In a few cases the solutions are compared with the results of a larger computer program described by Hauser (1977) who has also provided the examples referred to below. The program by Hauser is based on a star model of the type given in figure 6.2. In these cases the modified surface heat transfer coefficient has been used instead of α_C to get comparable results.

The different simplifications given above concerning the construction dynamics and the reduction of the number of heat flow paths, provide an opportunity freely to choose the degree of accuracy and complexity of the room model. This makes it possible to tailor models for unconventional system solutions both for qualitative studies and for the calculation of long term energy balances where the system dynamics are taken inte account.

7.1 CALCULATION OBJECT

The geometry of the calculated room is given in figure 7.1. In all calculation examples there are three different construction types: the outer wall, the inner walls, and floors and ceilings. Even if floors and ceilings are identical they may have different thermal characteristics as seen from the room.

The boundary conditions are defined by the incident solar radiation, the outside air temperature, and the adjacent room temperatures which in all cases are assumed to equal the resulting room air temperature.

Other variables considered in the calculations below are: window size and characteristics, internal heat sources, ventilation pattern and prefixed limits for the air temperature.

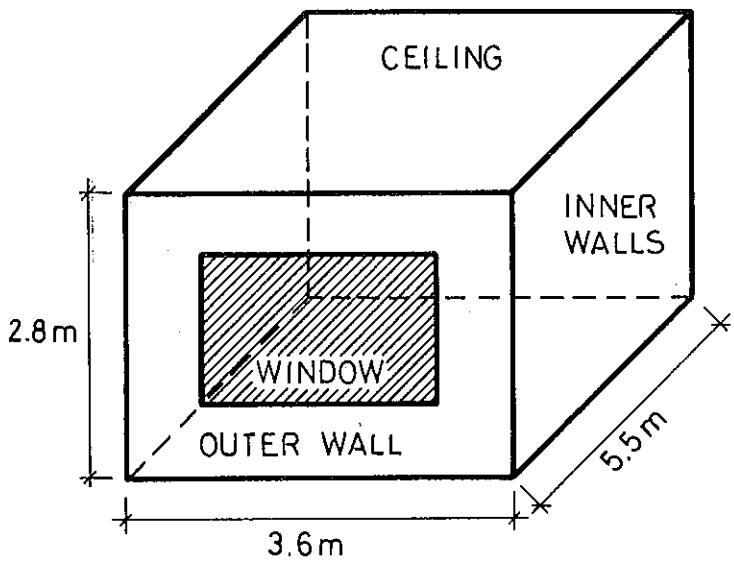

FIG. 7.1. Room geometry.

7.2 OVERHEATING PROBLEMS

Overheating in summer can be avoided in several ways. The conventional solution with a cooling battery is rather expensive due to installation, maintenance and energy costs. Other measures that in combination can provide an acceptable indoor comfort at a lower price are: reduction of the total solar gain through windows, forced nocturnal ventilation and use of the thermal inertia of the building components.

The construction specifications in the examples in this section are as follows.

Windows: $A = 4.03\ m^2$, $k = 3.15\ W/m^2K$, without sunprotection $F_1' = 0.65$ and $F_2' = 0.06$, with sun protection $F_1' = 0.21$ and $F_2' = 0.04$. In this case F_1' and F_2' are the fraction of the incident solar radiation transmitted through the window. They are given a constant average value during the day.

Outer walls: $A = 6.05\ m^2$, $k = 0.44\ W/m^2K$, $C_A = 1.39 \cdot 10^5\ J/Km^2$. $a_{outside} = 0.7$.

Inner walls: $A = 40.88\ m^2$. For the heavy-weight alternative $C_A = 2.35 \cdot 10^5\ J/Km^2$ and for the light-weight alternative $C_A = 0.12 \cdot 10^5\ J/Km^2$.

Floors: $A = 19.8\ m^2$, for the heavy-weight alternative $C_A = 0.95 \cdot 10^5\ J/Km^2$ and for the light-weight alternative $C_A = 1.27 \cdot 10^5\ J/Km^2$.

Ceilings: $A = 19.8\ m^2$, for the heavy-weight alternative $C_A = 3.0 \cdot 10^5\ J/Km^2$, for the light-weight alternative $C_A = 0.13 \cdot 10^5\ J/Km^2$.

The volume is $55.44\ m^3$.

The internal load is 200 W between 8 and 18 hours.

The outside temperature ϑ_0 and the incident solar radiation I are given in figure 7.2.

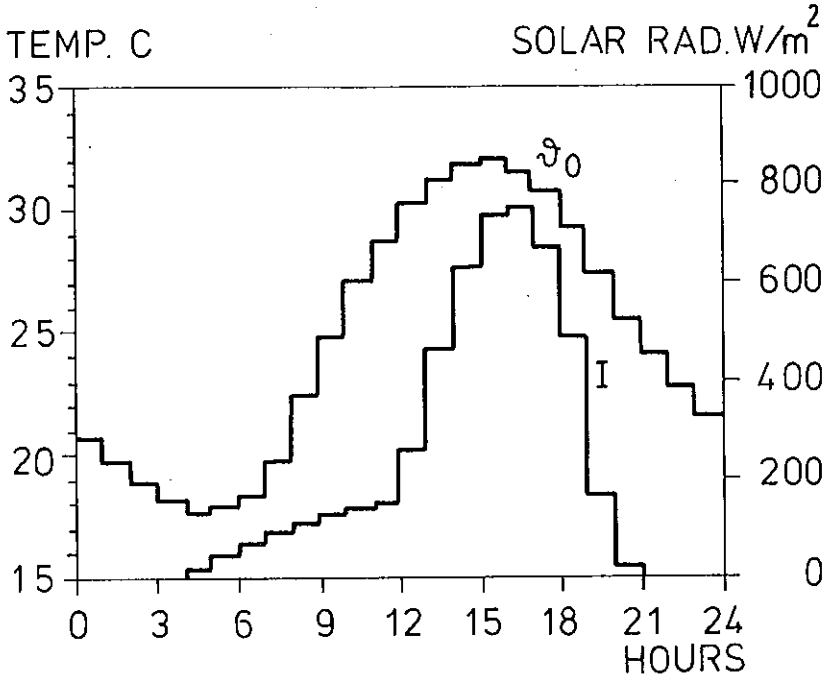

FIG. 7.2. Hourly mean values for incident solar radiation and outside air temperature. West oriented facade.

The active heat capacities above are calculated according to equation (5.43). The effective mean active heat capacity C^*_{AM} for the room is calculated according to equation (6.15). The reduction has a relatively larger effect for the light-weight alternative since light and heavy construction types are mixed.

light-weight $C_{AM} = 47400\ J/Km^2$
$C^*_{AM} = 37600\ J/Km^2$

heavy-weight $C_{AM} = 211100\ J/Km^2$
$C^*_{AM} = 189200\ J/Km^2$

The finite difference method in section 6.2.3 is then applied for the three following cases.

I. Window without sun protection and constant ventilation rate 0.8 h^{-1}. In this case the resulting temperatures exceed all limits. The light-weight construction gives maximum temperatures that are 5 K higher than for the heavy-weight alternative.

II. The window is equipped with sun protection and as a result the total solar transmission is reduced to 35% of its original value. The

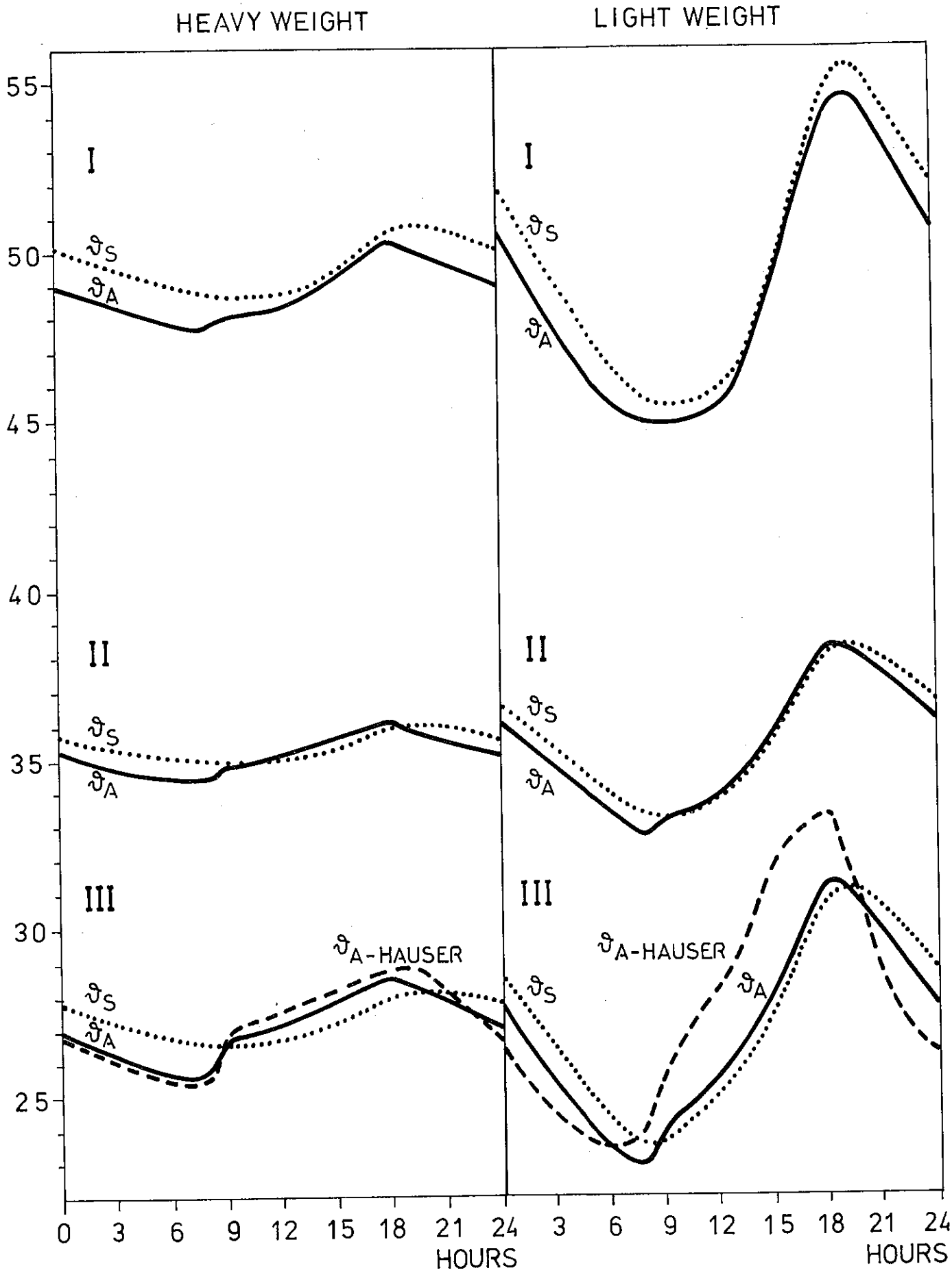

FIG. 7.3. Study of different measures to improve the indoor climate in summertime. Comparison with computer results of Hauser (1980).

temperatures are still too high.

III. From case II the ventilation pattern is changed so that between 18 hours p.m. and 6 hours a.m. the ventilation is 5 h^{-1} and 0.8 h^{-1} the rest of the day. In this case the heavy-weight alternative is 3 K lower than the light-weight with a maximum temperature of 28.5 ^{o}C.

These final results are compared with the computer results of Hauser (1980). The agreement is much better for the heavy-weight alternatives which is to be expected bearing in mind the results of Chapter 5. Figure 5.13 shows a poor agreement between the C-model and the real admittance at higher frequencies when a heavy material layer is screened off from the room by means of a light insulation layer. It must be emphasized that this comparison only concerns the different physical models and mathematical solutions. Since the α_C of the solutions in figure 7.3, has been adjusted to the modified α_C' of the computer model a comparison is made in figure 7.4 between the one-surface solutions for case III with two different values of α_C, 3 and 8 W/m^2K. The significant difference in mean value for the two alternatives stems from the high ventilation rate. When the ventilation rate is increased during the night the total heat transfer is overestimated for high values of α_C, as discussed in section 6.1.1.

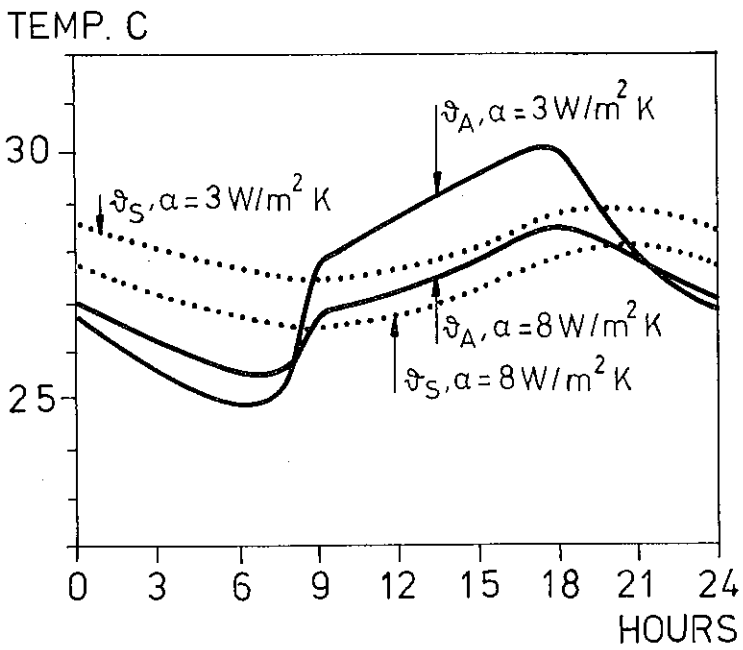

FIG. 7.4. Indoor temperatures calculated with two different values for α_C, 3 and 8 W/m^2K.

7.3 INTERMITTENT HEATING

For office moduls or dwellings which are intermittently occupied the power plant can be switched off resulting in lower indoor temperatures during some predetermined periods. If the system is linear the resulting energy savings can be estimated from the average drop in air temperature for the unconditioned period. The variation of temperatures and supplied power during the day is a non-steady process with a relatively large amount of high frequency components. In this section the one-surface model described above will be compared to computer results of Hauser (1980). The construction alternatives are the same as in section 7.2 case II except that the window size is altered to 1.76 m^2. The outside temperature and the incident solar radiation are given in figure 7.5. It is a cold sunny winter day.

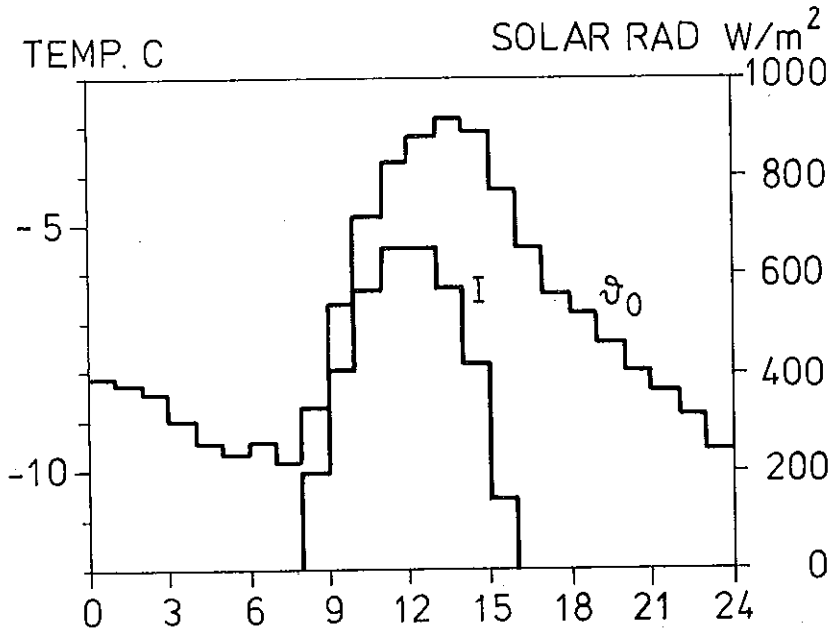

FIG. 7.5. Hourly mean values for incident solar radiation and outside air temperatures. South oriented facade.

The ventilation is constant 0.5 h^{-1}, the internal load is 200 W between 8 and 18 hours and the air temperature is conditioned to 20° C between 7 and 17 hours. There is a small discrepancy between the results from the computer run and the simpler calculation model since ΔQ_C^t in equation (6.51) is calculated to give the prefixed temperature at the end of a period while in the computer program the prefixed temperature is achieved momentanously.

The resulting indoor temperatures and power loads are given in figure 7.6. Even though the lowest temperature is the same for both models and for both construction types the average temperature during the unconditioned period is lower for the computer results. As a result of this the calculated energy consumption during the day is different. For the computer calculation the energy consumption is 4.9 kWh for the heavy-weight and 3.9 kWh for the light-weight while for the one-surface model it amounts to 6.0 and 5.6 kWh respectively.

As for the case III of figure 7.3 the intermittent heating process is expected to be sensitive to the chosen α_C especially when the power is supplied to the room air. In figure 7.7 temperatures and supplied power for the light-weight alternative of figure 7.6 are calculated for α_C equal 3 W/m^2K. Even though the air temperature is about 1 K lower at the end of the unconditioned period the maximum power load is reduced due to the limited heat transfer between the air and the surface. The energy consumption is slightly reduced but the surface warms up more slowly resulting in a less comfortable indoor climate during the conditioned period.

Dafgård (1977) treats intermittent heating by means of exponential functions for the cooling down and warming up phases. The time constants for the system are achieved from field measurements on the step response. A limitation is that all thermal loads have to be set constant for the three modes, steady state cooling down and warming up.

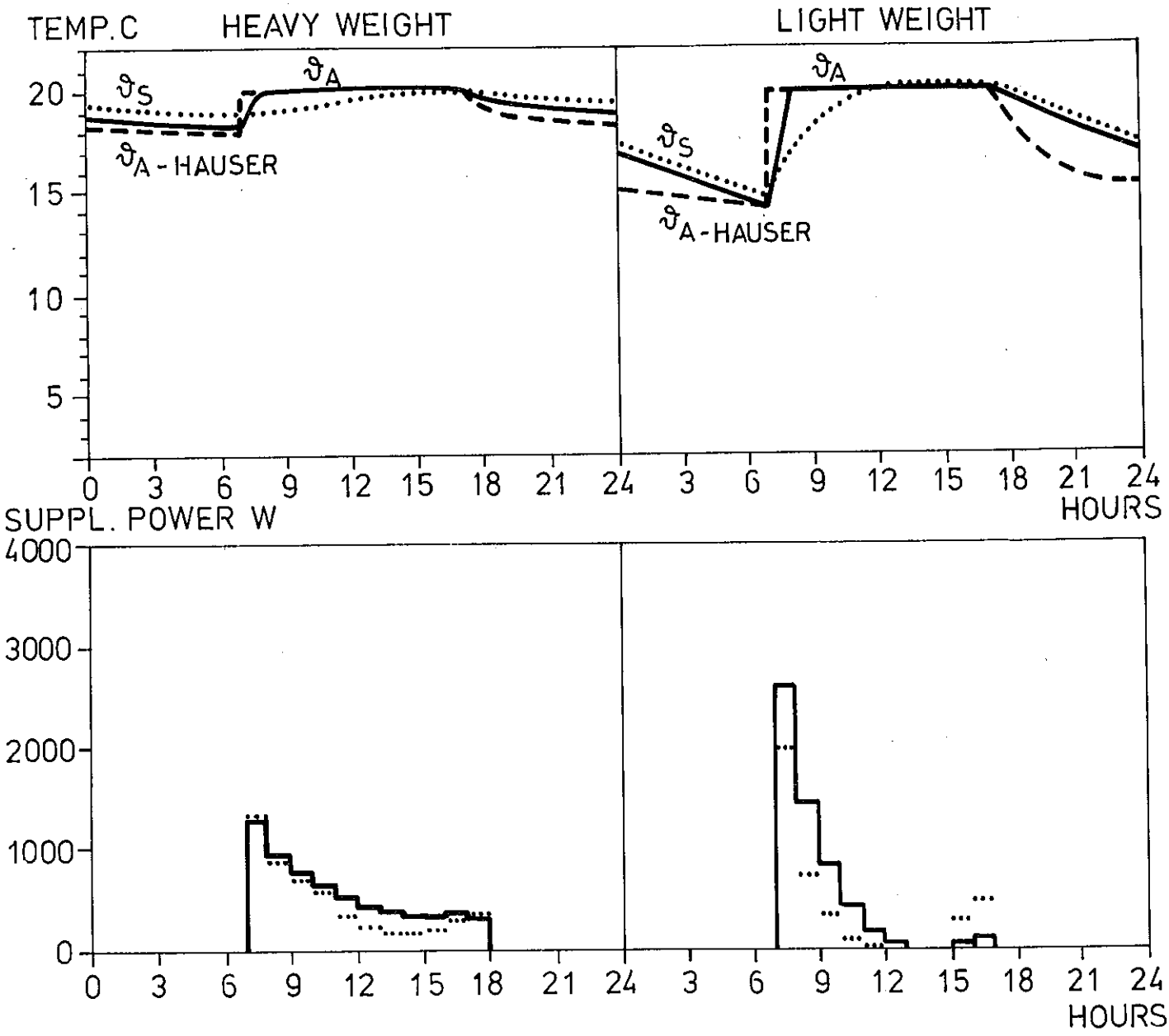

FIG. 7.6. Temperatures and power loads for an intermittently heated room.

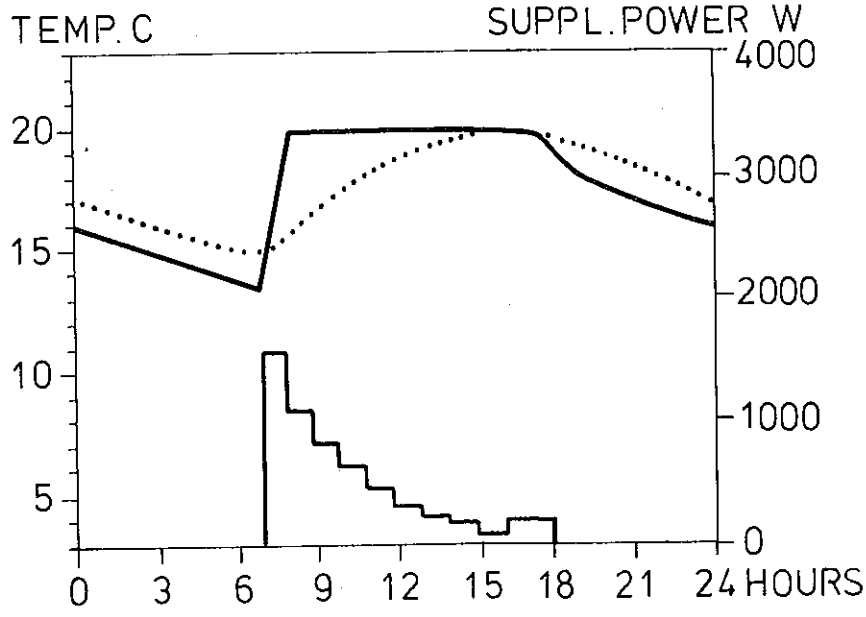

FIG. 7.7. Temperatures and supplied power for the light-weight alternative of figure 7.6 when α_C is altered to 3 W/m^2K.

7.4 ENERGY CONSUMPTION AND THERMAL INERTIA

Due to the relatively small ventilation and transmission loss for modern buildings the gratis heat for certain types of localities and for shorter periods exceeds the power load during parts of the heating season. Even if the power plant is shut down the temperatures rise, and at a certain limit the excess heat has to be removed by increased ventilation. This means that energy is lost at the same time as the long term energy consumption is considerable. With higher thermal inertia the temperature amplitude and the risk of over heating is reduced and a greater part of the gratis heat contributes to the long term energy balance.

The pattern of use is, however, just as important in this context. The influence of the heat capacity depends on the allowed limits for the temperature variation.

As an example the heat balance for the room of figure 7.1 is calculated with the one-surface model of section 6.2.3. The climate variables are valid for a cold but sunny February day in Stockholm. Figure 7.7 gives the hourly mean values for the outside air temperature and the solar radiation through a double glazed south-oriented window.

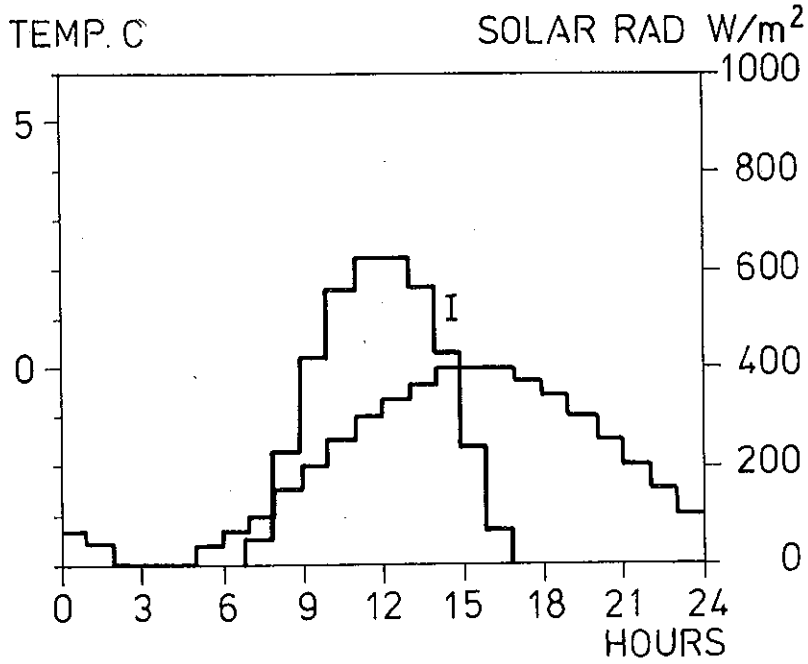

FIG. 7.8. Hourly mean values for the outside air temperature and the solar radiation through a double-glazed south oriented window. (Stockholm in February).

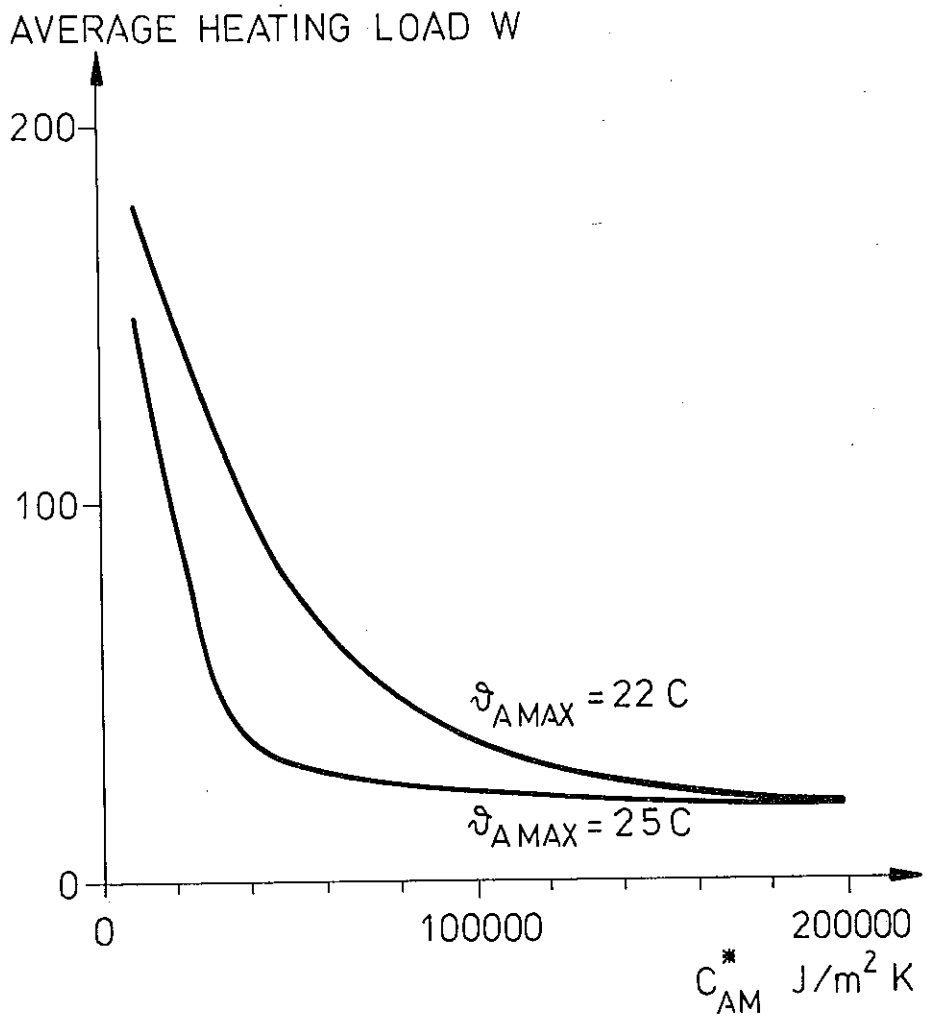

FIG. 7.9. Average heating load as a function of the effective mean active heat capacity.

The construction and operation specifications are as follows:

Window: $A = 3.0\ m^2$, $k = 2.0\ W/m^2K$, $F_1 = 0.36$, $F_2 = 0.07$

Outer wall: $A = 7.06\ m^2$, $k = 0.2\ W/m^2K$

The effective mean active heat capacity C^*_{AM} is given as a variable for the calculations.

The ventilation rate is $0.5\ h^{-1}$ between 7 and 18 hours and $0.2\ h^{-1}$ between 18 and 7 hours.

The internal load is 300 W between 8 and 18 hours.

The indoor air temperature is allowed to float between ϑ_{AMIN} and ϑ_{AMAX}. At lower temperatures power is supplied and higher temperatures are compensated by increased ventilation rate.

The average power load is given in figure 7.9 as a function of C^*_{AM} for ϑ_{AMIN} equal 20° C and two different ϑ_{AMAX}, 22 and 25° C.

The average power gain from solar radiation and internal sources is 330 W and the total average power load is 350 W.

LIST OF REFERENCES

Adamsson, B. (1970). Byggnadstekniska värmeproblem. Dep. for Building Science, Lund Institute of Technology.

Aittomäiki, A. (1974). Thermal Behaviour and Characterization of indoor Spaces. Technical Research Center of Finland, Helsinki.

Andersson, A.C. (1978). Köldbryggor i tilläggsisolerade ytterväggar. The National Swedish Board for Building Research, Report R 46:1978.

Andersson, A.C. (1980). ACA-STAT. Fortran IV. Computer program for two-dimensional steady-state potential flow. Not published. Div. of Building Technology, Lund Institute of Technology.

ASHRAE Handbook of Fundamentals, (1978). American Soc. of Heating and Air-Conditioning Engineers, Inc. New York.

Augenbroe, G.L.M. (1978). Finite Elements in Building Physics. Dep. for Building Physics. Delft University of Technology.

Bergquist, B., Hedberg, P.O., Johannesson, G., Skogström, L., Sommerhein, P. (1980). Mekaniskt ventilerad takkonstruktion som värmeväxlare och solfångare. The National Swedish Board for Building Research. Report R 111:1980.

Bondi, P., Di Filippo, P. Reale, G. (1977). Thermal Performance of Walls, Italian Studies and Research. Consiglio Nazionala delle Rierche, Rome.

Bring, A., Isfält, E. (1979). Computer Program BRIS. Manual. Trask Datacentral, Stockholm.

Brown, G. (1964). Metod för datamaskinberäkning av värme och ljusstrålning i rum. National Swedish Institute for Building Research, offprint 4:1964.

Brown, G., Isfält, E. (1969). Instrålning från sol och himmel i Sverige under klara dagar. National Swedish Institute for Building Research, Report R 19:1969.

Brown, G., Isfält, E. (1974). Solinstrålning och solavskärmning. National Swedish Institute for Building Research, R 19:1974.

van der Bruggen, R.J.A. (1978). Energy Consumption for Heating and Cooling in Relation to Building Design. Delft University of Technology.

Carslaw, H.S., Jaeger, J.C. (1959). Conduction of Heat in Solids. Oxford University Press.

Claesson, J. (1980). Personal Communication. Dep. of Mathematical Physics. University of Lund.

Crank, J. (1975). The Mathematics of Diffusion. Second edition. Oxford University Press.

Dafgård, N. (1979). Intermittent uppvärmning - nattsänkning. Dep. for Heating and Ventilating. Royal Institute of Technology.

Danter, E. (1973). Heat Exchange in a Room and the Definition of Room Temperatures. IHVE Symposium, June 1973.

DIN 67507 (1978). Lichttransmissionsgrade, Strahlungstransmissionsgrade und Gesamtenergiedurchlassgrade von Verglasungen.

Eckert, E.R.G., Drake, R.M. (1959). Heat and Mass Transfer. Mc Grawhill.

Gertis, K. (1976). Der instationäre Wärmedurchgang durch Aussenbauteile. Veröffentlichungen aus dem Institut für Bauphysik, Heft 75. Stuttgart.

Gertis, K., Hauser, G. (1976). Instationäre Berechnungsverfahren für den sommerliche Wärmeschutz im Hochbau. Veröffentlichungen aus dem Institut für Bauphysik, Heft 75. Stuttgart.

Halldórson, G., Sigurjónsson, J. (1978). Einangrun húsa. Rannsóknastofnun byggingaridnadarins, Reykjavik.

Hauri, H.H. (1977). Praktische Berechnung des instationären Wärmeflusses durch ein- und mehrschichtige Wände.

Hauser, G., Gertis, K. (1975). Kenngrössen des Instationären Wärmeschutzes von Aussenbauteilen. Veröffentlichungen aus dem Institut für Bauphysik, Heft 75. Stuttgart.

Hauser, G. (1977). Rehnerischer Vorherbestimmungen grosser Bauten. Universität Stuttgart.

Hauser, G. (1979). Die Wärmetechnische Beurteilung von Fenstern unter Berüchsichtigung der Sonneneinstrahlung während der Heizperiode. Bauphysik 1, 1979.

Hauser, G. (1980). Computer results for indoor climate. Personal communication. Dep. for Building Physics. University of Essen.

Höglund, I. (1973). Metod för beräkning av extrema yttemperaturer hos isolerade ytterkonstruktioner. National Swedish Institute for Building Research, Report R 6:1973.

IHVE Guide (1970). The Institution of Heating and Ventilating Engineers. London (1971).

Isfält, E. (1974). Optiska och termiska egenskaper hos fönster och solskydd. Dep. of Heating and Ventilating. Royal Institute of Technology, Stockholm.

Jensen, L. (1978). Digital reglering av klimatprocesser. Dep. of Automatic Control. Lund Institute of Tehcnology.

Johannesson, G. (1976). Köldbryggor i ytterväggar och den nya byggnormen. VVS 6-7, 1977.

Johannesson, G., Åberg, O. (1981). Köldbryggor i plåtkonstruktioner. Not yet printed. Div. of Building Technology, Lund Institute of Technology.

Kimura, K.I. (1977). Scientific Basis of Air Conditioning. Applied Science Publishers Ltd, London.

Kreith, F. (1965). Principles of Heat Transfer. Second edition. International Textbook Company.

Kreyzig, E. (1967). Advanced Engineering Mathematics. John Wiley & Sons.

Loudon, A.G. (1968). Summertime Temperatures in Building without Air-Conditioning. IHVE/BRS Symposium, February 24, 1968.

Love, T.J. (1968). Radiative Heat Transfer. Charles E. Merrill Publishing Company.

Mc Adams, W. (1954). Heat Transmission. International Student Edition.

Milbank, N.O., Harrington Lynn, J. (1974). Thermal Response and the Admittance Procedure. BSE May 1974.

Mitalas, G.P. (1965). An Assessment of Common Assumptions in Estimating Cooling Loads and Space Temperatures. ASHRAE Transactions 71, part II.

Mitalas, G.P., Stephenson, D.G. (1967). Room Thermal Response Factors. ASHRAE Transactions 73, Part I.

Muncey, R.W.R. (1979). Heat Transfer Calculations for Buildings. Applied Science Publishers, Ltd. London.

Nevander, L.E. (1961). Köldbryggor i väggkonstruktioner. Byggmästaren nr 2 1961.

Nevander, L.E., Bankvall, C. (1978). Värme. Div. of Building Technology. Lund Institute of Technology.

Pettersson, G., Ahlinder, S., Stabo, S. (1972). jω-metoden. Esselte Studium AB.

Rules Th. (1977). Rules for Calculating Practical Thermal Properties of Structural Components. Centre Scientifique et Technique du Batiment, Paris.

Sacchi, A. (1967). L'attenuazione delle oscillazioni termiche in pareti semplici e composte. Termocinetica del Trattato di Fisica Technica, Vol II.

Sacchi, A. (1977). Comparison among the Methods for the Calculation of Thermal Behaviour of Walls and Buildings in Non-Steady State Conditions. Istituto di Fisica Technica, Politecnico di Torino.

Sandberg, P.I. (1973). Byggnadsdelars fuktbalans i naturligt klimat. Div. of Building Technology. Lund Institute of Technology.

Sonderegger, R.C. (1977). Dynamic Models of House Heating Based on Equivalent Thermal Parameters. Report PU/CES 57. University of Princeton.

Swedish Building Code. (1975).

Tye, R., Spinney, S.C. (1978). Measurement of Specific Heat for Building Materials. ASHRAE Transcations 1978-6.

Verhoeven, A.C., Liem, T.H.J. (1976). Numerical Considerations on the Physical Behaviour of Thermal Bridges with Respect to Standardization. CIB 40-1976.

Vierveyzer, P. (1978). Energy Losses through Crawl Space Basements. Report CO 18. Dep. of Civil Engineering. Delft University of Technology.

Wieczynski, J. (1977). The Influence of Heat Transfer Coefficients on Indoor Climate. Dep. of Heating and Ventilating. Royal Institute of Technology, Stockholm.

Åström, J.J. (1968). Reglerteori. Almquist and Wicksell, Stockholm.